HIGH PRESSURE PROCESSING OF MIXED PEA PROTEIN-STARCH SYSTEMS: EFFECTS ON STRUCTURE AND *IN-VITRO* DIGESTIBILITY

A Dissertation

Presented to the Faculty of the Graduate School

of Cornell University

In Partial Fulfillment of the Requirements for the Degree of

Doctor of Philosophy

by

Yong Jie Shaun Sim

August 2019

HIGH PRESSURE PROCESSING OF MIXED PEA PROTEIN-STARCH SYSTEMS: EFFECTS ON STRUCTURE AND *IN-VITRO* DIGESTIBILITY

Yong Jie Shaun Sim, Ph.D.

Cornell University 2019

Pea proteins offer a relatively inexpensive and sustainable plant protein source that can be used to meet the increased consumer demand for protein. A major challenge in using pea protein ingredients to create novel food products is the undesirable "cooked" flavor formed during traditional thermal processing. Hence, a nonthermal method such as high pressure processing (HPP) may be key to expanding the range of pea-based products and their consumption. A review of the literature in Chapter One shows that the structures of protein and starch can be individually modified by HPP to create foods with unique textures and digestibility. However, it is not known how this occurs in protein-starch mixtures, which is important as starch is a major component in pea protein systems. Therefore, this dissertation describes work performed to understand how novel structures can be created using HPP treatment of pea protein-starch mixed systems, the mechanisms responsible for the formation of these structures, and the effect of HPP treatment on protein and starch digestibility.

The effects of pressure level and protein concentration on the pressure-induced structural changes in pea protein concentrates (PPC) were evaluated and compared to heat treatments in Chapter Two. HPP induced gel formation in PPC, with gel strength increasing with both pressure level and protein concentration, due to a greater extent of protein

denaturation, aggregation and network formation. Heat-treated samples exhibited greater gel strength than pressure-treated samples at the same protein concentration, due to the different type of structural transformations caused by the two processes.

Starch granules present in PPC retained their structure and were not gelatinized even after HPP treatment at the highest pressure level, but were gelatinized by heat. Since starch is a major component in pulses, the contributions of pea starch to pressure-induced structure formation in mixed protein-starch systems were examined in Chapter Three, using PPC and pea starch of varying protein and starch concentrations. Starch acted mainly as a filler in the pressure-induced protein gel matrix, and the increase in gel strength was more dependent on protein concentration than starch concentration. Starch granules were observed to be embedded in the protein network, and remained intact and ungelatinized after HPP.

As starch in the mixed systems remained ungelatinized after HPP, this was expected to have implications on its digestibility. At the same time, protein digestibility is also likely to be affected by the pressure treatment. The effects of HPP and heat on the protein and starch digestibility of mixed pea protein-starch systems were explored in Chapter Four. Pressure treatments led to higher protein and lower starch digestibility than heat treatments. Untreated controls had the highest protein and the lowest starch digestibility compared to the HPP and heat-treated samples. The implication of these results is that HPP-treated pea protein-starch mixtures could lead to the creation of novel pea-based products with lower glycemic-index and enhanced protein digestibility.

Overall, the findings of this work provide the knowledge foundation to develop novel pulse and pea protein foods using HPP, with significance both for their texture and digestibility.

BIOGRAPHICAL SKETCH

Having lived all his growing years in sunny Singapore, Shaun Sim thought it a great idea to experience some fine English weather. Thus he pursued his undergraduate education on a government scholarship in chemistry at the University of Cambridge, dabbling in some materials science on the side. When forced indoors by temperamental weather, Shaun discovered the joy of food and science, through watching videos on cooking and molecular gastronomy. Having just learnt the concept of phase diagrams, he wondered if he could construct one for cooking an egg. He also wondered how many ways of cooking an egg there were (many), and whether it was possible to uncook an egg (it is, with sodium borohydride). Shaun also subjected his poor friends to his cooking experiments (while not a great cook by any stretch, he thought his poached chocolate egg went rather well, though dark chocolate and egg white might have been a strange combination by the looks of his friends' faces). These activities bolstered his interest in the science of food, and after graduating with a First, he spent his mandatory one-year research attachment back home doing the next closest thing to food he knew then: clinical nutrition. He was fortunate to have an open-minded boss who allowed him to do a project on chocolate, and who introduced him to the existence of Food Science as a discipline. It was with great delight that Shaun decided to pursue his PhD in Food Science at Cornell University.

Shaun's fortune continued when Dr. Carmen Moraru accepted him as her student (though his luck with Ithacan weather did not). His interest in understanding food from its roots (literally) to its fate in the human body was fed through his minors in horticulture and human nutrition. He also had the privilege to present his research at local and international scientific conferences such as the Institute of Food Technologists Annual Meeting (IFT), the

Conference of Food Engineering (CoFE), and the World Congress of Food Science and Technology (IUFoST). When not pushing the knowledge boundaries of his field, Shaun has spent his time eating chocolate, making chocolate, buying chocolate, visiting chocolate factories, and teaching others about chocolate. He still experiments with food on his friends, but also has other interests in music: from playing in an orchestra, to making a violin under a local luthier's tutelage.

After completing his PhD, Shaun will return to the clinical nutrition research centre, where he will investigate novel food structures to improve human health.

To my parents and sister for their loving support,

especially through my rough seasons.

And to Jer Lin,

patiently waiting my return.

ACKNOWLEDGMENTS

I am really grateful to my advisor and committee chair, Dr. Carmen Moraru, for her generous guidance throughout my time here. She is the kindest and most supportive supervisor a student can ask for, and she has actively fostered an environment where all of us in her lab truly feel like a family. As a bonus, she also makes an amazing black forest cake. Under her careful instruction, I have grown to be a more meticulous thinker. I would also like to thank my minor advisors Dr. Thomas Brenna (from Human Nutrition) and Dr. Neil Mattson (from Horticulture) for their intellectual input and support over the years. And to Dr. David Barbano, my field appointed member, for his valuable contributions in my exams.

I am indebted (literally) to the Agency for Science, Technology and Research (A*STAR, Singapore) for funding my undergraduate and PhD studies, and international conference travel through the National Science Scholarship program. I am also thankful for my project funding through the USDA-NIFA grant, and to the Cornell Graduate School for travel funding to present my work at local conferences.

I am also grateful to my collaborators from Rutgers University: Dr. Mukund Karwe, Noopur Gosavi, Sawali Navare, and Ender Arserim for their assistance with the initial HPP runs, and the later TIM-1 digestions.

I would like to thank all Moraru Lab members past and present, who have made my time here so special: Cat Boyles, Daniela Buosi, Lee Cadesky, Hanyu Chen, Emily Griep, Sheena Hilton, Jaqueline Moraes, Jer Lin Poh, Jiai Zhang, and Huijuan Zheng; Yifan Cheng for our nerdy conversations and for your help with SEM imaging; my fellow (tea) drinking buddies Pedro Menchik and Andreea Beldie; my HPP teammates Linran Wang and Allie Hall; and Kyle Kriner who is able to fix anything. And a shout out to all visiting scholars,

summer scholars, professional masters, research associates, lab assistants, and undergraduate students who have been with us.

I would also like to mention the friendship and support from fellow grad students: my house mates at Gamma Alpha, my friends from Cornell International Christian Fellowship, and my peers in the Department of Food Science.

Finally, special thanks to the incredible administrative staff in the Food Science Department, and the staff at Cornell Dairy Bar, whose sandwiches I eat almost daily.

TABLE OF CONTENTS

LIST OF FIGURES

LIST OF TABLES

LIST OF ABBREVIATIONS

HPP	High Pressure Processing
PPC	Pea protein concentrate
PS	Pea starch
DSC	Differential scanning calorimetry
LVR	Linear viscoelastic region
SEM	Scanning electron microscopy
ATR-FTIR	Attenuated total reflectance Fourier transform infrared
TIM-1	TNO Gastro-Intestinal Model 1
BCA	Bicinchoninic acid
BSA	Bovine serum albumin
G6P	Glucose-6-phosphate
NAD^+/NADH	Nicotinamide adenine dinucleotide

CHAPTER ONE

INTRODUCTION

1.1 Pea Protein: Market Demand, Processing Challenges and Opportunities

The demand for protein is increasing due to population growth and socio-economic changes (Henchion, Hayes, Mullen, Fenelon, & Tiwari, 2017). With growing incomes and changing consumption patterns, consumers not only want foods high in protein, but also from sustainable sources, with a smaller environmental footprint (Mintel, 2013). One such protein source is represented by pulses, which are the edible dried seeds of leguminous plants such as peas, chickpeas, lentils, and beans. Pulses contain about twice as much protein as whole grain cereals, are relatively inexpensive crops to grow, and have a low water footprint compared with other protein sources (FAO, 2016). Pulses are also not classified as major allergens (Boye, Zare, & Pletch, 2010). While pulses constitute a regular component of the daily diet in some parts of the world, this is not the case for many Western countries, including the US, as cooking pulses require lengthy preparation. ***One way to include pulse proteins in the modern Western diet is by using pulse protein ingredients in the creation of novel food products.*** Pea (*Pisum sativum L.)* is one of the eleven primary pulses, and account for about 26 % of all pulses produced worldwide (www.faostat.fao.org). The market for pea protein is growing and is expected to reach $313.5m by 2025 (Grand View Research, 2017), making it one of the most popular pulse protein ingredient used in food products.

1.1.1 The Challenges of Using Pea Protein Ingredients to Create Novel Food Products

The major components of pea proteins are the globular, water soluble albumins and

salt soluble globulins, which make up 15-25 % and 50-60 % of the total protein content, respectively (Gueguen & Barbot, 1988). Pea albumins include a major albumin protein of ~25 kDa molecular weight, and a minor albumin protein of ~6 kDa molecular weight (Rao, Costa, Croy, Boulter, & Gatehouse, 1989). The pea globulin fraction includes legumin (11S), vicilin (7S), and convicilin (7S). Legumin has a hexameric quaternary structure (~390 kDa) at pH 7, with each of the six subunits composed of an acidic (40 kDa) and a basic (20 kDa) polypeptide, joined by a disulfide bridge (Croy, Derbyshire, Krishna, & Boulter, 1979). Vicilin has a trimeric structure (~170 kDa) with subunits of ~50 kDa, and does not contain cysteine residues (Gatehouse, Croy, Morton, Tyler, & Boulter, 1981). Convicilin (~290 kDa) also has a trimeric structure with subunits of ~ 71 kDa, but contains cysteine residues (Croy, Gatehouse, Tyler, & Boulter, 1980).

Commercially available pea protein ingredients include protein isolates and concentrates, which are obtained by extracting pea protein from pea flour (Figure 1.1).

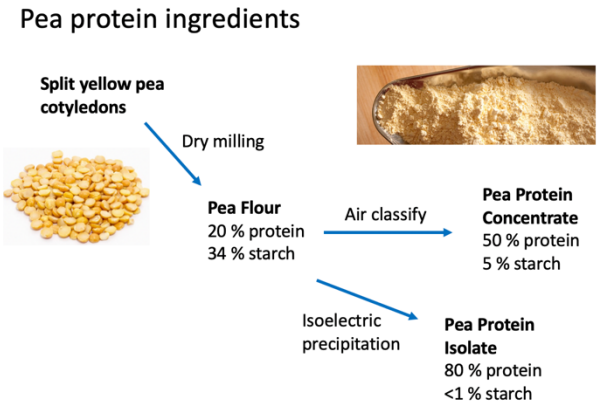

Figure 1.1. Overview of how pea protein ingredients are obtained. Images taken from http://www.agtfoods.com/products/pulse-ingredients.html

Pea flour is made by dry milling whole pea cotyledons. Yellow pea flour contains approximately 20 % protein, 34 % starch, 1.3 % fat and 2.5 % ash (Raghunathan et al., 2017;

Ribéreau et al., 2017). Pea protein isolates are typically obtained using isoelectric precipitation methods. The solubility of pea protein is high at alkaline pH and low at pH close to its isoelectric point (~pH 4-5) (Boye et al., 2010). Therefore, the process of making pea protein isolates involves dispersing pea flour in water, raising the pH to allow solubilization of proteins (sometimes at elevated temperatures of 55-65 °C to speed up the process), filtration to remove the insoluble starch and fiber, precipitation of proteins at isoelectric pH, centrifugation to recover the proteins, followed by washing to remove salts, neutralization and drying (Boye et al., 2010). While the protein content of pea protein isolates can reach 80-90 %, their functionality is affected by the harsh processing conditions used (Pelgrom, Vissers, Boom, & Schutyser, 2013).

A gentler technique to extract proteins from peas is air classification, which uses a spiral air stream to separate the denser starch particles from the lighter protein fractions in pea flour. Pea protein concentrates are typically made using this method. Due to the gentler process, pea protein concentrates retain a higher proportion of the native structure and functionality of proteins. However, the protein content of the concentrates is lower (between 50-60 %) compared to pea protein isolates, and they also contain ~5 % starch (Boye et al., 2010).

Pea protein ingredients are increasingly used for protein fortification or for their functional properties. Some examples include the replacement of eggs in vegan “mayonnaise” due to their emulsification properties, or as texturizing agents in plant-based meat replacements. Pea proteins also exhibit strong gelling properties and could be used to mimic the texture and mouthfeel of gelled dairy products.

In many cases, processing of pea protein ingredients involves a thermal treatment step, which can lead to the formation of a gel structure if the protein concentration is above a minimum level (Shand, Ya, Pietrasik, & Wanasundara, 2007; Sun & Arntfield, 2010). Other methods used to obtain pea-based gels include enzymatic treatments (Djoullah, Husson, & Saurel, 2017) and acid-induced gelation (Mession, Chihi, Sok, & Saurel, 2015). All these methods require the heat denaturation of pea proteins as the initial step. Unfortunately, a pronounced "cooked" flavor is formed due to the heating process (Malcolmson et al., 2014), which is undesirable to many consumers. ***Hence, a non-heat-based method to obtain gel structures, without the unpleasant, strong flavors specific to heat-treated pea products, may be key to expanding the range of pea-based products and their consumption.*** A processing method suitable for this purpose is high pressure processing.

1.1.2 High Pressure Structuring of Pea Proteins to Create Novel Textures

High pressure processing (HPP) is an emerging food processing method, which involves placing food (that is packaged in a flexible container such as a pouch or plastic bottle) in a high pressure (200-800 MPa) chamber. The high pressure is achieved via a hydraulic fluid medium such as water, and is transmitted uniformly throughout the chamber. Therefore, all food components are subjected to the same pressure. This process can be conducted at cold or ambient temperatures. The primary use of HPP currently is low-temperature microbial inactivation (cold pasteurization), but more recently HPP has been explored for food texture engineering. HPP can be used to form protein gels through the disruption of non-covalent interactions in proteins (Balasubramaniam, Martínez-Monteagudo, & Gupta, 2015; Cadesky, Walkling-Ribeiro, Kriner, Karwe, & Moraru, 2017).

The effect of pressure on globular proteins

Proteins contain primary, secondary, tertiary and quaternary structures. The primary structure consists of polypeptide chains formed by a sequence of amino acids covalently bonded through peptide bonds. These polypeptide chains form secondary structures – such as α-helices and β-sheets – via inter- or intramolecular hydrogen bonds. The tertiary structure is formed by folding the secondary structure domains into three-dimensional configurations via non-covalent interactions between amino acid side groups. These three-dimensional subunits can then assemble to form quaternary structures. The secondary, tertiary and quaternary structures are stabilized by a mix of non-covalent interactions such as electrostatic attraction, hydrogen bonds, hydrophobic interactions and disulfide linkages. Solvents such as water coordinate the protein structure via hydrogen bonds.

Changes in temperature, pressure, solvent and pH can disrupt the non-covalent interactions, leading to denaturation. In the case of applied pressure, the system will try to minimize the effect of the increasing pressure by favoring phenomena (phase transitions, chemical reactions, changes in molecular configuration) that lead to a reduction in overall volume (Cheftel, 1995). Proteins contain cavities in their hydrophobic core. Protein unfolding allows water to enter the hydrophobic cores, thus reducing molar volume (Frye & Royer, 1998; Roche et al., 2012). Rupturing and rearranging non-covalent bonds with solvent molecules also reduces the volume of hydration (Frye & Royer, 1998). Additionally, disrupting electrostatic interactions can decrease the solvation volume by electrostriction (Mozhaev et al., 1996). The net result is the disruption of non-covalent interactions and destabilization of the native protein structure. High pressures have little effect on the protein primary structure, and the extent of protein structure destabilization depends on the amount of

pressure applied (Figure 1.2). Protein quaternary oligomeric subunits can be dissociated under moderate pressure (50-200 MPa) (Mozhaev et al., 1996), but these changes are reversible. Pressures above 300 MPa however cause irreversible denaturation (Balny & Masson, 1993). In such situations, there may also be a change and/or conversion of one secondary structure to another (Balny & Masson, 1993).

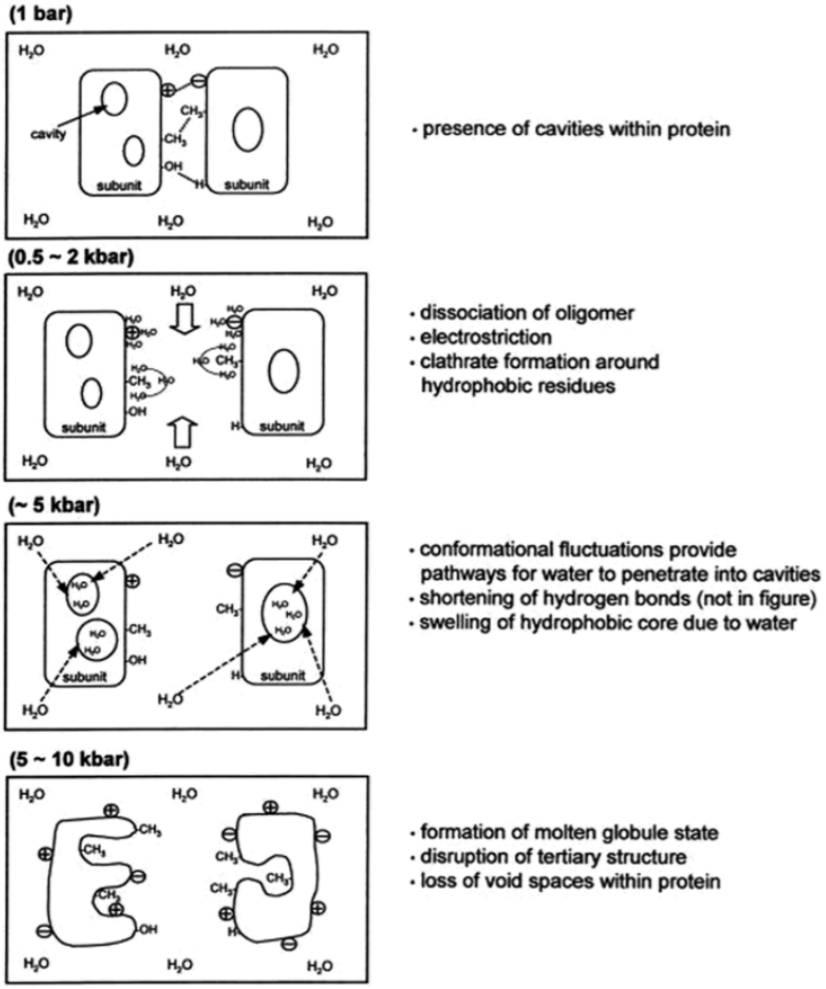

Figure 1.2. Effects of pressure on molecular interactions of protein molecules (from Boonyaratanakornkit et al., 2002).

Pressure-induced gelation occurs when the denatured or partially denatured proteins aggregate to form a network (Yang & Powers, 2016), provided that the protein concentration is above the minimum required to gel. The minimum protein concentration for gelation varies with the source of protein (Yang & Powers, 2016). Disulfide bonds exchange can occur under high pressure (Visschers & De Jongh, 2005). Gel strength was reported to increase at higher pressure levels (Alvarez et al., 2008; Van Camp & Huyghebaert, 1995; Van der Plancken et al., 2007). Other factors influencing pressure-induced gelation besides protein concentration and pressure intensity include pH and ionic strength of the protein solution. The protein gels formed by HPP have been found to be structurally and texturally different to their heat-treated counterpart (V. M. Balasubramaniam, Barbosa-Cánovas, & Lelieveld, 2016), opening the opportunity for a whole new palette of foods with novel textures.

Most of the work on pressure-induced gelation of plant proteins available to date has focused on soy proteins. It was found that the pressure-induced soy protein gels had increasing storage (G') and loss (G'') modulus with applied pressure and protein concentration (Alvarez et al., 2008; Apichartsrangkoon, 2003). At low soy protein concentrations (5 % and 10 %), the protein solution exhibited liquid-like properties (G'' > G') at all applied pressures (250-650 MPa) (Alvarez et al., 2008). The soy protein mixture exhibited solid-like gel properties from 15 % protein concentration and even under low applied pressures (250 MPa). A similar behavior is expected for pea protein.

There are however very few studies on pressure-induced gelation of pulse proteins in general, and none on pea proteins. Filling this knowledge gap may lead to the creation of novel pea protein products with interesting structures and superior sensory properties.

1.1.3 The Contributions of Starch to Structure Formation in High Pressure Treated Systems

Besides protein, starch is also a major component of pulses. This is important because HPP can also induce structural modifications in starch (Pei-Ling, Xiao-Song, & Qun, 2010). It has been reported before that in pure starch systems starch granules can be gelatinized by pressure, leading to gel formation (Ahmed, Singh, Ramaswamy, Pandey, & Raghavan, 2014; Leite, de Jesus, Schmiele, Tribst, & Cristianini, 2017). ***This suggests that starch could be a significant contributor to structure formation in pressure-treated protein gels.***

Starch is one of the main carbohydrates found in cereals and legumes. It is granular in form and is made up of two glucose polymers – amylose and amylopectin. Amylose is essentially linear, while amylopectin is highly branched due to α-(1→6) glycosidic bonds. This allows amylopectin to form a double helix configuration that is highly ordered and crystalline (Gallant et al., 1997). Starch granules have a porous "hilium" core, from which alternating crystalline (amylopectin) and amorphous (amylose and non-ordered amylopectin branches) layers grow outwards (Waigh et al., 1997), forming an ellipsoidal lamellar structure. This lamellar structure gives rise to birefringence and can be observed as a typical maltese cross pattern under plane polarized light. Clusters of amylopectin helices can be arranged in either densely packed A-type crystal structures found in cereal starches, or more open B-type structures found in tuber and root starches (Wang & Copeland, 2013). Legume starches (such as pea starch) are composed of C-type structures, which are mixtures of A- and B-type crystals.

Starch can be gelatinized by both temperature and pressure (Figure 1.3). Thermal energy disrupts the crystalline packing within and between the amylose and amylopectin

helical structures. Water is absorbed into the starch granules, forming hydrogen bonds with the amylopectin helical strands, causing the granules to swell and leach amylose into solution. This disruption of the crystalline structure results in the loss of birefringence. Differential scanning calorimetry (DSC) can be used to study this transition. Since starch gelatinization requires thermal energy to disrupt its crystalline structure, this endothermic peak can be detected under DSC. In heat-induced gelatinization, a phase transition occurs between 60-70 °C. The area of the peak is related to the total amount of heat energy absorbed and hence the amount of starch undergoing gelatinization.

HPP causes starch to swell in water, though the shape of the granules remains mostly intact and there is little leaching of amylose. It is thought that the absorption of water into the granule leads to an overall decrease in macroscopic starch volume (Muhr et al., 1982) to counter the equilibrium shift of the system when pressure is applied. Hydration of the crystalline regions causes helix-helix dissociation followed by helix-coil transition when gelatinization occurs. The disintegration of the macromolecule is incomplete, since hydrogen bonds stabilized by pressure favor the helix conformation (Knorr et al., 2006).

Factors that affect pressure-gelatinization of starch include starch type, applied pressure, temperature, hold time, and water content (Yang, Chaib, Gu, & Hemar, 2017). The degree of gelatinization increases with pressure. (Leite et al., 2017) found that pea starch did not gelatinize below 300 MPa, had 31 % gelatinization at 400 MPa, and complete gelatinization at 500 MPa. B-type starches like potato starch have the highest resistance to pressure. It was found that potato starch suspension completely gelatinized under pressure only after 700-900 MPa (Kawai et al., 2007; Kudta & Tomasik, 1992).

As heat-gelatinized starch solution cools, amylose leached into solution can reform double helices that can crosslink to form a network surrounding the liquid, and hence a gel (Leloup et al., 1992). It is unclear if the same mechanism occurs for pressure-gelatinized starch. Because amylose is not soluble at low temperatures, it can precipitate in a process known as retrogradation. The precipitation may lead to syneresis, which describes what happens when liquid separates from the solid phase.

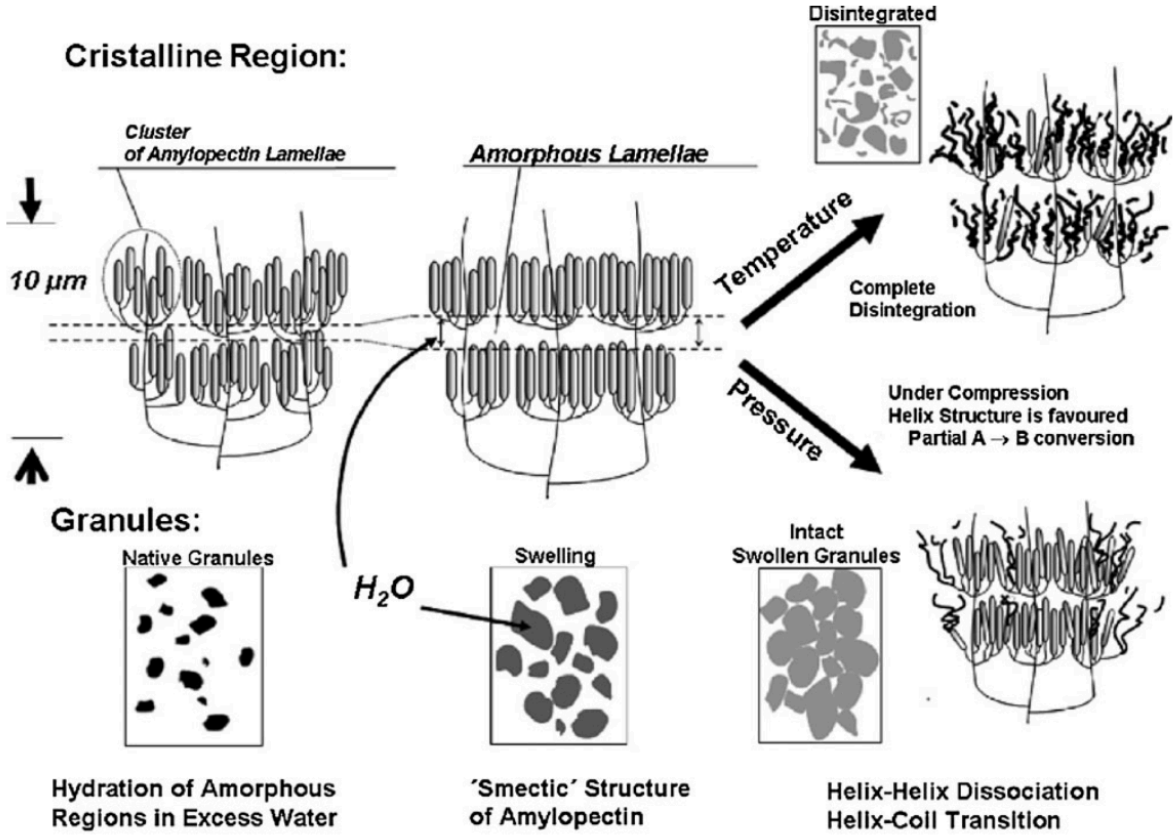

Figure 1.3. Cartoon depicting temperature and pressure-induced starch gelatinization in excess water (from Knorr et al., 2006).

Many food products (e.g. bread, pasta, and surimi) are made from protein-starch mixtures. Understanding how processing affects these mixtures could expand the food

structure design toolbox. For example, at a fixed solids content, the composite gel strength of heat-treated lentil protein-starch mixtures increased with increasing starch fraction (Joshi, Aldred, Panozzo, Kasapis, & Adhikari, 2014). In addition, as proteins and starch can experience attractive electrostatic forces between the negatively charged starch surface and positively charged side groups in proteins (Jamilah et al., 2009), pH modifications can affect subsequent protein-starch complexation and texture of heat-treated protein-starch mixtures (Marshall & Chrastil, 1992). The heat treatment temperature was also found to affect the rheological properties of corn starch-soy protein composites as starch gelatinizes at a lower temperature than protein denaturation (Li, Yeh, & Fan, 2007).

There is to date little published information on the structural effect of HPP on protein-starch mixed systems. The fundamental differences between the effects of pressure and heat treatments could lead to the formation of unique structures and textures. For example, while starch gelatinization occurs at a lower temperature than protein denaturation in heat treatments, both processes occur simultaneously during pressure treatments. Consequently, interesting properties and functionalities can be derived and used for different applications such as microencapsulation, texturing agents and edible films (Schmitt et al., 1998).

1.1.4 The Effect of High Pressure Processing on the Digestibility of High Pressure Treated Food

The unique pressure-induced structural changes in proteins and starch may also bring changes in the digestibility and nutritional properties of high pressure treated foods, but very little data addressing this issue exists to date. An increasing number of studies is however

focusing on evaluating the digestibility and bioavailability of processed foods. In such studies, *in vitro* digestion models are commonly used as a practical substitute to human models, and a number of systems that can mimic the mechanical and enzymatic transformations that occur in human digestion have been developed (Hur, Lim, Decker, & McClements, 2011). Depending on the requirements of the study, models with different levels of complexity (simple, static, or dynamic) can be employed. Dynamic models allow for more realistic simulation of *in vivo* conditions, such as biochemical changes and physical gastric motions.

The TNO Gastro-Intestinal Model (TIM-1) is one such dynamic model (Minekus, 2015). TIM-1 (Figure 1.4) contains four different compartments (stomach, duodenum, jejunum, and ileum) that allow the food to be exposed to different physiological environments (pH, gastric and intestinal secretions) as it transits through these compartments by the controlled action of peristaltic valve pumps. Digested products (e.g. sugars, peptides) are removed and collected through a dialysis filter system with a ~10 kDa molecular weight cut-off. The protein and glucose content of the digest can be measured and compared with the meal to determine respective digestibility.

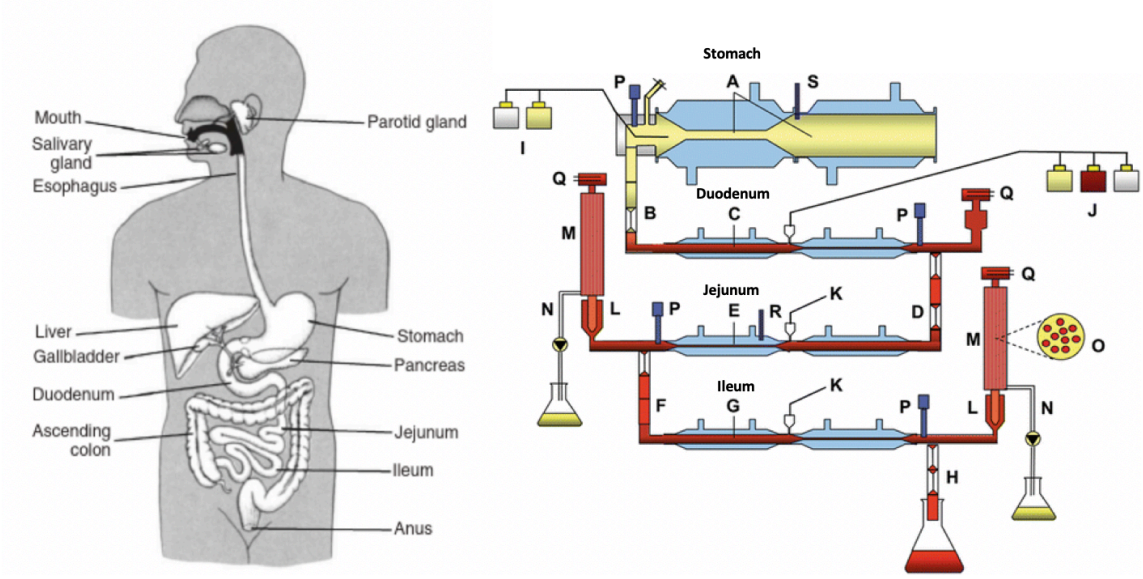

Figure 1.4. Schematic representation of TIM-1 to model the human gastrointestinal tract. A. gastric compartment; B. pyloric sphincter; C. duodenal compartment; D. peristaltic valve; E. jejunal compartment; F. peristaltic valve; G. ileal compartment; H. ileal-cecal valve; I. gastric secretion; J. duodenal secretion; K. bicarbonate secretion; L. pre-filter; M. filtration system; N. filtrate with bio-accessible fraction; O. hollow fiber system (cross section); P. pH electrodes; Q. level sensors; R. temperature sensors; S. pressure sensor (adapted from Minekus, 2015; Stipanuk and Caudill, 2012).

Pulses contain an array of antinutritional factors such as trypsin inhibitors and lectins that reduce protein digestibility (Nosworthy & House, 2017). Protein digestibility was found to be improved with the use of processing methods such as soaking and cooking due to the inactivation of these enzyme inhibitors (Boye et al., 2010). Heat-denatured proteins were also found to be more accessible to digestive proteases than untreated proteins (Chitra, Singh, & Venkateswara Rao, 1996). In pure protein systems, HPP affected protein digestibility through pressure-induced structure changes (Queirós, Saraiva, & da Silva, 2017) and the inactivation of antinutritional factors (Deng, Padilla-Zakour, Zhao, & Tao, 2015; Linsberger-Martin,

Weiglhofer, Thi Phuong, & Berghofer, 2013). Pressure-induced structural changes led to improved protein digestibility due to the exposure of proteolytic cleave sites in unfolded proteins, but also to decreased protein digestibility when the proteins aggregated and thus restricted digestive enzymes accessibility to the same cleavage sites (Queirós et al., 2017).

HPP can also influence the digestibility of starch. Factors that influence starch digestibility include starch type, mean granule size, degree of crystallinity (Tester, Karkalas, & Qi, 2004), and the presence of surface lipids and proteins (Wang & Copeland, 2013). Native starch is poorly hydrolyzed by amylases due to the highly crystalline starch structure and lower substrate accessibility (Wang & Copeland, 2013). Cooking was found to improve the enzymatic hydrolysis of starch, which increases with the degree of thermal gelatinization due to the breakdown of the crystalline order (Holm, Lundquist, Bjorck, Eliasson, & Asp, 1988). The effect of HPP on starch digestibility in pure starch systems was reported in a few studies, but their findings vary. Pressure-gelatinized starch was found to be more digestible than native starch, for reasons similar to an increase in digestibility after heat-gelatinization of starch (Deng et al., 2014; Hayashi & Hayashida, 1989; Noguchi et al., 2003; Zeng, Li, Gao, Liu, & Yu, 2018; Zhou et al., 2015). There were some studies however that showed that HPP treatments reduced starch digestibility. These occurred in low-moisture systems (Mercier, Charbonn, & Guilbot, 1968), which likely led to incomplete gelatinization (Yang et al., 2017), or in cases where the C-type starch structures converted to more amylase-resistant B-type structures under pressure (Liu et al., 2016; Liu et al., 2017). As pea starch is predominantly C-type, the starch digestibility of pressure-treated pea protein-starch mixtures may be reduced compared to untreated starch. If this were the case, HPP could result in foods that have low starch digestibility and low glycemic index, which may have certain health benefits.

For example, low glycemic diets represent one approach to manage the prevalence of type-2 diabetes (Brand-Miller, Hayne, Petocz, & Colagiuri, 2003). Recent strategies to produce low glycemic foods include the addition of denatured or hydrolyzed plant proteins that bind strongly to starch granules, restricting gelatinization and subsequent enzymatic cleavage (López-Barón, Gu, Vasanthan, & Hoover, 2017; López-Barón et al., 2018; Wee, Loud, Tan, & Forde, 2019), or the use of protein gel matrices to entrap starch granules, thus reducing digestive amylase accessibility (Lavoisier & Aguilera, 2019; Petitot, Abecassis, & Micard, 2009).

Based on the effects of pressure on protein and starch digestibility reported in literature, it may be possible to use HPP to treat protein-starch mixtures and produce low glycemic foods with high protein digestibility. ***There is currently no published literature investigating the effect of HPP on the digestibility of protein-starch mixed systems, hence filling this knowledge gap might facilitate the development of novel foods with nutritional benefits for the consumer.***

1.2 Objectives and Hypotheses for this Research

In response to the opportunities presented above, this dissertation describes the work performed to understand the possibility of creating novel structures using high pressure processing of pea protein ingredients, the mechanisms responsible for the structure formation, and the implications of the HPP treatment on protein and starch digestibility.

This work addressed the following objectives and hypotheses:

Objective 1. Examine the effects of pressure level and protein concentration on the pressure-induced structural changes in pea protein concentrates

Hypothesis:

A minimum protein concentration and pressure level are required to form a gel. The strength of pressure-induced gels increases with protein concentration and pressure level.

Objective 2. Evaluate the contributions of starch to pressure-induced structure formation in mixed pea protein-starch systems

Hypothesis:

At low starch concentration, starch behaves as a filler in a protein gel matrix. There is a critical protein to starch ratio where starch gel will begin to dominate the mixed system's structure and characteristics.

Objective 3. Investigate the effects of HPP or heat on the protein and starch digestibility of mixed pea protein-starch systems

Hypothesis:

Starch in the mixed pea protein-starch systems remains ungelatinized after HPP, and consequently it is less digestible than in heat-treated samples. Compared to untreated samples, protein digestibility of pressure-treated samples increases, due to the pressure-induced structural modifications in proteins.

The results for the three objectives are presented in Chapters Two, Three, and Four respectively. Overall, the findings from this dissertation could be used to develop novel pulse and pea protein foods using HPP, with possible implications both on their texture and digestibility.

REFERENCES

Ahmed, J., Singh, A., Ramaswamy, H. S., Pandey, P. K., & Raghavan, G. S. V. (2014). Effect of high-pressure on calorimetric, rheological and dielectric properties of selected starch dispersions. *Carbohydrate Polymers*, *103*, 12–21. https://doi.org/10.1016/J.CARBPOL.2013.12.014

Alvarez, P. A., Ramaswamy, H. S., & Ismail, A. A. (2008). High pressure gelation of soy proteins: Effect of concentration, pH and additives. *Journal of Food Engineering*, *88*(3), 331–340. https://doi.org/10.1016/j.jfoodeng.2008.02.018

Balasubramaniam, V., & Barbosa-Cánovas, G. (2016). *High Pressure Processing of Food*. Retrieved from http://link.springer.com/content/pdf/10.1007/978-1-4939-3234-4.pdf

Balasubramaniam, V. M. (Bala), Martínez-Monteagudo, S. I., & Gupta, R. (2015). Principles and Application of High Pressure–Based Technologies in the Food Industry. *Annual Review of Food Science and Technology*, *6*(1), 435–462. https://doi.org/10.1146/annurev-food-022814-015539

Balny, C., & Masson, P. (1993). Effects of high pressure on proteins. *Food Reviews International*, *9*(4), 611–628. https://doi.org/10.1080/87559129309540980

Boonyaratanakornkit, B. B., Park, C. B., & Clark, D. S. (2002). Pressure effects on intra- and intermolecular interactions within proteins. *Biochimica et Biophysica Acta*, *1595*(1–2), 235–249. https://doi.org/10.1016/S0167-4838(01)00347-8

Boye, J., Zare, F., & Pletch, A. (2010). Pulse proteins: Processing, characterization, functional properties and applications in food and feed. *Food Research International*, *43*(2), 414–431. https://doi.org/10.1016/j.foodres.2009.09.003

Brand-Miller, J., Hayne, S., Petocz, P., & Colagiuri, S. (2003). Low-glycemic index diets in the management of diabetes: a meta-analysis of randomized controlled trials. *Diabetes Care*, *26*(8), 2261–7. Retrieved from http://care.diabetesjournals.org/content/26/8/2261.short

Cadesky, L., Walkling-Ribeiro, M., Kriner, K. T., Karwe, M. V., & Moraru, C. I. (2017). Structural changes induced by high-pressure processing in micellar casein and milk protein concentrates. *Journal of Dairy Science*, *100*(9), 7055–7070. https://doi.org/10.3168/jds.2016-12072

Cheftel, J. C. (1995). Review : High-pressure, microbial inactivation and food preservation / Revision: Alta-presion, inactivacion microbiologica y conservacion de alimentos. *Food Science and Technology International*. https://doi.org/10.1177/108201329500100203

Chitra, U., Singh, U., & Venkateswara Rao, P. (1996). Phytic acid, in vitro protein digestibility, dietary fiber, and minerals of pulses as influenced by processing methods. *Plant Foods for Human Nutrition*, *49*(4), 307–316. https://doi.org/10.1007/BF01091980

Croy, R. R. D., Derbyshire, E., Krishna, T. G., & Boulter, D. (1979). LEGUMIN OF PISUM SATIVUM AND VICIA FABA. *New Phytologist*, *83*(1), 29–35. https://doi.org/10.1111/j.1469-8137.1979.tb00723.x

Croy, R. R., Gatehouse, J. A., Tyler, M., & Boulter, D. (1980). The purification and characterization of a third storage protein (convicilin) from the seeds of pea (Pisum sativum L.). *The Biochemical Journal*, *191*(2), 509–16. https://doi.org/10.1042/BJ1910509

Deng, Y., Jin, Y., Luo, Y., Zhong, Y., Yue, J., Song, X., & Zhao, Y. (2014). Impact of

continuous or cycle high hydrostatic pressure on the ultrastructure and digestibility of rice starch granules. *Journal of Cereal Science*, *60*(2), 302–310. https://doi.org/10.1016/J.JCS.2014.06.005

Deng, Y., Padilla-Zakour, O., Zhao, Y., & Tao, S. (2015). Influences of High Hydrostatic Pressure, Microwave Heating, and Boiling on Chemical Compositions, Antinutritional Factors, Fatty Acids, In Vitro Protein Digestibility, and Microstructure of Buckwheat. *Food and Bioprocess Technology*, *8*(11), 2235–2245. https://doi.org/10.1007/s11947-015-1578-9

Djoullah, A., Husson, F., & Saurel, R. (2017). Gelation behaviors of denaturated pea albumin and globulin fractions during transglutaminase treatment. *Food Hydrocolloids*. https://doi.org/10.1016/J.FOODHYD.2017.11.005

FAO. (2016). Pulses are praised for their health, environmental and economic benefits. How can their full potential be tapped? | Global Forum on Food Security and Nutrition (FSN Forum). Retrieved November 16, 2017, from http://www.fao.org/fsnforum/activities/discussions/pulses

Frye, K. J., & Royer, C. A. (1998). Probing the contribution of internal cavities to the volume change of protein unfolding under pressure. *Protein Science : A Publication of the Protein Society*, *7*(10), 2217–22. https://doi.org/10.1002/pro.5560071020

Gallant, D. J., Bouchet, B., & Baldwin, P. M. (1997). Microscopy of starch: evidence of a new level of granule organization. *Carbohydrate Polymers*, *32*(3–4), 177–191. https://doi.org/10.1016/S0144-8617(97)00008-8

Gatehouse, J. A., Croy, R. R. D., Morton, H., Tyler, M., & Boulter, D. (1981). Characterisation and Subunit Structures of the Vicilin Storage Proteins of Pea (Pisum sativum L.). *Eur. J. Biochem*, *118*, 627–633. Retrieved from http://onlinelibrary.wiley.com/store/10.1111/j.1432-1033.1981.tb05565.x/asset/j.1432-1033.1981.tb05565.x.pdf?v=1&t=ja90y4yj&s=c7baefbcd3f03965c12c507f123cd993608a40b5

Grand View Research. (2017). Pea Protein Market Size Worth $313.5 Million By 2025 | CAGR: 17.4%. Retrieved November 16, 2017, from http://www.grandviewresearch.com/press-release/global-pea-proteins-market

Gueguen, J., & Barbot, J. (1988). Quantitative and qualitative variability of pea (Pisum sativum L.) protein composition. *Journal of the Science of Food and Agriculture*, *42*(3), 209–224. https://doi.org/10.1002/jsfa.2740420304

Hayashi, R., & Hayashida, A. (1989). Increased Amylase Digestibility of Pressure-Treated Starch. *Agricultural and Biological Chemistry*, *53*(9), 2543–2544. https://doi.org/10.1080/00021369.1989.10869672

Henchion, M., Hayes, M., Mullen, A., Fenelon, M., & Tiwari, B. (2017). Future Protein Supply and Demand: Strategies and Factors Influencing a Sustainable Equilibrium. *Foods*, *6*(7), 53. https://doi.org/10.3390/foods6070053

Holm, J., Lundquist, I., Bjorck, I., Eliasson, A. C., & Asp, N. G. (1988). Degree of starch gelatinization, digestion rate of starch in vitro, and metabolic response in rats. *American Journal of Clinical Nutrition*, *47*(6), 1010–1016. https://doi.org/10.1093/ajcn/47.6.1010

Hur, S. J., Lim, B. O., Decker, E. A., & McClements, D. J. (2011, March 1). In vitro human digestion models for food applications. *Food Chemistry*. Elsevier. https://doi.org/10.1016/j.foodchem.2010.08.036

Jamilah, B., Mohamed, A., Abbas, K. A., Abdul Rahman, R., Karim, R., & Hashim, D. M. (2009). Protein-starch interaction and their effect on thermal and rheological characteristics of a food system: A review. *Journal of Food, Agriculture and Environment*, *7*(2), 169–174. Retrieved from https://www.academia.edu/27458465/Protein-starch_interaction_and_their_effect_on_thermal_and_rheological_characteristics_of_a_food_system_a_review

Joshi, M., Aldred, P., Panozzo, J. F., Kasapis, S., & Adhikari, B. (2014). Rheological and microstructural characteristics of lentil starch-lentil protein composite pastes and gels. *Food Hydrocolloids*, *35*, 226–237. https://doi.org/10.1016/j.foodhyd.2013.05.016

Kawai, K., Fukami, K., & Yamamoto, K. (2007). Effects of treatment pressure, holding time, and starch content on gelatinization and retrogradation properties of potato starch–water mixtures treated with high hydrostatic pressure. *Carbohydrate Polymers*, *69*(3), 590–596. https://doi.org/10.1016/j.carbpol.2007.01.015

Knorr, D., Heinz, V., & Buckow, R. (2006). High pressure application for food biopolymers. *Biochimica et Biophysica Acta (BBA) - Proteins and Proteomics*, *1764*(3), 619–631. https://doi.org/10.1016/j.bbapap.2006.01.017

Kudta, E., & Tomasik, P. (1992). The Modification of Starch by High Pressure. Part I: Air- and Oven-dried Potato Starch. *Starch - Stärke*, *44*(5), 167–173. https://doi.org/10.1002/star.19920440503

Lavoisier, A., & Aguilera, J. M. (2019). Effect of a Whey Protein Network Formed by Cold Gelation on Starch Digestibility. *Food Biophysics*, *14*(2), 214–224. https://doi.org/10.1007/s11483-019-09573-3

Leite, T. S., de Jesus, A. L. T., Schmiele, M., Tribst, A. A. L., & Cristianini, M. (2017). High pressure processing (HPP) of pea starch: Effect on the gelatinization properties. *LWT - Food Science and Technology*, *76*, 361–369. https://doi.org/10.1016/j.lwt.2016.07.036

Leloup, V. M., Colonna, P., Ring, S. G., Roberts, K., & Wells, B. (1992). Microstructure of amylose gels. *Carbohydrate Polymers*, *18*(3), 189–197. https://doi.org/10.1016/0144-8617(92)90063-V

Li, J. Y., Yeh, A. I., & Fan, K. L. (2007). Gelation characteristics and morphology of corn starch/soy protein concentrate composites during heating. *Journal of Food Engineering*, *78*(4), 1240–1247. https://doi.org/10.1016/j.jfoodeng.2005.12.043

Linsberger-Martin, G., Weiglhofer, K., Thi Phuong, T. P., & Berghofer, E. (2013). High hydrostatic pressure influences antinutritional factors and in vitro protein digestibility of split peas and whole white beans. *LWT - Food Science and Technology*, *51*(1), 331–336. https://doi.org/10.1016/j.lwt.2012.11.008

Liu, H., Guo, X., Li, Y., Li, H., Fan, H., & Wang, M. (2016). In vitro digestibility and changes in physicochemical and textural properties of tartary buckwheat starch under high hydrostatic pressure. *Journal of Food Engineering*, *189*, 64–71. https://doi.org/10.1016/j.jfoodeng.2016.05.015

Liu, M., Wu, N.-N., Yu, G.-P., Zhai, X.-T., Chen, X., Zhang, M., … Tan, B. (2017). Physicochemical properties, structural properties, and in vitro digestibility of pea starch treated with high hydrostatic pressure. *Starch - Stärke*, 1700082. https://doi.org/10.1002/star.201700082

López-Barón, N., Gu, Y., Vasanthan, T., & Hoover, R. (2017). Plant proteins mitigate in vitro

wheat starch digestibility. *Food Hydrocolloids*, *69*, 19–27. https://doi.org/10.1016/J.FOODHYD.2017.01.015

López-Barón, N., Sagnelli, D., Blennow, A., Holse, M., Gao, J., Saaby, L., … Vasanthan, T. (2018). Hydrolysed pea proteins mitigate in vitro wheat starch digestibility. *Food Hydrocolloids*, *79*, 117–126. https://doi.org/10.1016/j.foodhyd.2017.12.009

Malcolmson, L., Frohlich, P., Boux, G., Bellido, A.-S., Boye, J., & Warkentin, T. D. (2014). Aroma and flavour properties of Saskatchewan grown field peas (Pisum sativum L.). *Canadian Journal of Plant Science*, *94*(8), 1419–1426. https://doi.org/10.4141/cjps-2014-120

Marshall, W. E., & Chrastil, J. (1992). Interaction of Food Proteins with Starch. In *Biochemistry of Food Proteins* (pp. 75–97). Boston, MA: Springer US. https://doi.org/10.1007/978-1-4684-9895-0_3

Mercier, C., Charbonn, R., & Guilbot, A. (1968). Influence of pressure treatment on granular structure and susceptibility to enzymatic amylolysis of various starches. *Starch - Stärke*, *20*(1), 6–11.

Mession, J.-L., Chihi, M. L., Sok, N., & Saurel, R. (2015). Effect of globular pea proteins fractionation on their heat-induced aggregation and acid cold-set gelation. *Food Hydrocolloids*, *46*, 233–243. https://doi.org/10.1016/J.FOODHYD.2014.11.025

Minekus, M. (2015). The TNO gastro-intestinal model (TIM). In *The Impact of Food Bioactives on Health: In Vitro and Ex Vivo Models* (pp. 37–46). Cham: Springer International Publishing. https://doi.org/10.1007/978-3-319-16104-4_5

Mintel. (2013). US consumers have a healthy appetite for high protein food. The US leads the way in global launches of high protein products | Mintel.com. Retrieved November 16, 2017, from http://www.mintel.com/press-centre/food-and-drink/us-consumers-have-a-healthy-appetite-for-high-protein-food-the-us-leads-the-way-in-global-launches-of-high-protein-products

Mozhaev, V. V, Heremans, K., Frank, J., Masson, P., & Balny, C. (1996). High pressure effects on protein structure and function. *Proteins*, *24*(1), 81–91. https://doi.org/10.1002/(SICI)1097-0134(199601)24:1<81::AID-PROT6>3.0.CO;2-R

Muhr, A. H., Wetton, R. E., & Blanshard, J. M. V. (1982). Effect of hydrostatic pressure on starch gelatinisation, as determined by DTA. *Carbohydrate Polymers*, *2*(2), 91–102. https://doi.org/10.1016/0144-8617(82)90055-8

Noguchi, T., Taniguchi-Yamada, A., Sato, H., Suzuki, T., Matsumoto, S., & Takano, K. (2003). Effect of high-pressure treatment on decomposition of potato and wheat starch by alpha-amylase. *Food Preservation Science*, *29*(6), 335–339. https://doi.org/10.5891/jafps.29.335

Nosworthy, M. G., & House, J. D. (2017, January 1). Factors influencing the quality of dietary proteins: Implications for pulses. *Cereal Chemistry*. John Wiley & Sons, Ltd. https://doi.org/10.1094/CCHEM-04-16-0104-FI

Pei-Ling, L., Xiao-Song, H., & Qun, S. (2010). Effect of high hydrostatic pressure on starches: A review. *Starch - Stärke*, *62*(12), 615–628. https://doi.org/10.1002/star.201000001

Pelgrom, P. J. M., Vissers, A. M., Boom, R. M., & Schutyser, M. A. I. (2013). Dry fractionation for production of functional pea protein concentrates. *Food Research International*, *53*(1), 232–239. https://doi.org/10.1016/J.FOODRES.2013.05.004

Petitot, M., Abecassis, J., & Micard, V. (2009). Structuring of pasta components during processing: impact on starch and protein digestibility and allergenicity. *Trends in Food Science & Technology*, *20*(11–12), 521–532. https://doi.org/10.1016/J.TIFS.2009.06.005

Queirós, R. P., Saraiva, J. A., & da Silva, J. A. L. (2017). Tailoring structure and technological properties of plant proteins using high hydrostatic pressure. *Critical Reviews in Food Science and Nutrition*, 1–19. https://doi.org/10.1080/10408398.2016.1271770

Raghunathan, R., Hoover, R., Waduge, R., Liu, Q., & Warkentin, T. D. (2017). Impact of molecular structure on the physicochemical properties of starches isolated from different field pea (Pisum sativum L.) cultivars grown in Saskatchewan, Canada. *Food Chemistry*, *221*, 1514–1521. https://doi.org/10.1016/j.foodchem.2016.10.142

Rao, R., Costa, A., Croy, R. R. D., Boulter, D., & Gatehouse, J. A. (1989). Variation in polypeptides of the major albumin protein of pea (Pisum sativum L.) : Inheritance and molecular analysis. *MGG Molecular & General Genetics*, *219*(1–2), 277–281. https://doi.org/10.1007/BF00261188

Ribéreau, S., Aryee, A. N. A., Tanvier, S., Han, J., & Boye, J. I. (2017). Composition, digestibility, and functional properties of yellow pea as affected by processing. *Journal of Food Processing and Preservation*, e13375. https://doi.org/10.1111/jfpp.13375

Roche, J., Caro, J. A., Norberto, D. R., Barthe, P., Roumestand, C., Schlessman, J. L., … Royer, C. A. (2012). Cavities determine the pressure unfolding of proteins. *Proceedings of the National Academy of Sciences of the United States of America*, *109*(18), 6945–50. https://doi.org/10.1073/pnas.1200915109

Schmitt, C., Sanchez, C., Banon, S. D., & Hardy, J. (1998). Structure and technofunctional properties of protein-polysaccharide complexes: A review. *Crit. Rev. Food Sci. Nutr.*, *38*(8), 689–753. https://doi.org/10.1080/10408699891274354

Shand, P. J., Ya, H., Pietrasik, Z., & Wanasundara, P. K. J. P. D. (2007). Physicochemical and textural properties of heat-induced pea protein isolate gels. *Food Chemistry*, *102*(4), 1119–1130. https://doi.org/10.1016/j.foodchem.2006.06.060

Stipanuk, M. H., & Caudill, M. A. (2012). Biochemical, physiological, and molecular aspects of human nutrition. Retrieved from https://ebookcentral.proquest.com

Sun, X. D., & Arntfield, S. D. (2010). Gelation properties of salt-extracted pea protein induced by heat treatment. *Food Research International*, *43*(2), 509–515. https://doi.org/10.1016/J.FOODRES.2009.09.039

Tester, R. F., Karkalas, J., & Qi, X. (2004). Starch structure and digestibility Enzyme-Substrate relationship. *World's Poultry Science Journal*, *60*(2), 186–195. https://doi.org/10.1079/WPS200312

Van Camp, J., & Huyghebaert, A. (1995). High pressure-induced gel formation of a whey protein and haemoglobin protein concentrate. *LWT - Food Science and Technology*. https://doi.org/10.1016/S0023-6438(95)80021-2

Van der Plancken, I., Van Loey, A., & Hendrickx, M. E. (2007). Foaming properties of egg white proteins affected by heat or high pressure treatment. *Journal of Food Engineering*, *78*(4), 1410–1426. https://doi.org/10.1016/j.jfoodeng.2006.01.013

Visschers, R. W., & De Jongh, H. H. J. (2005). Bisulphide bond formation in food protein aggregation and gelation. *Biotechnology Advances*. https://doi.org/10.1016/j.biotechadv.2004.09.005

Waigh, T. A., Hopkinson, I., Donald, A. M., Butler, M. F., Heidelbach, F., & Riekel, C. (1997). Analysis of the Native Structure of Starch Granules with X-ray Microfocus Diffraction. *Macromolecules*, *30*(13), 3813–3820. https://doi.org/10.1021/ma970075w

Wang, S., & Copeland, L. (2013). Molecular disassembly of starch granules during gelatinization and its effect on starch digestibility: A review. *Food and Function*. https://doi.org/10.1039/c3fo60258c

Wee, M. S. M., Loud, D. E., Tan, V. W. K., & Forde, C. G. (2019). Physical and sensory characterisation of noodles with added native and denatured pea protein isolate. *Food Chemistry*, *294*, 152–159. https://doi.org/10.1016/j.foodchem.2019.05.042

Yang, J., & Powers, J. R. (2016). Effects of High Pressure on Food Proteins. In V. M. Balasubramaniam, G. V Barbosa-Cánovas, & H. L. M. Lelieveld (Eds.), *High Pressure Processing of Food: Principles, Technology and Applications* (pp. 353–389). New York, NY: Springer New York. https://doi.org/10.1007/978-1-4939-3234-4_18

Yang, Z., Chaib, S., Gu, Q., & Hemar, Y. (2017). Impact of pressure on physicochemical properties of starch dispersions. *Food Hydrocolloids*, *68*, 164–177. https://doi.org/10.1016/j.foodhyd.2016.08.032

Zeng, F., Li, T., Gao, Q., Liu, B., & Yu, S. (2018). Physicochemical properties and in vitro digestibility of high hydrostatic pressure treated waxy rice starch. *International Journal of Biological Macromolecules*, *120*, 1030–1038. https://doi.org/10.1016/J.IJBIOMAC.2018.08.121

Zhou, Z., Ren, X., Wang, F., Li, J., Si, X., Cao, R., … Blanchard, C. (2015). High pressure processing manipulated buckwheat antioxidant activity, anti-adipogenic properties and starch digestibility. *Journal of Cereal Science*, *66*, 31–36. https://doi.org/10.1016/j.jcs.2015.09.002

CHAPTER TWO

HIGH PRESSURE STRUCTURING OF PEA PROTEIN CONCENTRATES

2.1 ABSTRACT

This work demonstrates the use of high pressure processing (HPP) to induce structural modifications in pea protein concentrates (PPC). Reconstituted PPC with 8-24 g protein /100 g water were subjected to HPP at 250-550 MPa for 15 min, at 20-33 °C, or heat treatments at 95 °C for 15 min. Structural changes were investigated using dynamic rheology, scanning electron microscopy, differential scanning calorimetry, and mid-infrared spectroscopy. Gel formation occurred at 16 g protein /100 g water concentration and 250 MPa for the HPP-treated samples, and at 12 g protein /100 g water concentration for the heat-treated samples. Gel strength increased with both pressure level and protein concentration. Heat-treated samples exhibited greater gel strength than pressure-treated samples at the same protein concentration. A greater extent of protein denaturation, aggregation and network formation occurred with increasing pressure level, due to protein tertiary and quaternary conformation changes. Starch granules present in PPC retained their structure and were not gelatinized even at 550 MPa. These findings can be used to create novel pea protein products with interesting structures and superior sensory and nutritional properties.

2.2 INTRODUCTION

As the demand for protein is increasing (Mintel, 2013), pulse proteins are increasingly explored for the development of high protein foods. Pulses, including peas, chickpeas, lentils, and beans, contain about twice as much protein as whole grain cereals, are relatively

inexpensive crops to grow, have a low water footprint compared with other protein sources, and also are not major allergens (Boye, Zare, & Pletch, 2010; FAO, 2016). Among pulses, peas (*Pisum sativum L.)* account for about a quarter of all pulses produced worldwide, and the pea protein market is expected to reach $313.5 million by 2025 (Grand View Research, 2017). Commercially available pea protein ingredients include protein isolates, made using isoelectric precipitation, and protein concentrates, obtained by air classification. While the protein content of pea protein isolates can reach 80-90%, their functionality is affected by the harsh processing conditions used (Pelgrom, Vissers, Boom, & Schutyser, 2013). By comparison, pea protein concentrates have a lower protein content (50-60%), but retain a high proportion of the native structure and functional properties of the proteins (Boye et al., 2010).

In many cases, processing of pea protein ingredients involves a thermal treatment step, which can lead to the formation of a gel structure if the protein concentration is above a minimum level (Shand, Ya, Pietrasik, & Wanasundara, 2007; Sun & Arntfield, 2010). Other methods used to obtain pea-based gels include enzymatic treatments (Djoullah, Husson, & Saurel, 2017) and acid-induced gelation (Mession, Chihi, Sok, & Saurel, 2015). During the heat denaturation of pea proteins, a pronounced "cooked" flavor is formed (Malcolmson et al., 2014), which is undesirable to many consumers. Hence, a non-heat-based method of processing that can result in a gel structure, without the unpleasant, strong flavors specific to heat-treated pea products, may be key to expanding the range of pea-based products and their consumption. A processing method suitable for this purpose is high pressure processing (HPP).

HPP, a nonthermal processing method primarily used for microbial inactivation, was shown to disrupt non-covalent interactions and cause structural changes in proteins

(Balasubramaniam, Martínez-Monteagudo, & Gupta, 2015; Cadesky, Walkling-Ribeiro, Kriner, Karwe, & Moraru, 2017). Moderate pressures (50-200 MPa) can reversibly dissociate oligomeric subunits of proteins (Mozhaev, Heremans, Frank, Masson, & Balny, 1996), while pressures above 300 MPa can cause irreversible denaturation of globular proteins (Balny & Masson, 1993). Pressure-induced gelation of the denatured proteins was shown to occur above a minimum protein concentration, which varies with the pressure level and the source of protein (Queirós, Saraiva, & da Silva, 2017; Yang & Powers, 2016). Such pressure-induced protein gels can be used to make novel high protein foods with superior sensory and nutritional properties compared to heat-treated products. Due to the microbial inactivation effect of HPP, such products could also have built-in safety and extended microbiological shelf-life. To date, there is no published information on pressure-induced gelation of pea proteins. To address this gap, the goal of this work was to evaluate the pressure-induced structural changes in pea protein concentrates (PPC), and to investigate the effect of pressure level and protein concentration on these changes.

2.3 MATERIALS AND METHODS

Materials

Commercial pea protein concentrate (PPC) obtained by air classification (Pea Protein 55, AGT Foods, Regina, SK, Canada) was used as a source of pea protein. Pea protein isolate was not used, as preliminary investigation using differential scanning calorimetry found that the proteins were denatured. The composition of PPC powder, determined at Dairy One Laboratories (Ithaca, NY), was: 54.5 g/100 g (dry weight) protein, 4.3 g/100 g (dry weight) starch, 2.8 g/100 g (dry weight) fat, 6.7 g/100 g (dry weight) ash, and 7.2 g/100 g moisture.

Sample Preparation

Five protein concentrations (8, 12, 16, 20 and 24 g protein / 100 g water) were chosen to represent a wide range of protein concentrations. The 8 g/100 g concentration was below the critical pea protein concentration for thermal gelation (Withana-Gamage, Wanasundara, Pietrasik, & Shand, 2011), while the 24 g/100 g concentration was close to the solubility limit of the PPC powder. To uniformly hydrate the proteins, a bulk 24 g/100 g protein solution was first made, then diluted to obtain the target protein concentrations.

To prepare the bulk protein solution, PPC powder was added to Milli-Q water with stirring at 1,200 rpm for 15 min at 25 °C. The solution was then cooled in an ice bath with continued stirring for 15 min. To ensure good dispersion of proteins, the solution was subsequently high-shear mixed at 18,000 rpm for 7.5 min in an ice bath, using a high shear mixer (UltraTurrax Model T25 fitted with a S25N-18G dispersion tool, IKA Works Inc., Wilmington, NC), ensuring that the solution did not exceed 26 °C. The solution was then stirred at 500 rpm for 15 min at 25 °C. To obtain the targeted protein concentrations, different proportions of bulk protein solution and Milli-Q water were weighed and mixed with stirring at 700 rpm for 15 min at 25 °C. The pH of the protein solutions was ~ 6.0. Finally, the protein solutions were filled in pre-cut storage bags (FoodSaver Vacuum-Seal Roll, Sunbeam Products Inc., Boca Raton, FL) and vacuum sealed. The packaged PPC samples were stored overnight at 4 °C before HPP treatment.

HPP Treatment

The protein samples were high pressure processed using a vertical 10 L HPP unit (Elmhurst Research Inc., Albany, NY) located at Rutgers University (New Brunswick, NJ). Samples were subjected to pressure treatments at 250, 350, 450 and 550 MPa, for a 15 min

hold time. The processing parameters (temperature and pressurization rates) are shown in Table 2.1. The 15 min hold time for the pressure treatments was based on previous work conducted on the same unit (Cadesky et al., 2017). The HPP-treated samples were stored at 4 °C to minimize microbial activity and analyzed within 48 h. Some of the 550 MPa pressure treatments were repeated using a 55 L HPP unit (Hiperbaric, Spain) at Cornell University (Geneva, NY). These samples were only used for generating additional replicates for differential scanning calorimetry analyses.

Table 2.1. Temperature and pressure data for the pressure treatments. The HPP treatments were conducted using a vertical 10 L HPP unit (Elmhurst Research Inc., Albany, NY), in triplicate.

Treatment pressure (MPa)	Initial temperature (°C)	Maximum temperature (°C)	Maximum pressure (MPa)	Pressurization rate (MPa/s)	Depressurization rate (MPa/s)
250	20.6 ± 2.1	26.8 ± 2.4	259.4 ± 0.2	2.8 ± 0.1	52.3 ± 0.2
350	21.4 ± 1.5	29.8 ± 1.9	356.7 ± 0.8	3.0 ± 0.1	71.1 ± 0.2
450	20.7 ± 1.5	31.8 ± 1.7	459.5 ± 0.9	3.2 ± 0.1	90.5 ± 0.2
550	19.8 ± 0.8	33.1 ± 0.9	556.7 ± 1.3	3.4 ± 0.1	110.9 ± 1.4

Heat Treatment

For comparison purposes, heat-treated pea protein gels were also obtained by immersing packaged PPC samples in a water bath at 95 °C for 15 min. These heat treatment conditions were selected based on previous reports. Shand, Ya, Pietrasik, & Wanasundara (2007) and Sun & Arntfield (2010) found that heating at 95 °C was sufficient to fully denature pea proteins. The 15 min heating time allowed for complete structural transformation of the sample, under the conditions used in this study. The heat-treated samples were immediately

cooled in an ice bath for 15 min, then stored at 4 °C and analyzed within 48 h.

Rheological Analyses

Dynamic rheological testing of the HPP and heat-treated protein samples was conducted using an ARES strain-controlled rheometer (TA Instruments, New Castle, DE). For samples of softer consistency, a 50 mm diameter Teflon parallel plate with an interplaten gap of 1 mm was used. Two mL aliquots of the protein sample were loaded onto the lower plate, with care taken to avoid air bubble formation. For stronger gel samples, a 25 mm diameter Teflon parallel plate with an interplaten gap of 2 mm was used. The gels were sliced 2 mm thick and placed between the plates. All measurements were performed at 25 °C, maintained using a Peltier temperature control system. An isothermal chamber enclosed the parallel plates to minimize sample dehydration during measurements. The samples were subjected to a 1 min relaxation step before measurement.

Dynamic strain sweeps were first conducted for each sample to identify the linear viscoelastic region (LVR), at a frequency of 1 rad/s. Frequency sweeps were then performed at a strain value within the LVR, over the frequency range 0.1-100 rad/s. The storage modulus (G'), loss modulus (G"), and loss tangent (tan δ = G"/G') were recorded. All measurements were performed in triplicate, except for 250, 350 and 450 MPa pressure treatments of 8 g/100 g PPC solutions, for which single measurements were made. These intermediate pressures were only evaluated once, because for 8 g/100 g PPC concentration no significant differences in G' were observed between untreated and pressure-treated samples up to 550 MPa. Also, no rheological measurements were conducted for heat-treated 8 g/ 100 g PPC, due to the inhomogeneous structure of the sample.

Microstructural Analyses by Scanning Electron Microscopy (SEM)

Small amounts of untreated and pressure-treated (250 MPa and 550 MPa) PPC samples of 16 g/100 g and 24 g/100 g concentrations, and heat-treated PPC samples of 24 g/100 g concentration were deposited onto clean glass slides and air dried for 40 min. Thin cross-sections were used for strong gel samples. Samples were fixated with 2.5% (w/v) glutaraldehyde in 0.05 M sodium cacodylate buffer for 2 h, and washed three times for 5 min each with the cacodylate buffer. A secondary fixation was done using 1% (w/v) osmium tetroxide in cacodylate buffer for 1 h, and samples washed three times in the cacodylate buffer. Samples were then dehydrated using graded ethanol solutions in the order 25%, 50%, 70%, 95% (v/v) and three times with 100% (v/v) for 10 min each, followed by critical point drying using carbon dioxide. Dried surfaces were mounted on SEM stubs with carbon tape, then thinly coated with a gold/palladium alloy. A Zeiss LEO 1550 field emission scanning electron microscope (Carl Zeiss Microscopy LLC, Jena, Germany) was used for imaging at 3 kV. Images were acquired using the SmartSEM® software accompanying the instrument.

Differential Scanning Calorimetry

Thermograms of untreated, HPP and heat-treated 24 g/100 g PPC samples were obtained using a differential scanning calorimeter (DSC Model Q1000, TA Instruments, New Castle, DE), calibrated using indium and sapphire standards. PPC samples were weighed into DSC aluminum pans, which were then hermetically sealed and scanned between 15 °C and 110 °C, at a heating rate of 1 °C/min. An empty hermetically sealed aluminum pan was used as reference. The onset temperature (T_o), peak temperature (T_d), end temperature (T_{end}), and the enthalpy (ΔH) of thermal transitions were calculated by manual peak integration using the equipment software (TA Instruments, New Castle, DE).). All DSC measurements were

performed in duplicate.

Protein Secondary Structure Analyses by Fourier Transformed Infrared Spectroscopy

The protein secondary structure of untreated, HPP and heat-treated 24 g/100 g PPC solutions were evaluated using attenuated total reflectance Fourier transformed infrared spectroscopy. The data was collected using a Fourier Transform Infrared Spectrophotometer (IRAffinity-1S, Shimadzu Corp., Kyoto, Japan), equipped with a Quest ATR Diamond Accessory (Specac Inc., Swedesboro, NJ), and analyzed using the Lab Solutions IR integrated software. Spectra of Milli-Q water and the PPC solutions were collected in absorbance mode, with Happ-Genzel apodization. For each sample, an average of 128 scans were recorded at a high-resolution setting of 1.0 cm^{-1} in the range of 400 cm^{-1} to 4,000 cm^{-1}, with background subtraction. Final PPC spectral data were corrected by subtracting the infrared spectrum of Milli-Q water measured on the same day, under identical conditions. Deconvolution of the spectra was unnecessary, due to the high resolution used. Manual peak integration and the peak areas were calculated using Origin 9 software (OriginLab Corp., Northampton, MA). All measurements were performed in triplicate.

Statistical Analyses

Data was analyzed using R v. 3.2.2 (R Foundation for Statistical Computing, Vienna, Austria). A one-way analysis of variance (ANOVA) was conducted to determine if the mean values of measured parameters differed significantly as a function of pea protein concentration and treatment. The significance was established using Tukey HSD or Dunnett's post-hoc tests. A probability level of $p < 0.05$ was considered significant. All values are expressed as means ± 1 standard deviation.

2.4 RESULTS

Establishing the HPP Holding Time

To establish the HPP hold time, pressurization hold times from 5 min to 20 min at a pressure of 550 MPa were first tested, using a PPC solution of 24 g/100 g concentration. All samples formed gels after the HPP treatment, and showed a solid like behavior, with G' > G" over the entire frequency range (Figure 2.1a). The gel strength was generally higher for longer hold times compared to shorter hold times, although G' did not increase linearly with hold time. The value of the storage modulus at a frequency of 1 rad/s (G'_{1rad}) was selected as a quantitative parameter to compare the different treatments. The 15 min hold time gave the highest G'_{1rad} (Figure 2.1b), indicating that the largest extent of structure formation occurred at this hold time. Therefore, all subsequent pressure treatments were therefore conducted using a 15 min hold time.

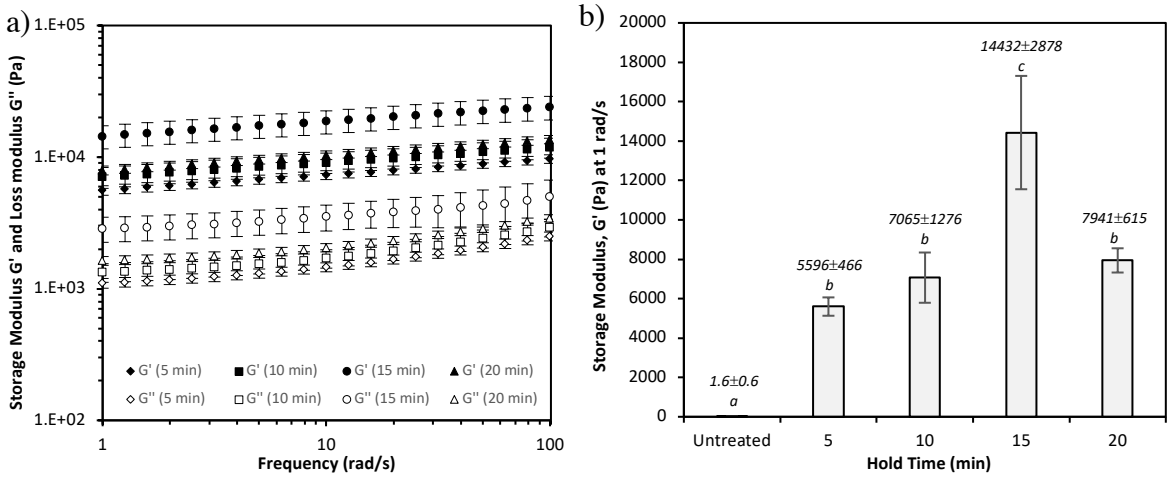

Figure 2.1. The effect of HPP hold time on rheological properties of 24 g/100 g concentration PPC solutions treated at 550 MPa for different hold times. **(a)** Frequency sweeps (G' and G'' vs. frequency); **(b)** Storage modulus at 1 rad/s ($G'_{1rad/s}$). Values represent averages of three processing replicates, and error bars represent 1 standard deviation. Values connected by the same letter are not significantly different from each other ($p>0.05$).

Visual and Microstructural Observations of HPP and Heat-Treated PPC

Samples treated by HPP were examined visually and by SEM. Figure 2.2 shows photographs of the variety of structures (from soft gels to hard gels) that were obtained after HPP treatment. SEM images of untreated, pressure-treated, and heat-treated 24 g/100 g concentration PPC samples are shown in Figure 2.3. Generally, HPP treatment resulted in a network structure made up by fibrillar aggregates. A thicker and more defined structure was observed for the 550 MPa treatments compared to 250 MPa, suggesting a greater extent of protein aggregation and network formation at the higher pressure. The voids between the network fibrils were possibly formed as a result of the expansion of the entire structure when pressure was released. By comparison, the heat-treated samples had a denser and more homogeneous network structure than the pressure-treated samples. The 16 g/100 g concentration PPC sample pressure-treated at 550 MPa (Figure 2.4) had a less organized structure compared to the 24 g/100 g concentration PPC sample treated at 550 MPa (Figure 2.3), probably due to the lower amount of protein available for network formation. It should be noted that for this particular sample intact starch granules embedded in the protein network were occasionally observed.

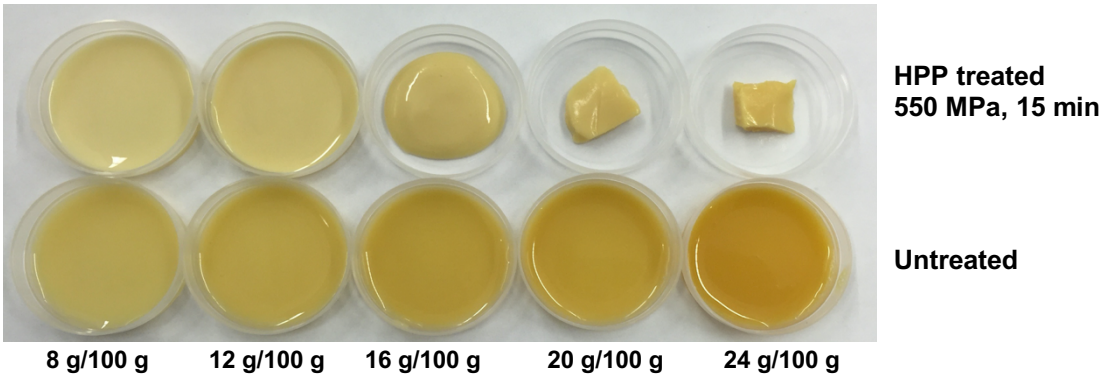

Figure 2.2. Visual appearance of PPC samples of different concentrations treated at 550 MPa for 15 min.

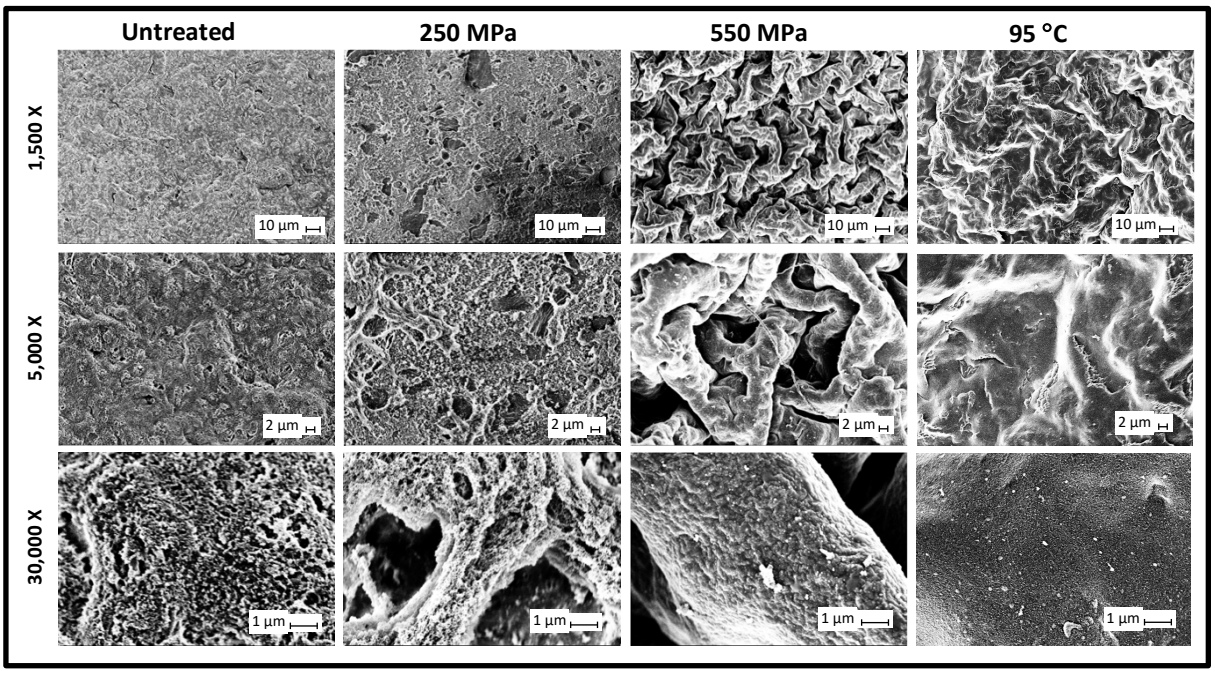

Figure 2.3. SEM micrographs of untreated, pressure-treated and heat-treated PPC solutions of 24 g/100 g concentration. A greater extent of aggregation and network formation is observed after treatment at higher pressures.

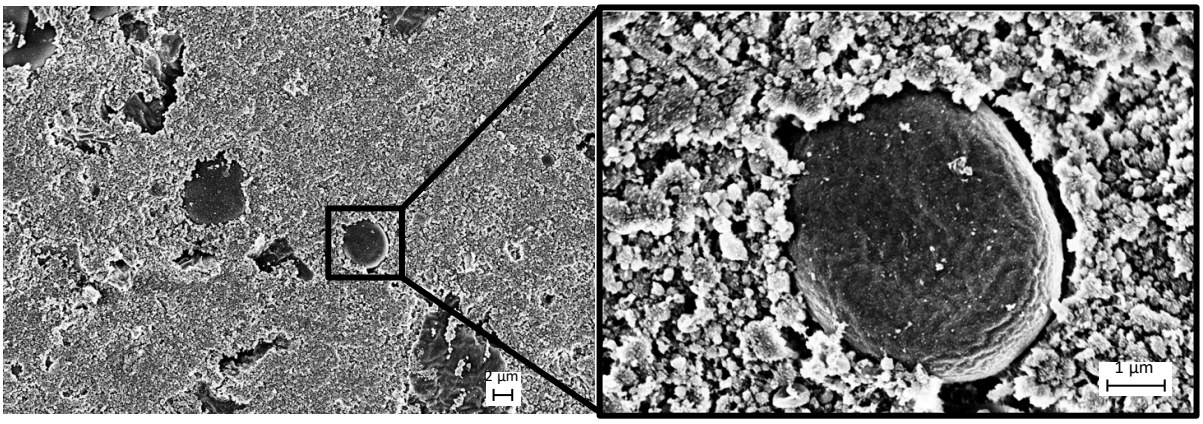

Figure 2.4. SEM micrographs of 16 g/100 g concentration PPC solutions pressure-treated at 550 MPa for 15 min. The spherical particles represent starch granules embedded in the protein-dominated gel network, which remained intact after the pressure treatment.

Effect of HPP and Heat Treatments on the Rheological Properties of PPC

The frequency sweeps of untreated, pressure-treated, and heat-treated PPC samples (Figure 2.5) showed that G' > G" for all samples investigated in this study, except for the untreated samples at frequencies above 10 rad/s, for which G' ~ G". Therefore, G' was considered the prevailing modulus for all samples. To make direct comparisons between the rheological properties of the different samples, two parameters were used: $G'_{1rad/s}$ and the frequency dependence parameter *m*, determined as the slope of the log(G') vs. log(frequency) curve.

There were no significant differences in $G'_{1rad/s}$ among untreated samples of different protein concentrations (Figure 2.6). The untreated samples had tan δ values ranging from 0.6-2.0, and frequency parameter *m* values between 0.33-0.40 (Figure 2.7). These values are indicative of a weakly associated concentrated dispersion (Beliciu & Moraru, 2013). There were also no significant differences in $G'_{1rad/s}$ between untreated and HPP-treated samples of 8 g/100 g and 12 g/100 g concentration. For these concentrations, tan δ decreased from 0.6-2.0 for the untreated samples, to 0.4-1.3 for the HPP-treated samples. The frequency parameter *m* also decreased from 0.33-0.34 for the untreated samples, to 0.24-0.31 for the HPP-treated samples. This demonstrates an increase in the solid-like character of the samples after HPP treatment, likely due to enhanced intermolecular interactions in the protein matrix.

$G'_{1rad/s}$ values increased by nearly 2 orders of magnitude after HPP treatment of the 16 g/100 g concentration samples (Figure 2.6). For the 20 g/100 g and 24 g/100 g samples pressure-treated at 350 MPa and above, there was a significant increase by up to four orders of magnitude in $G'_{1rad/s}$ compared to the untreated samples. For the 16 g/100 g, 20 g/100 g and 24 g/100 g samples, HPP treatment at 250 MPa led to tan δ between 0.2-0.7 and *m* values

between 0.17-0.19, which are indicative of a weak gel-like structure, while HPP treatments at 350 MPa and above resulted in smaller tan δ (between 0.2-0.3) and *m* (~ 0.1), which are characteristic of strong gels (Steffe, 1996). This data suggests that gelation occurred at 16 g/100 g concentration and 250 MPa. This minimum protein concentration for gel formation is similar to values reported elsewhere (14-16 g/100 g) for heat-treated pea protein isolate (O'Kane, Vereijken, Gruppen, & Boekel, 2005; Withana-Gamage et al., 2011). Overall, gel strength increased with pressure and protein concentration. In this study, gel formation in the heat-treated samples occurred at a lower protein concentration, of 12 g/100 g. The heat-treated samples formed a stronger network than the pressure-treated samples of the same concentration, as evidenced by the higher $G'_{1rad/s}$ (Figure 2.6), lower tan δ (~0.2), and lower *m* (~ 0.1) values (Figure 2.7).

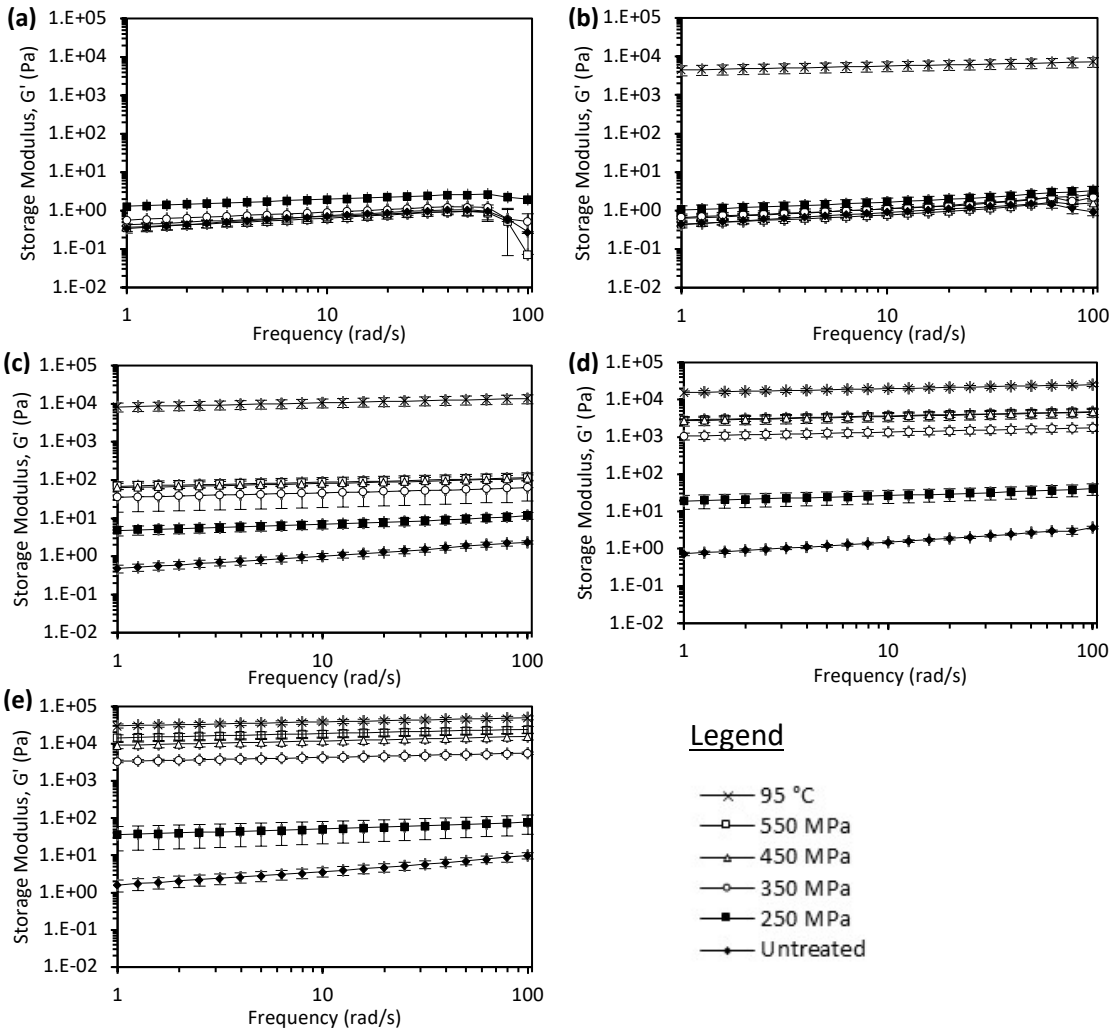

Figure 2.5. Frequency sweeps (G' vs frequency) for untreated, pressure treated, and heat treated PPC solutions of **(a)** 8 g/100 g, **(b)** 12 g/100 g, **(c)** 16 g/100 g, **(d)** 20 g/100 g, and **(e)** 24 g/100 g protein concentration. Error bars represent 1 standard deviation (n=3).

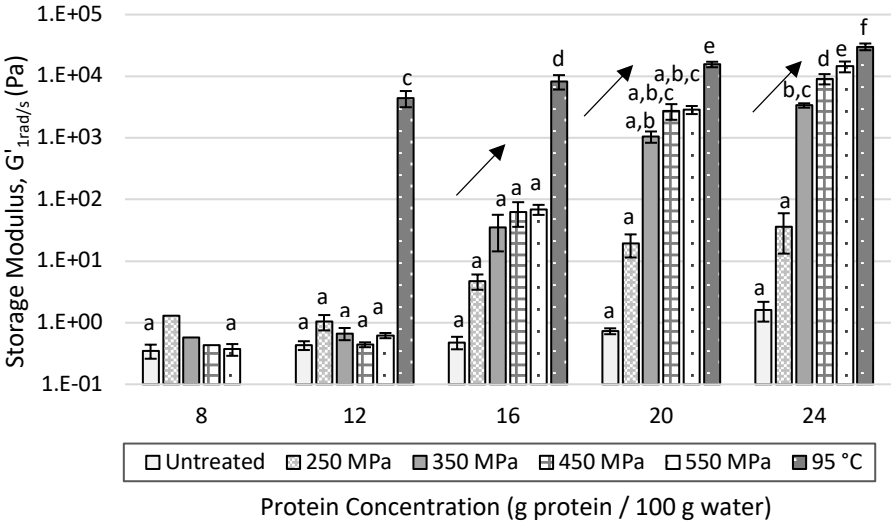

Figure 2.6. Storage modulus at 1 rad/s ($G'_{1rad/s}$) for untreated, pressure-treated and heat-treated PPC solutions. Error bars represent 1 standard deviation (n=3). Data points connected by the same letter are not significantly different from each other ($p>0.05$). *Note: only single data points exist for the 250, 350 and 450 MPa treatments of 8 g/100 g samples; these data points were not included in the statistical analyses.*

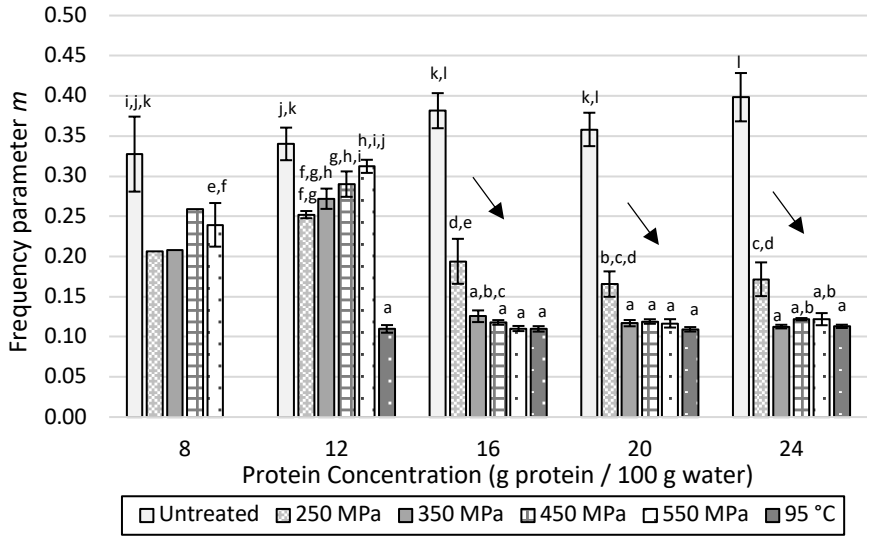

Figure 2.7. Frequency dependence parameter *m* of untreated, pressure-treated, and heat-treated PPC solutions. Error bars represent 1 standard deviation (n=3). Bars with the same letter are not significantly different from each other ($p>0.05$). *Note: only single data points exist for the 250, 350 and 450 MPa treatments of 8 g/100 g samples; these data points were not included in the statistical analyses.*

Evaluation of Thermal Transitions in PPC samples

DSC analyses was conducted for the untreated, pressure-treated and heat-treated 24 g/100 g PPC samples, to investigate the conformational changes that occurred in the protein samples as a result of the pressure and heat treatment. The DSC thermograms are shown in Figure 2.8, and the characteristic temperatures (onset, peak, and end) and enthalpy of the identified thermal transitions are summarized in Table 2.2.

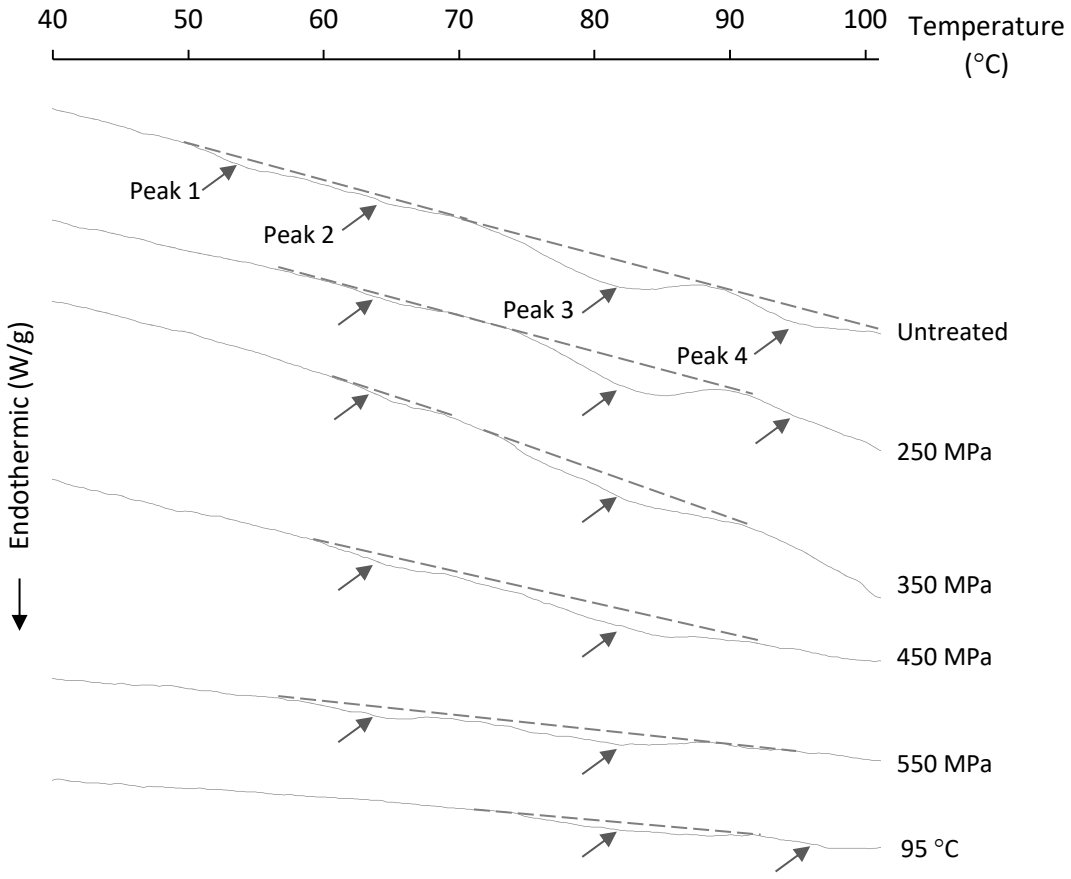

Figure 2.8. DSC thermograms for untreated, pressure-treated, and heat-treated PPC of 24 g/100 g protein concentration. A greater extent of protein denaturation occurred with increasing pressure.

Four major peaks were observed in the untreated PPC sample. Peak 1 (T_{peak} ~ 54 °C) was attributed to the melting of endogenous lipid crystals, Peak 2 (T_{peak} ~ 66 °C) corresponds to the gelatinization of pea starch (Ratnayake, Hoover, Shahidi, Perera, & Jane, 2001), Peak 3 (T_{peak} ~ 82 °C) corresponds to protein denaturation (Shand et al., 2007), and Peak 4 (T_{peak} ~ 96 °C) to the dissociation of amylose-lipid complexes formed during starch gelatinization, between leached amylose and the endogenous lipids (Eliasson, 1994).

Lipid transition. The lipid crystal melting peak (Peak 1) was not detected in the thermograms for any of the pressure-treated samples. The melting peak was also absent from the thermogram for the heat-treated samples, presumably due to lipid melting during heat treatment.

Starch transition. The enthalpy of starch gelatinization for the untreated samples (1.95 J/g starch) was smaller than values reported for pure pea starch systems (Leite, de Jesus, Schmiele, Tribst, & Cristianini, 2017). The starch gelatinization peak (Peak 2) was not detected on the thermogram for heat-treated samples, which indicates complete starch gelatinization due to the heat treatment. An increase in starch gelatinization enthalpy was observed for all pressure treatments, and the enthalpy values of samples pressure-treated at 350 MPa and higher became significantly greater than the untreated samples.

Protein transition. There was a decrease in protein denaturation enthalpy with increasing pressure level, with the values significantly lower than the untreated sample at 450 MPa. Thermal treatment resulted in an even significantly smaller transition enthalpy for Peak 3. This is due to greater protein denaturation at higher pressure levels and by thermal treatment.

Amylose-lipid transition. The heat treatment (95 °C) and the lowest pressure level (250

MPa) were sufficient only to partially dissociate the amylose-lipid complex (Peak 4), as indicated by the smaller enthalpy of dissociation for these two treatments compared to the untreated samples, but the differences were not statistically significant. The dissociation peak was absent for pressure treatments at 350 MPa and above.

Table 2.2. Parameters of the thermal transitions identified for untreated, pressure-treated, and heat-treated 24 g/100 g concentration PPC solutions. The enthalpy of peak 4 was calculated per gram of starch. The 550 MPa pressure treatments were repeated using a 55 L HPP unit (Hiperbaric, Spain). All measurements were conducted in duplicate. Values connected by the same letter in each column of each peak are not significantly different from each other ($p>0.05$).

Treatment	T_{onset} (°C)	T_{peak} (°C)	T_{end} (°C)	ΔT (°C)	ΔH (J/g component)	Change compared to untreated
Peak 1 (Lipid)						
Untreated	51.23 ± 0.82	53.73 ± 0.63	57.22 ± 1.29	5.98 ± 0.73	5.74 ± 0.95	-
250 MPa	Not Detected	Not Detected	Not Detected	Not Detected	Not Detected	Disappearance
350 MPa	Not Detected	Not Detected	Not Detected	Not Detected	Not Detected	Disappearance
450 MPa	Not Detected	Not Detected	Not Detected	Not Detected	Not Detected	Disappearance
550 MPa	Not Detected	Not Detected	Not Detected	Not Detected	Not Detected	Disappearance
95 °C	Not Detected	Not Detected	Not Detected	Not Detected	Not Detected	Disappearance
Peak 2 (Starch)						
Untreated	63.57 ± 0.18*a*	66.16 ± 1.01*a*	69.18 ± 1.11*a*	5.62 ± 0.97*a*	1.95 ± 0.42*a*	-
250 MPa	63.18 ± 1.19*a*	65.36 ± 0.32*a,b*	69.60 ± 0.18*a*	6.42 ± 1.15*a,b*	3.23 ± 0.62*a,b*	↑
350 MPa	63.21 ± 0.82*a*	65.26 ± 0.32*a,b*	69.38 ± 0.49*a*	6.17 ± 0.70*a*	3.40 ± 0.56*b*	↑
450 MPa	62.47 ± 0.59*a,b*	65.04 ± 0.44*a,b*	69.10 ± 0.72*a*	6.62 ± 0.31*a,b*	3.78 ± 0.67*b*	↑
550 MPa	61.25 ± 1.09*b*	64.62 ± 0.39*b*	69.78 ± 0.81*a*	8.54 ± 1.56*b*	5.22 ± 0.69*c*	↑
95 °C	Not Detected	Not Detected	Not Detected	Not Detected	Not Detected	Disappearance
Peak 3 (Mixed 7S and 11S globulins)						
Untreated	73.94 ± 0.71*a*	81.78 ± 0.51*a*	88.91 ± 0.71*a,b*	14.98 ± 0.28*a*	3.74 ± 0.75*a*	-
250 MPa	75.19 ± 1.29*a*	83.09 ± 0.39*a*	89.49 ± 0.55*a,b*	14.30 ± 1.75*a*	3.70 ± 0.46*a*	↓
350 MPa	74.82 ± 0.93*a*	82.80 ± 0.31*a*	89.97 ± 0.89*a,b*	15.15 ± 1.79*a*	2.86 ± 0.54*a*	↓
450 MPa	75.03 ± 0.92*a*	83.49 ± 0.81*a*	90.08 ± 1.09*a,b*	15.05 ± 1.79*a*	1.34 ± 0.55*b*	↓
550 MPa	74.06 ± 2.68*a*	82.82 ± 1.11*a*	88.74 ± 0.85*a*	14.69 ± 3.20*a*	1.32 ± 0.12*b*	↓
95 °C	78.16 ± 4.39*a*	84.04 ± 2.00*a*	90.91 ± 1.23*b*	12.75 ± 5.39*a*	0.70 ± 0.55*b*	↓
Peak 4 (Amylose-lipid complex)						
Untreated	92.49 ± 2.28*a*	96.12 ± 1.39*a,b*	101.68 ± 2.32*a*	9.19 ± 3.77*a*	14.27 ± 8.07*a*	-
250 MPa	92.73 ± 0.40*a,b*	95.06 ± 1.33*a*	99.84 ± 2.10*a*	7.10 ± 2.49*a*	4.36 ± 4.30*a*	↓
350 MPa	Not Detected	Not Detected	Not Detected	Not Detected	Not Detected	Disappearance
450 MPa	Not Detected	Not Detected	Not Detected	Not Detected	Not Detected	Disappearance
550 MPa	Not Detected	Not Detected	Not Detected	Not Detected	Not Detected	Disappearance
95 °C	95.28 ± 0.19*b*	98.20 ± 0.71*b*	102.75 ± 0.71*a*	7.47 ± 0.57*a*	6.76 ± 1.67*a*	↓

Changes to Protein Secondary Structure in HPP and Heat Treated PPC

The FTIR spectra for untreated, HPP, and heat-treated 24 g/100 g PPC solutions are shown in Figure 2.9. The amide I range of 1600-1700 cm^{-1} was selected for its association with protein secondary structure and the assignment of the component bands was based on previous work (Shevkani, Singh, Kaur, & Rana, 2015; Withana-Gamage et al., 2011). Nineteen bands were observed, and key band centers and relative band areas are summarized in tables 2.3 and 2.4 respectively.

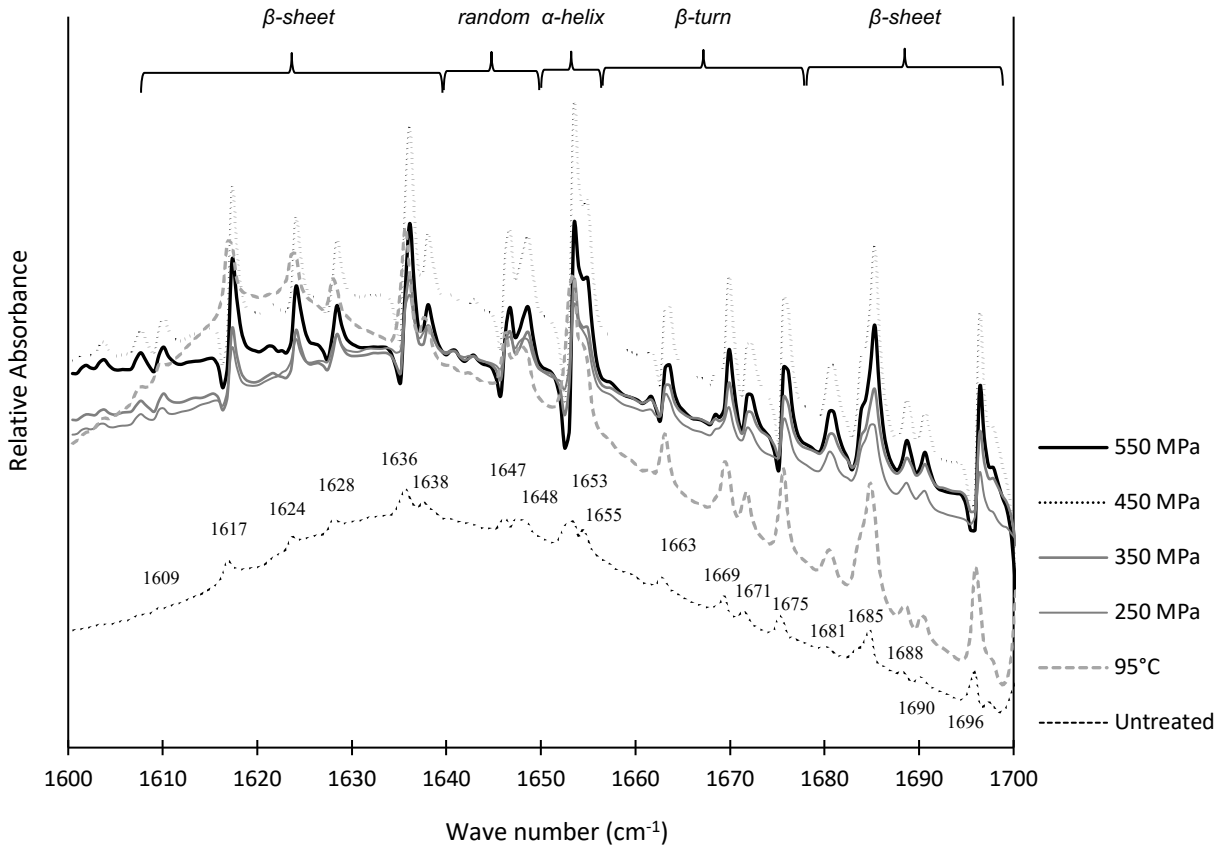

Figure 2.9. Attenuated total reflectance Fourier transform infrared spectra in the amide I region for 24 g/100 g concentration PPC solutions at various treatment conditions. Assignment of spectral regions for various conformations (α-helices, random structures, β-turns and β-sheets) done according to Withana-Gamage et al. (2011), and Shevkani et al. (2015).

There were small but significant increases in the absorption wave number (by ~1 cm^{-1}) for some band centers with pressure treatments (Table 2.3). These bands include shoulder β-sheets (1609, 1617, 1690, 1696 cm^{-1}) that have been associated with aggregation bands (Shevkani et al., 2015). Heat treatment only significantly affected three bands. These small increases (≤ 6 cm^{-1}) indicate weakening intermolecular hydrogen bonds within the secondary structures (Arrondo & Goñi, 1999; Lefèvre & Subirade, 2001). Small shifts in wave number after pressure treatment have also been observed in soy proteins (Tang & Ma, 2009) and milk proteins (Cadesky et al., 2017).

Untreated PPC had about 47 % β-sheets, 8 % random structures, 12 % α-helix and 10 % β-turns (Table 2.4). The proportions of β-sheets and α-helix in untreated pea protein is similar to previous work (Subirade, Gueguen, & Pézolet, 1994). There were however no statistically significant differences in relative band areas between the untreated, pressure or heat-treated samples. Overall, there were no significant changes in protein secondary structures due to pressure and heat treatments.

Table 2.3. Conformations in the protein secondary structure identified based on band centers (cm^{-1}) in attenuated total reflectance Fourier transform infrared spectra of untreated, HPP-treated and heat-treated 24 g/100 g concentration PPC solutions. All measurements were conducted in triplicate. Values labelled with an asterisk (*) in each row are significantly different ($p<0.05$) from the untreated sample, as determined by Dunnett's test.

Assignment	Untreated	250 MPa	350 MPa	450 MPa	550 MPa	95 °C
β-sheet	1609.4 ± 0.3	1610.4 ± 0.6*	1610.1 ± 0.0	1610.1 ± 0.0	1610.4 ± 0.6*	1609.6 ± 0.0
β-sheet	1617.0 ± 0.3	1617.3 ± 0.0*	1617.3 ± 0.0*	1617.3 ± 0.0*	1617.3 ± 0.0*	1616.8 ± 0.0
β-sheet	1637.6 ± 0.0	1638.1 ± 0.0*	1638.1 ± 0.0*	1638.1 ± 0.0*	1637.9 ± 0.3	1637.6 ± 0.0
Random	1647.7 ± 0.7	1648.2 ± 0.0	1648.7 ± 0.0*	1648.7 ± 0.0*	1648.7 ± 0.0*	1648.0 ± 0.3
α-helix	1652.8 ± 0.3	1653.2 ± 0.6	1653.5 ± 0.0	1653.5 ± 0.0	1653.7 ± 0.3*	1653.5 ± 0.0
β-turn	1662.8 ± 0.3	1663.1 ± 0.0	1663.5 ± 0.3*	1663.6 ± 0.0*	1663.5 ± 0.3*	1663.1 ± 0.0
β-turn	1669.4 ± 0.0	1669.9 ± 0.0*	1669.9 ± 0.0*	1669.9 ± 0.0*	1669.9 ± 0.0*	1669.4 ± 0.0
β-turn	1671.3 ± 0.0	1671.8 ± 0.0*	1672.0 ± 0.3*	1672.1 ± 0.3*	1672.0 ± 0.3*	1671.8 ± 0.0*
β-turn	1675.2 ± 0.0	1675.7 ± 0.0*	1675.7 ± 0.0*	1675.7 ± 0.0*	1675.8 ± 0.3*	1675.7 ± 0.0*
β-sheet	1684.8 ± 0.0	1685.2 ± 0.3*	1685.3 ± 0.0*	1685.3 ± 0.0*	1685.3 ± 0.0*	1684.8 ± 0.0
β-sheet	1688.2 ± 0.0	1688.7 ± 0.0*	1688.7 ± 0.0*	1688.7 ± 0.0*	1688.7 ± 0.0*	1688.7 ± 0.0*
β-sheet	1690.1 ± 0.0	1690.6 ± 0.0*	1690.8 ± 0.3*	1690.6 ± 0.0*	1690.6 ± 0.0*	1690.5 ± 0.3
β-sheet	1695.8 ± 0.3	1696.2 ± 0.3*	1696.4 ± 0.0*	1696.4 ± 0.0*	1696.4 ± 0.0*	1695.9 ± 0.0

Table 2.4. ATR-FTIR relative peak areas (in %) for 24 g/100 g concentration PPC solutions treated by HPP and heat. All measurements were conducted in triplicate. Values within the same column labeled with the same letter are not significantly different ($p>0.05$) from each other, based on Tukey's test.

Treatment	Relative proportion of secondary structures			
	β-sheet (%)	*Random/disordered (%)*	*α-helix (%)*	*β-turns (%)*
Untreated	46.63 ± 3.23[a]	8.45 ± 3.15[a]	12.02 ± 5.98[a]	9.77 ± 2.07[a]
250 MPa	45.29 ± 5.72[a]	9.15 ± 0.50[a]	14.81 ± 1.52[a]	12.35 ± 1.26[a]
350 MPa	41.24 ± 7.96[a]	7.30 ± 2.28[a]	11.55 ± 1.21[a]	13.70 ± 2.64[a]
450 MPa	40.23 ± 2.98[a]	8.63 ± 1.09[a]	13.44 ± 2.93[a]	11.47 ± 1.01[a]
550 MPa	41.43 ±0.48[a]	6.76 ± 1.78[a]	10.39 ± 1.25[a]	15.11 ± 4.05[a]
95 °C	48.54 ± 0.56[a]	8.99 ± 0.36[a]	17.64 ± 0.40[a]	15.27 ± 0.28[a]

2.5 DISCUSSION

A wide range of structures were obtained by changing protein concentration and applied pressures, from soft gels (G'~10^2 Pa) to strong gels (G'~10^4 Pa). The observed increase in gel strength with pressure can be explained by the structural changes of protein. Protein denaturation, which is required for aggregation and gelation to happen, occurred after pressure treatments. The degree of denaturation increased with pressure, as evidenced by the decrease in protein denaturation enthalpy with increasing pressure levels (Table 2.2). This could be explained by the different protein fractions denaturing at different pressure levels. Pea vicilin (7S) was found to be completely denatured at 240 MPa (Pedrosa & Ferreira, 1994). While there are no current data on how pressure affects pea legumin (11S), the 11S fraction in soy (glycinin) was found to unfold at 350 MPa (Ahmed, Ayad, Ramaswamy, Alli, & Shao, 2007), and a similar behavior can be expected for pea legumin. It is important to note that, according to previous work, the different depressurization rates may also play a role in gel formation (Fertsch, Müller, & Hinrichs, 2003). However, the individual effect of depressurization on gel formation could not be tested with the experimental setup used in this study.

Pressure-treated samples can achieve similar gel strengths to heat-treated samples under certain conditions. For example, heat-treated samples of 12 g/100 g protein concentration had similar gel strength to both 20 g/100 g samples pressure-treated at 550 MPa, and 24 g/100 g samples pressure-treated at 350 MPa. There were however some differences in the gelling behavior between the pressure and heat-treated samples: heat-treated samples had a lower apparent minimum protein concentration for gelation, and the gel strength of the heat-treated samples was greater than the pressure-treated samples at the same

protein concentration. As there was no significant difference in the extent of protein denaturation, as assessed by the enthalpy of denaturation, between the 450 MPa, 550 MPa and the heat-treated samples, other components in PPC could be involved.

One possible component is starch (there is < 2 g starch / 100 g water in the highest (24 g/100 g) protein concentration sample). Starch was affected differently by the two treatments: while the heat treatment resulted in complete starch gelatinization, starch was not gelatinized in the pressure-treated samples even after 550 MPa treatment, a pressure level found to induce total gelatinization of pea starch in the presence of excess water (Leite et al., 2017). The absence of gelatinization for the HPP-treated samples could be due to the limited availability of water for starch gelatinization. As both starch gelatinization and protein denaturation occur simultaneously during pressure treatment, starch and proteins compete for water, since the water holding capacity of the proteins increases after pressure denaturation (Queirós et al., 2017). Leite et al. (2017) also reported that pea starch dispersed in a water deficient environment did not gelatinize at all after HPP treatments. Furthermore, it was reported that high pressures can cause reordering of starch molecules into more crystal-like structures in low water systems (Pei-Ling, Xiao-Song, & Qun, 2010), which could also explain the increase in gelatinization enthalpy with increasing pressure level. Starch granules therefore remained intact (as also seen in Figure 2.4).

On the other hand, as the temperature of PPC solution taken from cold storage increases during heat treatment, starch gelatinization (T_{peak} ~ 66 °C) occurs before protein denaturation (T_{peak} ~ 82 °C), and water is available for starch gelatinization. Starch granules swell during thermal gelatinization, possibly reducing the volume occupied by protein molecules, and leading to an increase in local protein concentration, thus explaining the lower

apparent minimum protein concentration for thermal gelation. Additionally, the swollen starch granules can reinforce the protein gel (Kim & Lee, 1987), resulting in greater gel strength than the pressure-treated samples at the same protein concentration. (Joshi, Aldred, Panozzo, Kasapis, & Adhikari, 2014) also found that the gel strength of heat-treated lentil protein-lentil starch composite gels increased with greater lentil starch fraction. Further investigation is needed to better understand the structuring effects of starch in pressure-treated PPC.

2.6 CONCLUSIONS

The data presents an evaluation of the effect of low temperature pressure treatments on pea protein concentrates, at different pressures and protein levels. Pressure treatments above 250 MPa induced protein denaturation and subsequent gel structure formation. Starch granules did not seem to be affected by the pressure treatment, but the effect of HPP on starch in a mixed system requires further investigation. From a practical perspective, a wide range of structures and textures can be created by controlling the pressure level and protein concentration of HPP-treated pea protein concentrates. This approach can be used to create novel pea-based products, such as puddings or tofu analogs. The low temperature of the treatment will help preserve the sensory and nutritional properties of such products.

2.7 ACKNOWLEDGMENTS

This work was funded by the USDA-NIFA grant 2016-67017-24635. We acknowledge the use of the DSC and electron microscope at the Cornell Center for Materials Research (CCMR), supported by NSF-MRSEC (DMR 1120296). We would like to thank

Noopur Gosavi and Sawali Navare from Rutgers University for their assistance with the HPP treatments, Dr. Yifan Cheng from Cornell University for assistance with SEM imaging, and AGT Foods for supplying the PPC powder.

REFERENCES

Ahmed, J., Ayad, A., Ramaswamy, H. S., Alli, I., & Shao, Y. (2007). Dynamic Viscoelastic Behavior of High Pressure Treated Soybean Protein Isolate Dispersions. *International Journal of Food Properties*, *10*(2), 397–411. https://doi.org/10.1080/10942910601045313

Arrondo, J. L. R., & Goñi, F. M. (1999, November 1). Structure and dynamics of membrane proteins as studied by infrared spectroscopy. *Progress in Biophysics and Molecular Biology*. Pergamon. https://doi.org/10.1016/S0079-6107(99)00007-3

Balasubramaniam, V. M. (Bala), Martínez-Monteagudo, S. I., & Gupta, R. (2015). Principles and Application of High Pressure–Based Technologies in the Food Industry. *Annual Review of Food Science and Technology*, *6*(1), 435–462. https://doi.org/10.1146/annurev-food-022814-015539

Balny, C., & Masson, P. (1993). Effects of high pressure on proteins. *Food Reviews International*, *9*(4), 611–628. https://doi.org/10.1080/87559129309540980

Beliciu, C. M., & Moraru, C. I. (2013). Physico-chemical changes in heat treated micellar casein - Soy protein mixtures. *LWT - Food Science and Technology*, *54*(2), 469–476. https://doi.org/10.1016/j.lwt.2013.06.013

Boye, J., Zare, F., & Pletch, A. (2010). Pulse proteins: Processing, characterization, functional properties and applications in food and feed. *Food Research International*, *43*(2), 414–431. https://doi.org/10.1016/j.foodres.2009.09.003

Cadesky, L., Walkling-Ribeiro, M., Kriner, K. T., Karwe, M. V., & Moraru, C. I. (2017). Structural changes induced by high-pressure processing in micellar casein and milk protein concentrates. *Journal of Dairy Science*, *100*(9), 7055–7070. https://doi.org/10.3168/jds.2016-12072

Djoullah, A., Husson, F., & Saurel, R. (2017). Gelation behaviors of denaturated pea albumin and globulin fractions during transglutaminase treatment. *Food Hydrocolloids*. https://doi.org/10.1016/J.FOODHYD.2017.11.005

Eliasson, A. C. (1994). Interactions between starch and lipids studied by DSC. *Thermochimica Acta*, *246*(2), 343–356. https://doi.org/10.1016/0040-6031(94)80101-0

FAO. (2016). Pulses are praised for their health, environmental and economic benefits. How can their full potential be tapped? | Global Forum on Food Security and Nutrition (FSN Forum). Retrieved November 16, 2017, from http://www.fao.org/fsnforum/activities/discussions/pulses

Fertsch, B., Müller, M., & Hinrichs, J. (2003). Firmness of pressure-induced casein and whey protein gels modulated by holding time and rate of pressure release. *Innovative Food Science and Emerging Technologies*, *4*(2), 143–150. https://doi.org/10.1016/S1466-8564(03)00008-0

Grand View Research. (2017). Pea Protein Market Size Worth $313.5 Million By 2025 | CAGR: 17.4%. Retrieved November 16, 2017, from

http://www.grandviewresearch.com/press-release/global-pea-proteins-market
Joshi, M., Aldred, P., Panozzo, J. F., Kasapis, S., & Adhikari, B. (2014). Rheological and microstructural characteristics of lentil starch-lentil protein composite pastes and gels. *Food Hydrocolloids*, *35*, 226–237. https://doi.org/10.1016/j.foodhyd.2013.05.016
Kim, J. M., & Lee, C. M. (1987). Effect of Starch of Textural Properties of Surimi Gel. *Journal of Food Science*, *52*(3), 722–725. https://doi.org/10.1111/j.1365-2621.1987.tb06711.x
Lefèvre, T., & Subirade, M. (2001). Molecular structure and interaction of biopolymers as viewed by Fourier transform infrared spectroscopy: model studies on β-lactoglobulin. *Food Hydrocolloids*, *15*(4–6), 365–376. https://doi.org/10.1016/S0268-005X(01)00056-X
Leite, T. S., de Jesus, A. L. T., Schmiele, M., Tribst, A. A. L., & Cristianini, M. (2017). High pressure processing (HPP) of pea starch: Effect on the gelatinization properties. *LWT - Food Science and Technology*, *76*, 361–369. https://doi.org/10.1016/j.lwt.2016.07.036
Malcolmson, L., Frohlich, P., Boux, G., Bellido, A.-S., Boye, J., & Warkentin, T. D. (2014). Aroma and flavour properties of Saskatchewan grown field peas (Pisum sativum L.). *Canadian Journal of Plant Science*, *94*(8), 1419–1426. https://doi.org/10.4141/cjps-2014-120
Mession, J.-L., Chihi, M. L., Sok, N., & Saurel, R. (2015). Effect of globular pea proteins fractionation on their heat-induced aggregation and acid cold-set gelation. *Food Hydrocolloids*, *46*, 233–243. https://doi.org/10.1016/J.FOODHYD.2014.11.025
Mintel. (2013). US consumers have a healthy appetite for high protein food. The US leads the way in global launches of high protein products | Mintel.com. Retrieved November 16, 2017, from http://www.mintel.com/press-centre/food-and-drink/us-consumers-have-a-healthy-appetite-for-high-protein-food-the-us-leads-the-way-in-global-launches-of-high-protein-products
Mozhaev, V. V, Heremans, K., Frank, J., Masson, P., & Balny, C. (1996). High pressure effects on protein structure and function. *Proteins*, *24*(1), 81–91. https://doi.org/10.1002/(SICI)1097-0134(199601)24:1<81::AID-PROT6>3.0.CO;2-R
O'Kane, F. E., Vereijken, J. M., Gruppen, H., & Boekel, M. A. J. S. (2005). Gelation Behavior of Protein Isolates Extracted from 5 Cultivars of Pisum sativum L. *Journal of Food Science*, *70*(2), C132–C137. https://doi.org/10.1111/j.1365-2621.2005.tb07073.x
Pedrosa, C., & Ferreira, S. T. (1994). Deterministic pressure-induced dissociation of vicilin, the 7S storage globulin from pea seeds: effects of pH and cosolvents on oligomer stability. *Biochemistry*, *33*(13), 4046–55. Retrieved from http://www.ncbi.nlm.nih.gov/pubmed/8142407
Pei-Ling, L., Xiao-Song, H., & Qun, S. (2010). Effect of high hydrostatic pressure on starches: A review. *Starch - Stärke*, *62*(12), 615–628. https://doi.org/10.1002/star.201000001
Pelgrom, P. J. M., Vissers, A. M., Boom, R. M., & Schutyser, M. A. I. (2013). Dry

fractionation for production of functional pea protein concentrates. *Food Research International*, *53*(1), 232–239. https://doi.org/10.1016/J.FOODRES.2013.05.004

Queirós, R. P., Saraiva, J. A., & da Silva, J. A. L. (2017). Tailoring structure and technological properties of plant proteins using high hydrostatic pressure. *Critical Reviews in Food Science and Nutrition*, 1–19. https://doi.org/10.1080/10408398.2016.1271770

Ratnayake, W. S., Hoover, R., Shahidi, F., Perera, C., & Jane, J. (2001, August 1). Composition, molecular structure, and physicochemical properties of starches from four field pea (Pisum sativum L.) cultivars. *Food Chemistry*. Elsevier. https://doi.org/10.1016/S0308-8146(01)00124-8

Shand, P. J., Ya, H., Pietrasik, Z., & Wanasundara, P. K. J. P. D. (2007). Physicochemical and textural properties of heat-induced pea protein isolate gels. *Food Chemistry*, *102*(4), 1119–1130. https://doi.org/10.1016/j.foodchem.2006.06.060

Shevkani, K., Singh, N., Kaur, A., & Rana, J. C. (2015). Structural and functional characterization of kidney bean and field pea protein isolates: A comparative study. *Food Hydrocolloids*, *43*, 679–689. https://doi.org/10.1016/j.foodhyd.2014.07.024

Steffe, J. F. (1996). *Rheological methods in food process engineering*. Freeman press.

Subirade, M., Gueguen, J., & Pézolet, M. (1994). Conformational changes upon dissociation of a globular protein from pea: a Fourier transform infrared spectroscopy study. *Biochimica et Biophysica Acta (BBA) - Protein Structure and Molecular Enzymology*, *1205*(2), 239–247. https://doi.org/10.1016/0167-4838(94)90239-9

Sun, X. D., & Arntfield, S. D. (2010). Gelation properties of salt-extracted pea protein induced by heat treatment. *Food Research International*, *43*(2), 509–515. https://doi.org/10.1016/J.FOODRES.2009.09.039

Tang, C.-H., & Ma, C.-Y. (2009). Effect of high pressure treatment on aggregation and structural properties of soy protein isolate. *LWT - Food Science and Technology*, *42*(2), 606–611. https://doi.org/10.1016/j.lwt.2008.07.012

Withana-Gamage, T. S., Wanasundara, J. P., Pietrasik, Z., & Shand, P. J. (2011). Physicochemical, thermal and functional characterisation of protein isolates from Kabuli and Desi chickpea (Cicer arietinum L.): A comparative study with soy (Glycine max) and pea (Pisum sativum L.). *Journal of the Science of Food and Agriculture*, *91*(6), 1022–1031. https://doi.org/10.1002/jsfa.4277

Yang, J., & Powers, J. R. (2016). Effects of High Pressure on Food Proteins. In V. M. Balasubramaniam, G. V Barbosa-Cánovas, & H. L. M. Lelieveld (Eds.), *High Pressure Processing of Food: Principles, Technology and Applications* (pp. 353–389). New York, NY: Springer New York. https://doi.org/10.1007/978-1-4939-3234-4_18

CHAPTER THREE

HIGH PRESSURE PROCESSING OF PEA PROTEIN-STARCH MIXED SYSTEMS: EFFECT OF STARCH ON STRUCTURE FORMATION

3.1 ABSTRACT

This work explores the structural effects of high pressure processing (HPP) on starch in mixed pea protein-starch systems of varying concentrations. Reconstituted pea protein concentrate containing 9 %, 12 %, and 15 % (w/w) protein, without added starch or in combination with 4 % or 8 % (w/w) pea starch, respectively, were subjected to HPP at 600 MPa for 4 min, at 5 °C. Structural changes were investigated using dynamic rheology, scanning electron microscopy, and differential scanning calorimetry (DSC). The addition of starch enabled the formation of weak gels, at protein concentrations below the minimum required for gelation. Above the minimum protein concentration for gelation, starch addition resulted in stronger gels. Starch acted mainly as a filler in the pressure-induced protein gel matrix, and starch granules remained intact after HPP. DSC analyses confirmed that starch remained ungelatinized after HPP, likely due to the limited availability of water in the mixed systems during HPP.

3.2 INTRODUCTION

The food industry is experiencing a growing demand for pulse proteins, due to their perceived health benefits and lower environmental impact of pulse crops (Henchion, Hayes, Mullen, Fenelon, & Tiwari, 2017). To capitalize on this trend, innovative processing methods are being explored to create new food products with interesting structures and textures using

pulse proteins. An example of a suitable processing method is high pressure processing (HPP). HPP, a nonthermal processing method used primarily for microbial inactivation, is able to disrupt non-covalent interactions, leading to protein denaturation and subsequent structural changes (Balasubramaniam, Martínez-Monteagudo, & Gupta, 2015; Cadesky, Walkling-Ribeiro, Kriner, Karwe, & Moraru, 2017). Unique gel structures can be formed above a minimum protein concentration by pressure-induced gelation of the denatured proteins (Queirós, Saraiva, & da Silva, 2017). The structural modifications induced by HPP in pea protein concentrates were demonstrated in Chapter Two. Gel formation occurred from 12 % (w/w) protein concentration and a pressure treatment at 250 MPa, with gel strength increasing with both pressure level and protein concentration. This was due to a greater extent of protein denaturation, aggregation and network formation with increasing pressure levels.

Besides protein, starch is also a major component found in pulses, and pea protein concentrates contain a small amount of starch as well. This is important because HPP can also induce structural modifications in starch (Pei-Ling, Xiao-Song, & Qun, 2010). It has been reported before that in pure starch systems starch granules can be gelatinized by pressure, leading to gel formation (Ahmed, Singh, Ramaswamy, Pandey, & Raghavan, 2014; Leite, de Jesus, Schmiele, Tribst, & Cristianini, 2017). The extent of starch pressure induced gelatinization is influenced by starch type, applied pressure, temperature, hold time, and water content (Yang, Chaib, Gu, & Hemar, 2017). This suggests that starch could be a significant contributor to structure formation in pressure-treated protein gels.

Many food products (e.g. bread, pasta, and surimi) are made from protein-starch mixtures. Understanding how processing affects these mixtures could expand the food structure design toolbox. For example, the textural properties of heat-induced composite

protein-starch gels can be controlled by adjusting protein-starch ratios and temperature in thermally-treated protein-starch mixtures (Joshi, Aldred, Panozzo, Kasapis, & Adhikari, 2014; Li, Yeh, & Fan, 2007). To date, there is little published information on the effect of pressure on starch in mixed protein-starch systems, most of which focus on animal based proteins (Barrios-Peralta, Pérez-Won, Tabilo-Munizaga, & Briones-Labarca, 2012; Oh, Anema, Pinder, & Wong, 2009). In the previous chapter, there was some evidence that starch granules in pea protein concentrates of high protein and low starch concentration were not gelatinized after HPP treatment. Therefore, the objective of this work was to investigate the role of starch in the pressure induced structural changes in pea protein-starch systems of varying protein and starch concentrations.

3.3 MATERIALS AND METHODS

Materials

Pea protein concentrate (PPC) obtained by air classification (Pea Protein 55, AGT Foods, Regina, SK, Canada) was used as a source of pea protein. Pea protein isolate was not used, as preliminary investigation using differential scanning calorimetry found that the proteins were denatured. The composition of PPC powder was: 54.5 % (dry weight) protein, 4.3 % (dry weight) starch, 2.8 % (dry weight) fat, 6.7 % (dry weight) ash, and 7.2 % moisture. Pea starch (PS) was provided by World Food Processing LLC. (Turtle Lake, WI) and contained 0.7 % (dry weight) protein, 94.0 % (dry weight) starch, 0.1 % (dry weight) fat, 0.15 % (dry weight) ash, and 10.7 % moisture. All compositions were determined at Dairy One Laboratories (Ithaca, NY).

Sample Preparation

Three protein concentrations of 9, 12, and 15 % (w/w) were chosen to represent different structuring behavior. The minimum pea protein concentration for pressure gelation as determined by previous work was 12 %, while 15 % was close to the solubility limit of the PPC powder. To each protein concentration, PS was added to give final starch concentrations of 4 or 8 % (w/w). The starch concentrations are comparable to existing protein-starch composite products such as surimi (Hunt, Getty, & Park, 2009). In total, nine formulations (9P, 9P/4S, 9P/8S, 12P, 12P/4S, 12P/8S, 15P, 15P/4S, and 15P/8S) were prepared. An 8 % (w/w) starch-only system, 8S, was made for comparison purposes. In this chapter, the different mixtures will be referred to as *x*P/*y*S with *x* % protein and *y* % starch. *x*P represents the PPC-only system with *x* % protein, which only contain a small amount of starch. The complete composition information for all formulations is shown in Table 3.1.

To prepare the solutions, PPC and/or PS powders were added to Milli-Q water with stirring at 1,200 rpm for 30 min at 25 °C. The solutions were then cooled in an ice bath with continued stirring for 15 min. To achieve good dispersion, the solutions were subsequently high-shear mixed at 18,000 rpm for 7.5 min in an ice bath, using a high shear mixer (UltraTurrax Model T25 fitted with a S25N-18G dispersion tool, IKA Works Inc., Wilmington, NC), ensuring that the solutions did not exceed 25 °C. Finally, the mixed solutions were filled in pre-cut storage bags (FoodSaver Vacuum-Seal Roll, Sunbeam Products Inc., Boca Raton, FL) and vacuum sealed. The packaged samples were stored overnight at 4 °C before HPP treatment.

Table 3.1. The protein and starch percentages in all formulations arranged in decreasing protein-to-starch ratios.

Formulation	% protein (w/w)	% starch (w/w)	Protein-to-starch ratio	% total solids (w/w)
PPC powder	50.6	4.0	12.6	92.8
15P	15.0	1.19	12.6	27.5
12P	12.0	0.95	12.6	22.0
9P	9.0	0.71	12.6	16.5
15P/4S	15.0	4.0	3.8	30.5
12P/4S	12.0	4.0	3.0	25.3
9P/4S	9.0	4.0	2.3	20.0
15P/8S	15.0	8.0	1.9	34.8
12P/8S	12.0	8.0	1.5	29.5
9P/8S	9.0	8.0	1.1	24.3
*Pea Flour**	26.1	47.7	0.6	92.1
8S	< 0.1	8.0	< 0.01	8.5

*Average protein and starch percentages in pea flour according to Chung et al. (2008), shown for comparison purposes.

HPP Treatment

The samples were high pressure processed using a 55 L HPP unit (Hiperbaric, Spain). Samples were subjected to pressure treatment at 600 MPa for a 4 min hold time, which is a typical processing parameter for microbial inactivation used by the food industry. The initial temperature of the pressurizing medium (filtered water) was 5 °C. The HPP-treated samples were stored at 4 °C to minimize microbial activity, and analyzed within 48 h. All processing runs were conducted in triplicate.

Rheological Analyses

Dynamic rheological testing of the samples was conducted using an ARES strain-controlled rheometer (TA Instruments, New Castle, DE). For samples of softer consistency, a 50 mm diameter Teflon parallel plate with an interplaten gap of 1 mm was used. Two mL

aliquots of the protein sample were loaded onto the lower plate, with care taken to avoid air bubble formation. For stronger gel samples, a 25 mm diameter Teflon parallel plate with an interplaten gap of 2 mm was used. The gels were sliced 2 mm thick and placed between the plates.

All measurements were performed at 25 °C, maintained using a Peltier temperature control system. An isothermal chamber enclosed the parallel plates to minimize sample dehydration during measurements. The samples were subjected to a 1 min relaxation step before measurements. Dynamic strain sweeps were first conducted for each sample to identify the linear viscoelastic region (LVR), at a frequency of 1 rad/s. Frequency sweeps were then performed at a strain value within the LVR, over the frequency range 0.1-100 rad/s. The storage modulus (G'), loss modulus (G"), and loss tangent (tan δ = G"/G') were recorded. The storage modulus at 1 rad/s ($G'_{1rad/s}$) and a frequency dependence parameter (*m*) were used to make direct comparisons between samples. *m* is the slope of the log(prevailing modulus) vs. log(frequency) curve. The prevailing modulus was chosen as G' for samples with solid-like behavior and G" for liquid-like behavior. All measurements were performed in triplicate. No rheological measurements were conducted for 8 % starch-only samples due to sedimentation of the untreated sample, and phase separation of the HPP-treated sample.

Microstructural Analyses by Scanning Electron Microscopy (SEM)

Small amounts of untreated and HPP-treated 15P PPC-only and 15P/8S mixed samples, and the solid phase of HPP-treated 8S starch-only sample were deposited onto clean glass slides and air dried for 40 min. Thin cross-sections were used for strong gel samples. Samples were fixated with 2.5 % (w/v) glutaraldehyde in 0.05 M sodium cacodylate buffer for 2 h, and washed three times for 5 min each with the cacodylate buffer. A secondary

fixation was done using 1 % (w/v) osmium tetroxide in cacodylate buffer for 1 h, and samples washed three times in the cacodylate buffer. Samples were then dehydrated using graded ethanol solutions in the order 25 %, 50 %, 70 %, 95 % (v/v) and three times with 100 % (v/v) for 10 min each, followed by critical point drying using carbon dioxide. Dried surfaces were mounted on SEM stubs with carbon tape, then thinly coated with a gold/palladium alloy. A Zeiss LEO 1550 field emission scanning electron microscope (Carl Zeiss Microscopy LLC, Jena, Germany) was used for imaging at 3 kV. Images were acquired using the SmartSEM® software accompanying the instrument.

Differential Scanning Calorimetry

Thermograms of untreated and HPP-treated samples were obtained using a differential scanning calorimeter (DSC Model Q1000, TA Instruments, New Castle, DE), which was calibrated using indium and sapphire standards. A heat-treated (95 °C for 15 min, followed by quenching in an ice bath for 15 min) 8S sample was also measured for comparison. The solid phases of the heat-treated and pressure-treated 8S samples were blended respectively with their liquid phases before measurement, to ensure comparable water content with the untreated sample. Samples were weighed into DSC aluminum pans, which were then hermetically sealed and scanned between 15 °C and 110 °C, at a heating rate of 2 °C/min. An empty hermetically sealed aluminum pan was used as reference. The onset temperature (T_{onset}), peak temperature (T_{peak}), and the enthalpy (ΔH) of thermal transitions were calculated by manual peak integration using the equipment software (TA Instruments, New Castle, DE). Merged peaks were deconvoluted using Origin 9 software (OriginLab Corp., Northampton, MA) with Gaussian curve fitting function (adjusted R^2 values above 0.99). The enthalpy of deconvoluted peaks were calculated from the relative integral area of the fitted curve. All

measurements were performed in triplicate.

Statistical Analyses

Statistical analysis was performed using R v. 3.2.2 (R Foundation for Statistical Computing, Vienna, Austria). A one-way analysis of variance (ANOVA) was conducted to determine if the mean values of measured parameters differed significantly as a function of formulation and treatment. The significance was established using Tukey HSD post-hoc tests. A probability level of $p < 0.05$ was considered significant. All values are expressed as means ± 1 standard deviation.

3.4 RESULTS

Effect of HPP on the Rheological Properties of the PPC-only and Mixed Systems

Figures 3.1 and 3.2 show frequency sweeps of untreated and pressure-treated samples. $\tan \delta < 1$ (hence $G' > G''$) for all samples, except untreated samples at frequencies above 10 rad/s. The rheological behavior of the different samples was evaluated by comparing G' values at 1 rad/s ($G'_{1rad/s}$) and the slope of the G' vs frequency curves (m), respectively.

For the untreated samples, while there were no significant differences among different formulations, $G'_{1rad/s}$ increased with total solids content (Figure 3.3). The untreated samples had tan δ values between 0.5-1.7, and frequency parameter *m* values between 0.31-0.38 (Figure 3.4). These values are indicative of a weakly associated concentrated dispersion (Beliciu & Moraru, 2013). Most untreated samples had a liquid-like behavior, even when starch was added (Figure 3.2). Interestingly, the tan δ values for the 15P/8S mixed samples were smaller than for the other samples, suggesting an increase in the solid-like character, possibly due to lower mobility of the components in the highly concentrated system.

$G'_{1rad/s}$ values increased by up to 3 orders of magnitude for HPP-treated samples compared to untreated samples (Figure 3.3). For each protein concentration, $G'_{1rad/s}$ increased with starch concentration. Gel formation did not occur for the pressure-treated 9P PPC-only samples, as evidenced by tan δ between 0.4-1.0 and no significant decrease in *m* value after HPP treatment, since the protein concentration was below the minimum protein concentration for gelation as shown in Chapter Two. Weak gels were however formed with the addition of starch for the pressure-treated 9P/4S and 9P/8S mixed samples (tan δ between 0.2-0.7 and *m* values of 0.15-0.17 after HPP treatment). HPP treatment of the 12 % and 15 % protein concentration PPC-only and mixed systems resulted in even smaller tan δ (between 0.2-0.3) and *m* (~ 0.1), which are characteristic of strong gels (Steffe, 1996). In particular, self-standing gels were formed when starch was added to 12P samples ($G'_{1rad/s} \sim 10^3$ Pa). Notably, gel strength was more dependent on protein concentration than the increase in total solids from added starch. For example, pressure-treated 12P samples had higher $G'_{1rad/s}$ than pressure-treated 9P/8S mixed samples, even though the latter had a greater total solids content. A similar behavior was also seen in pressure-treated 15P and 12P/8S samples.

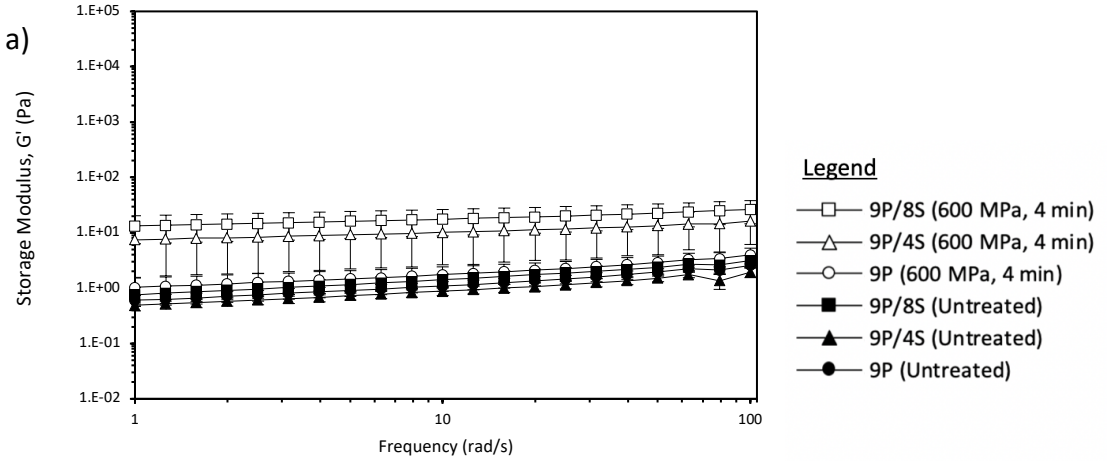

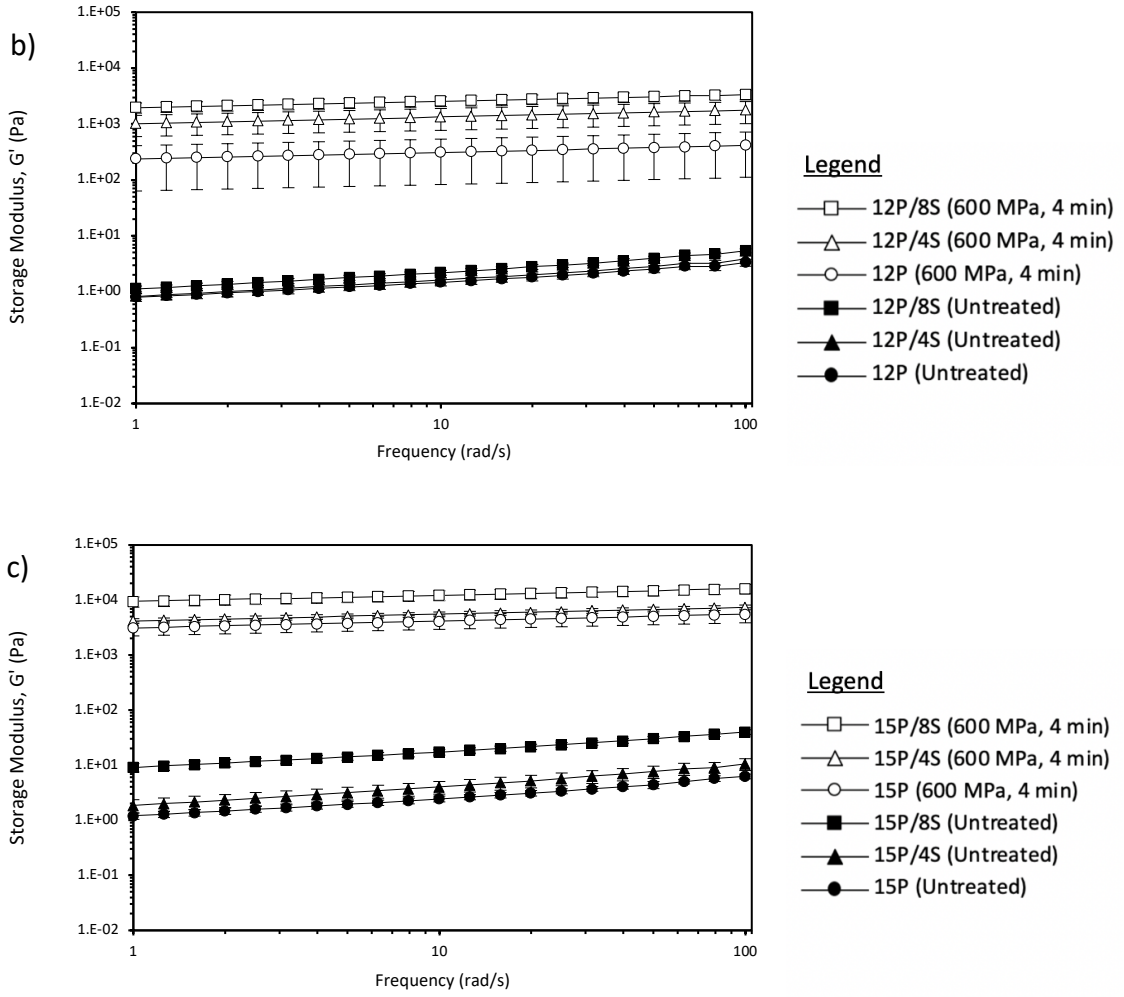

Figure 3.1. Frequency sweeps (G' vs frequency) for untreated and pressure-treated PPC-only and mixed protein-starch samples, at different protein concentrations: **(a)** 9 %, **(b)** 12 %, and **(c)** 15 % (w/w). Starch concentration in the mixed samples was 4 % or 8 % (w/w). Error bars represent 1 standard deviation (n=3).

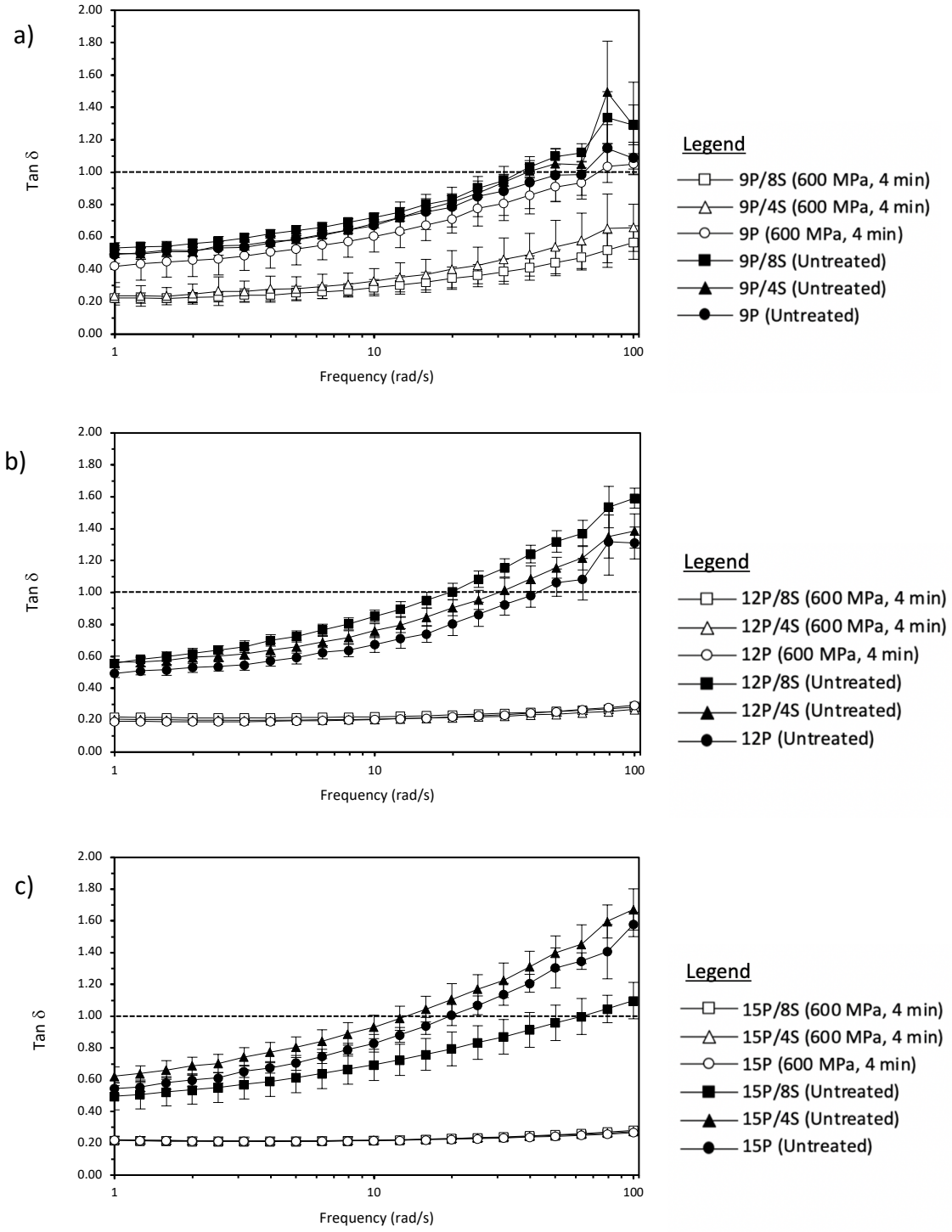

Figure 3.2. Tan δ vs frequency for untreated and pressure-treated PPC-only and mixed protein-starch samples, at different protein concentrations: **(a)** 9 %, **(b)** 12 %, and **(c)** 15 % (w/w). Starch concentration in the mixed samples was 4 % or 8 % (w/w). Error bars represent 1 standard deviation (n=3).

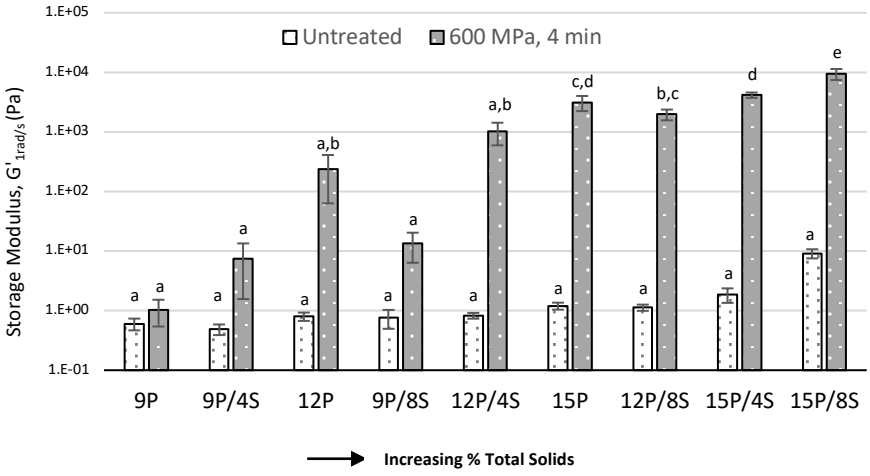

Figure 3.3. Storage modulus at 1 rad/s ($G'_{1rad/s}$) for untreated and pressure-treated PPC-only and mixed protein-starch samples with increasing total solids content. *x*P represents PPC-only systems with *x* % protein, and *x*P/*y*S represents mixed systems with *x* % protein and *y* % starch. Error bars represent 1 standard deviation (n=3). Data points connected by the same letter are not significantly different from each other ($p>0.05$).

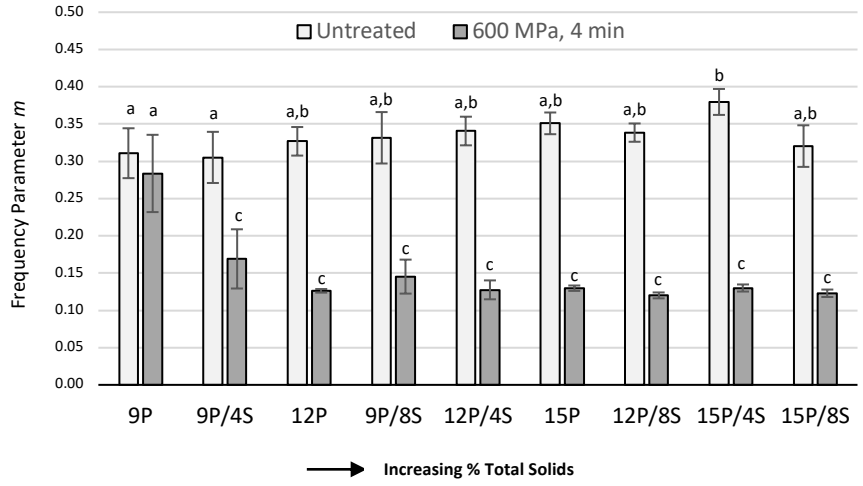

Figure 3.4. Frequency dependence parameter *m* of untreated and pressure-treated PPC-only and mixed protein-starch samples with increasing total solids content. *x*P represents PPC-only systems with *x* % protein, and *x*P/*y*S represents mixed systems with *x* % protein and *y* % starch. Error bars represent 1 standard deviation (n=3). Bars with the same letter are not significantly different from each other ($p>0.05$).

Microstructural Observations of Untreated and HPP-Treated Samples

Even though the samples were well mixed just prior to HPP treatment, HPP-treated 8 % starch-only (8S) samples showed macroscopic phase separation into a solid phase and a liquid phase, which is consistent with the findings reported by Leite et al. (2017) for pea starch solutions treated at pressures above 500 MPa. The solid phase was analyzed by SEM, and was found to consist of intact, disrupted, and fused starch granules (Figure 3.5). Sedimentation and subsequent pressure-driven compacting of the dense starch granules during the pressure ramp-up and hold time could have led to phase separation. The starch granules remained fused even after pressure was released.

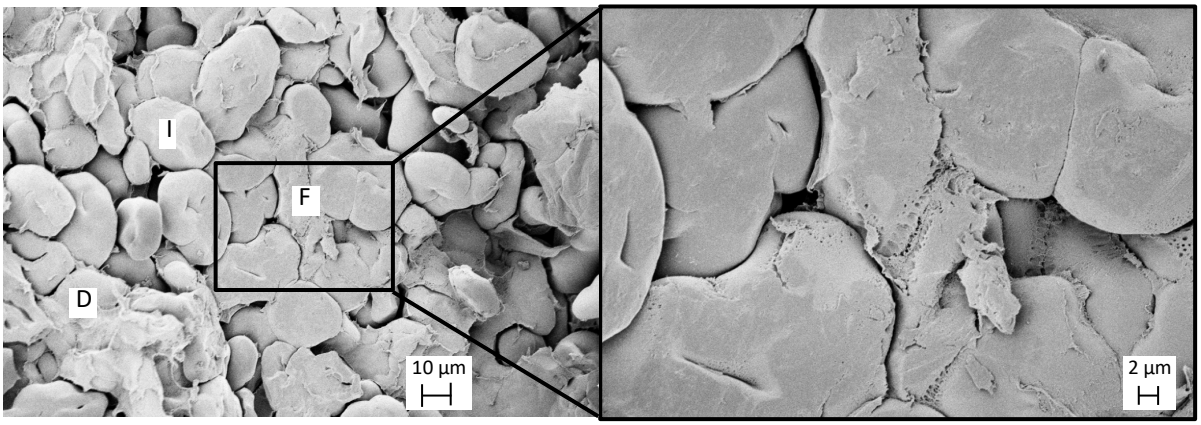

Figure 3.5. SEM micrographs of the solid phase of pressure-treated 8 % (w/w) starch-only (8S) sample. The solid phase is composed of intact (I), disrupted (D), and fused (F) starch granules.

SEM imaging was also conducted on untreated and pressure-treated 15P and 15P/8S samples (Figure 3.6). As shown in the insert for the HPP-treated 15P sample, the gel structure was made up by a network of protein aggregates. More starch granules were seen in the 15P/8S samples than the 15P samples. The intact starch granules were embedded in the protein network and seemed to behave as a filler. Unlike the 8S samples, phase separation did not occur, likely due to reduced starch sedimentation in the more viscous PPC solutions, and the entrapment of the starch granules in the protein matrix when pressure was released.

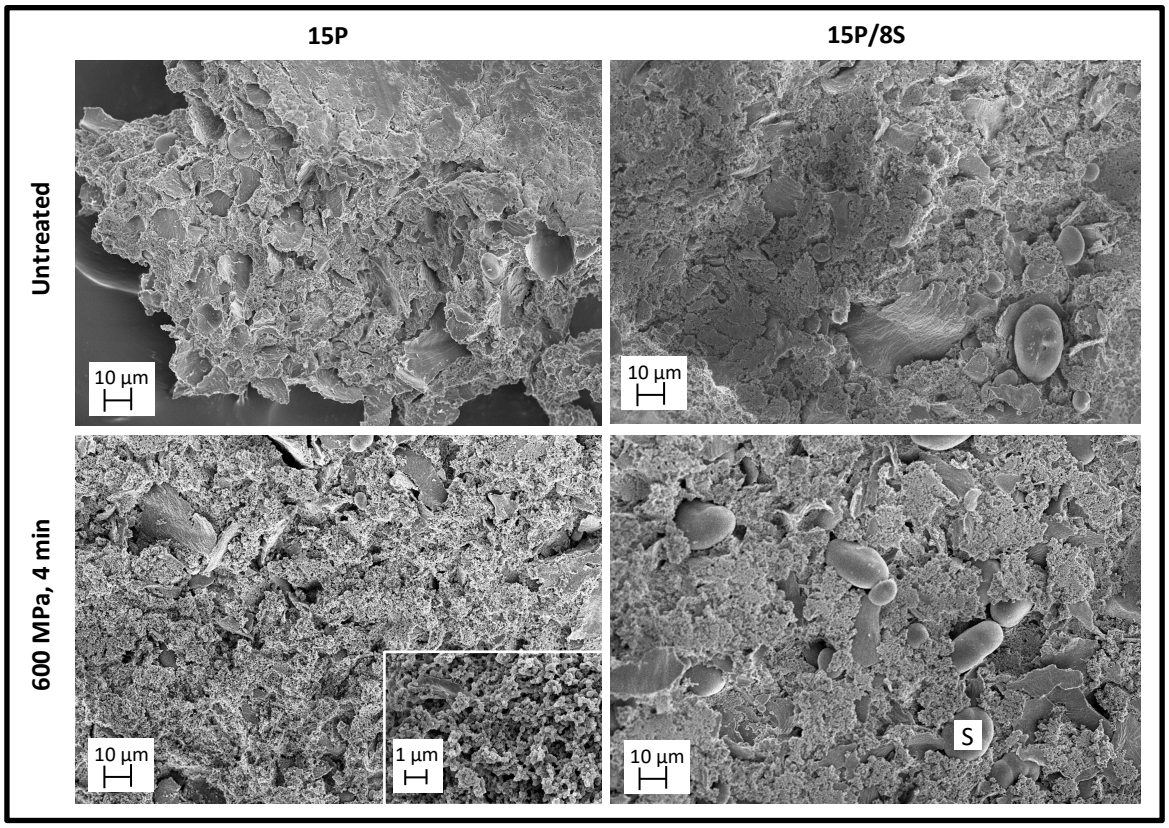

Figure 3.6. SEM micrographs of untreated and pressure-treated 15 % (w/w) protein PPC-only (15P), and 15 % (w/w) protein with 8 % (w/w) starch mixed (15P/8S) samples. The PPC-only samples naturally contain a small amount of starch. The insert shows the protein gel formed by a network of aggregates. More starch granules (S) are seen embedded in the protein network for the 15P/8S samples.

Effect of HPP on the Thermal Properties of the PPC-only and Mixed Systems

Thermal analyses by DSC was conducted for untreated, pressure-treated, and heat-treated 8S starch-only samples, and all PPC-only and mixed samples. The DSC thermograms are shown in Figures 3.7 and 3.8, the characteristic temperatures (onset and peak) and enthalpy of the identified thermal transitions are summarized in Table 3.2, and the identification of these peaks is discussed below.

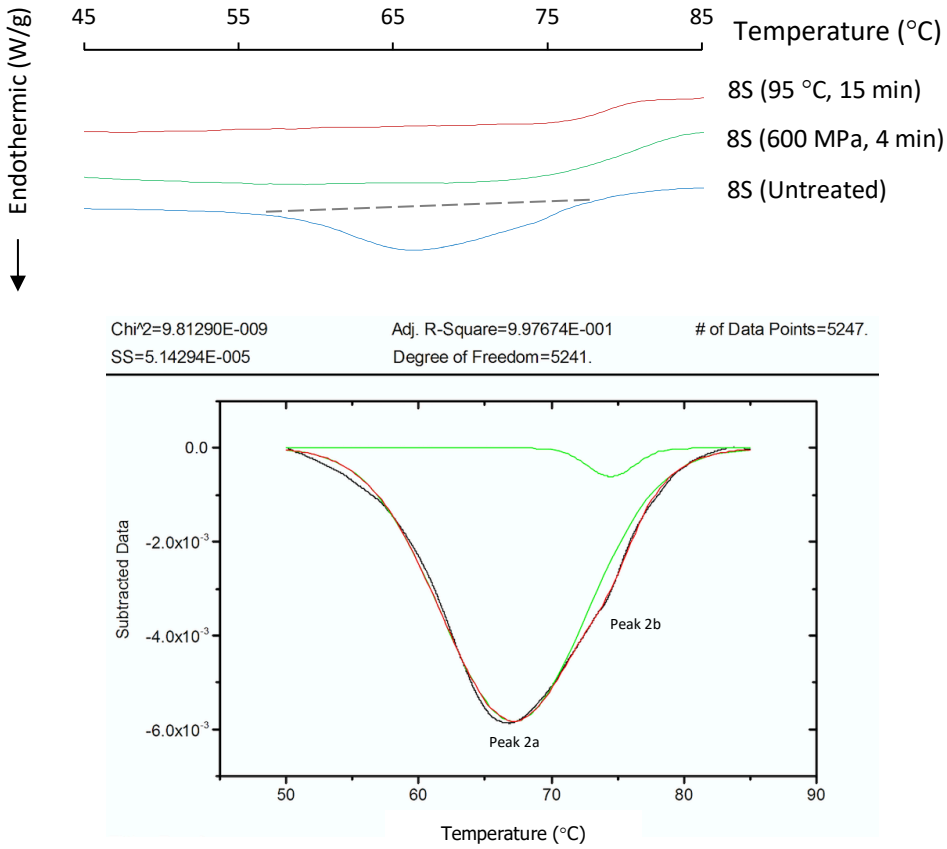

Figure 3.7. Top: DSC thermograms for untreated, pressure-treated, and heat-treated 8 % (w/w) starch-only (8S) samples. Bottom: deconvolution of the untreated 8S sample gives Peaks 2a and 2b.

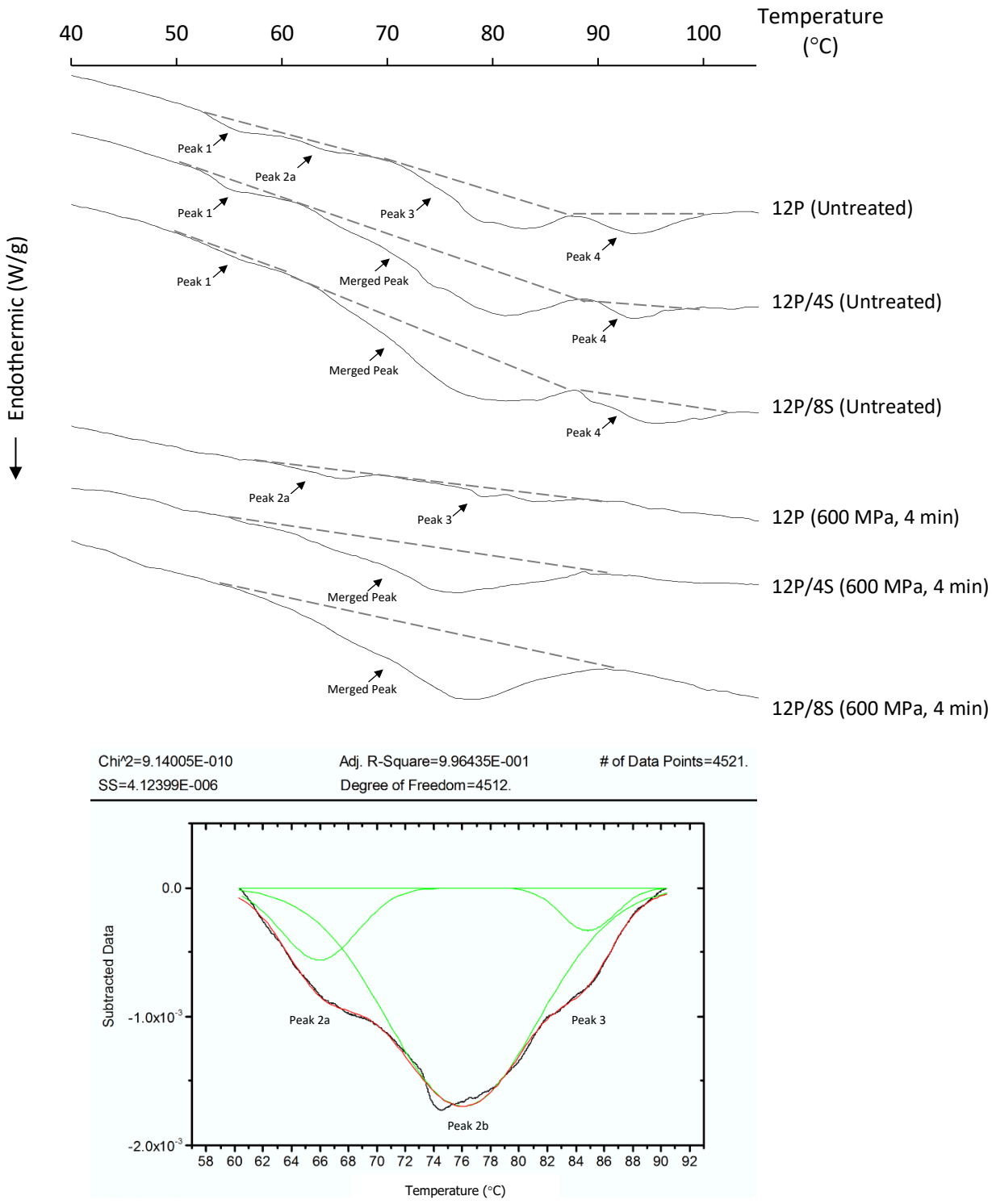

Figure 3.8. Top: DSC thermograms for untreated and pressure-treated 12 % (w/w) protein PPC-only (12P), and 12 % (w/w) protein with 4 % or 8 % (w/w) starch mixed (12P/4S or 12P/8S) samples. The thermogram is also representative for 9 % and 15 % (w/w) protein concentration samples. Bottom: deconvolution of merged peak yields Peaks 2a, 2b, and 3.

For the 8S untreated starch-only sample, one peak (T_{peak} ~ 66 °C) was observed (Figure 3.7), which corresponds to the gelatinization of pea starch (Ratnayake, Hoover, Shahidi, Perera, & Jane, 2001). Deconvolution of this peak revealed two peaks: Peak 2a (T_{peak} ~ 64 °C) and Peak 2b (T_{peak} ~ 71 °C), which corresponds to the B-type and A-type polymorphs of pea starch respectively (Bogracheva, Morris, Ring, & Hedley, 1998).

For the untreated PPC-only samples, four major peaks were observed (Figure 3.8, top). Peak 1 (T_{peak} ~ 56 °C) was attributed to the melting of endogenous lipid crystal; Peak 2a (T_{peak} ~ 65 °C), as discussed above, corresponds to the gelatinization of B-type crystal form of starch; Peak 3 (T_{peak} ~ 81 °C) corresponds to protein denaturation (Shand, Ya, Pietrasik, & Wanasundara, 2007); and Peak 4 (T_{peak} ~ 94 °C) to the dissociation of amylose-lipid complexes formed during starch gelatinization, between leached amylose and the endogenous lipids (Eliasson, 1994).

For the untreated mixed samples, in addition to Peak 1 and Peak 4, a large peak with T_{peak} ~ 74 °C was observed (Figure 3.8, top). This is consistent with the findings of Chung et al. (2008), who also found a major peak at T_{peak} ~ 72 °C in pea flour, a system which contains more starch than protein. Peaks 2a, 2b, and 3, with the same transition temperatures as above, were obtained from the deconvolution of the merged peak (Figure 3.8, bottom). For the HPP-treated mixed samples. only the merged peak was observed (Figure 3.8, top).

An analysis of the thermal transitions described above indicates that protein denaturation occurred after pressure treatment, as evidenced by the significantly lower protein denaturation enthalpy (Table 3.2). This is consistent with the observations in Chapter Two.

For starch, the enthalpy of B-type starch gelatinization (Peak 2a) for both the untreated

PPC and mixed samples (~ 2 J/g starch) was much smaller than for untreated pure pea starch (~ 32 J/g starch), which was attributed to the presence of lipids in the PPC powder. A decrease in the enthalpy of starch gelatinization in the presence of lipids was reported before (Eliasson, 1994). In contrast, the enthalpy of A-type starch gelatinization (Peak 2b) for the untreated PPC and mixed samples was similar to the untreated pure pea starch system. The peak temperatures of both B-type and A-type starch gelatinization for the untreated samples significantly increased with protein and starch content, which was likely due to reduced availability of water as more solids were added (Lund & Lorenz, 1984). Pure pea starch (8S sample) fully gelatinized under both heat and pressure treatments, as indicated by the lack of a gelatinization peak in Figure 3.7 (top panel). In contrast, starch in the PPC-only and mixed samples did not undergo pressure-gelatinization under the conditions used in this study. In fact, an increase in B-type starch gelatinization enthalpy (Peak 2a) was observed for all pressure-treated samples, although not all increases were statistically significant (Table 3.2). There were no significant changes in A-type starch gelatinization enthalpy with pressure treatment.

Table 3.2. Thermal transition parameters identified for untreated and pressure-treated mixed pea protein-starch solutions. *x*P represents PPC-only systems with *x* % protein, *x*P/*y*S represents mixed systems with *x* % protein and *y* % starch, and 8S represents the starch-only system with 8 % starch. The enthalpy of peak 4 was calculated per gram of lipid. For each peak, untreated and pressure-treated values of each parameter (T_{onset}, T_{peak} and ΔH) connected by the same letter are not significantly different from each other ($p>0.05$). No T_{onset} values for deconvoluted samples were available and therefore left blank. n.d.: not detected. Values represent averages of three replicates ± 1 stdev.

Sample	T_{onset} (°C)		T_{peak} (°C)		ΔH (J/g component)	
	Untreated	600 MPa, 4 min	Untreated	600 MPa, 4 min	Untreated	600 MPa, 4 min
Peak 1 (Lipid)						
9P	53.25 ± 0.39*a*	n.d.	56.22 ± 0.05*a*	n.d.	4.26 ± 1.15*ab*	n.d.
9P/4S	53.24 ± 0.42*a*	n.d.	55.35 ± 0.17*a*	n.d.	1.67 ± 0.06*a*	n.d.
9P/8S	53.70 ± 1.56*a*	n.d.	55.82 ± 0.58*a*	n.d.	2.45 ± 1.76*a*	n.d.
12P	52.05 ± 2.13*a*	n.d.	56.64 ± 0.90*a*	n.d.	6.55 ± 1.90*abc*	n.d.
12P/4S	53.24 ± 0.51*a*	n.d.	56.25 ± 0.97*a*	n.d.	4.83 ± 2.00*abc*	n.d.
12P/8S	52.91 ± 1.42*a*	n.d.	55.82 ± 0.84*a*	n.d.	3.23 ± 1.42*ab*	n.d.
15P	52.87 ± 1.82*a*	n.d.	56.20 ± 1.36*a*	n.d.	9.85 ± 2.44*c*	n.d.
15P/4S	52.19 ± 0.72*a*	51.39 ± 4.79*a*	56.18 ± 0.06*a*	54.49 ± 3.61*a*	8.66 ± 1.84*bc*	3.58 ± 2.77*ab*
15P/8S	52.40 ± 0.48*a*	n.d.	55.73 ± 0.23*a*	n.d.	4.21 ± 1.75*ab*	n.d.
8S	n.d.	n.d.	n.d.	n.d.	n.d.	n.d.
Peak 2a (Starch)						
9P	61.81 ± 2.09*ab*	58.30 ± 0.55*a*	63.12 ± 1.63*a*	64.64 ± 0.86*abc*	1.53 ± 1.50*a*	6.24 ± 0.94*bc*
9P/4S			65.38 ± 0.62*abc*	68.25 ± 2.65*bc*	0.87 ± 0.14*a*	9.19 ± 4.42*c*
9P/8S			66.93 ± 1.11*abc*	66.24 ± 1.36*abc*	1.58 ± 1.45*ab*	3.08 ± 1.06*ab*
12P	61.88 ± 0.94*ab*	61.96 ± 0.54*ab*	64.91 ± 0.79*abc*	65.75 ± 0.60*abc*	2.05 ± 0.62*ab*	4.00 ± 1.17*ab*
12P/4S			66.62 ± 0.41*abc*	66.20 ± 0.60*abc*	1.92 ± 1.05*ab*	3.05 ± 1.54*ab*
12P/8S			68.38 ± 0.26*bc*	66.57 ± 0.66*abc*	1.91 ± 0.85*ab*	2.45 ± 0.34*ab*
15P	64.72 ± 2.12*b*	63.08 ± 1.23*b*	66.96 ± 1.51*abc*	66.65 ± 0.53*abc*	2.00 ± 1.16*ab*	5.77 ± 1.87*abc*
15P/4S			68.47 ± 1.05*bc*	67.01 ± 0.15*abc*	2.58 ± 0.73*ab*	2.63 ± 1.16*ab*
15P/8S			68.71 ± 0.96*c*	68.48 ± 0.53*c*	2.48 ± 1.06*ab*	4.02 ± 1.12*ab*
8S			64.41 ± 3.81*ab*	n.d.	31.84 ± 22.24	n.d.
Peak 2b (Starch)						
9P	n.d.	n.d.	n.d.	n.d.	n.d.	n.d.
9P/4S			73.57 ± 0.21*ab*	74.93 ± 0.70*bc*	18.80 ± 4.46*a*	5.83 ± 4.95*a*
9P/8S			74.49 ± 0.73*abc*	74.77 ± 0.32*bc*	10.13 ± 2.73*a*	6.40 ± 2.97*a*
12P	n.d.	n.d.	n.d.	n.d.	n.d.	n.d.
12P/4S			75.44 ± 0.73*bcd*	76.12 ± 0.62*bcde*	16.64 ± 12.12*a*	13.93 ± 2.07*a*

12P/8S			76.56 ± 0.37*bcde*	76.85 ± 0.32*bcde*	10.84 ± 3.81*a*	12.56 ± 2.10*a*
15P	n.d.	n.d.	n.d.	n.d.	n.d.	n.d.
15P/4S			78.77 ± 0.11*de*	77.78 ± 0.74*cde*	13.04 ± 1.30*a*	12.15 ± 1.73*a*
15P/8S			77.91 ± 0.50*cde*	78.78 ± 0.35*e*	11.92 ± 0.59*a*	13.48 ± 1.01*a*
8S			71.01 ± 3.95*a*	n.d.	11.62 ± 10.57*a*	n.d.
Peak 3 (Protein)						
9P	70.52 ± 1.00*a*	80.16 ± 2.06*c*	79.26 ± 0.83*a*	84.17 ± 0.38*cde*	2.49 ± 0.11*de*	0.39 ± 0.14*a*
9P/4S			82.20 ± 0.92*bcd*	82.71 ± 2.58*bcd*	0.76 ± 0.57*abc*	0.81 ± 0.82*abc*
9P/8S			82.50 ± 0.47*bcd*	83.06 ± 1.17*bcd*	0.89 ± 0.35*abc*	0.93 ± 0.82*abc*
12P	73.53 ± 1.08*ab*	77.88 ± 3.11*bc*	80.97 ± 1.78*ab*	84.30 ± 0.50*cde*	2.69 ± 0.19*de*	0.70 ± 0.49*abc*
12P/4S			82.62 ± 0.85*bcd*	84.86 ± 0.96*de*	1.71 ± 0.64*bcd*	0.58 ± 0.19*ab*
12P/8S			83.61 ± 0.34*bcde*	86.11 ± 0.17*e*	1.12 ± 0.40*abc*	0.35 ± 0.01*a*
15P	73.66 ± 0.13*ab*	73.24 ± 2.65*ab*	81.90 ± 0.58*abc*	84.05 ± 0.75*cde*	3.15 ± 0.28*e*	0.72 ± 0.16*abc*
15P/4S			84.00 ± 0.11*cde*	86.22 ± 0.29*e*	1.51 ± 0.29*abcd*	0.28 ± 0.15*a*
15P/8S			84.62 ± 0.25*cde*	86.27 ± 0.53*e*	1.93 ± 0.04*cde*	0.67 ± 0.39*ab*
8S	n.d.	n.d.	n.d.	n.d.	n.d.	n.d.
Peak 4 (Amylose-lipid complex)						
9P	87.16 ± 0.32*a*	93.10 ± 0.88*cde*	92.14 ± 0.81*a*	95.33 ± 1.28*bcd*	18.91 ± 8.99*abc*	3.34 ± 1.33*a*
9P/4S	88.40 ± 0.37*ab*	94.86 ± 3.68*e*	92.44 ± 0.82*ab*	97.44 ± 2.07*d*	18.85 ± 6.61*abc*	7.76 ± 4.50*ab*
9P/8S	88.69 ± 0.27*ab*	n.d.	93.69 ± 1.29*abc*	n.d.	16.02 ± 1.85*abc*	n.d.
12P	89.50 ± 0.71*abc*	n.d.	93.78 ± 0.50*abc*	n.d.	18.02 ± 6.02*abc*	n.d.
12P/4S	89.87 ± 0.22*abcd*	n.d.	94.01 ± 0.80*abc*	n.d.	21.53 ± 3.61*bc*	n.d.
12P/8S	89.94 ± 1.51*abcd*	n.d.	94.93 ± 0.17*abcd*	n.d.	28.69 ± 7.72*c*	n.d.
15P	90.00 ± 0.47*abcd*	n.d.	94.68 ± 0.58*abcd*	n.d.	28.26 ± 2.06*c*	n.d.
15P/4S	91.40 ± 0.60*bcde*	93.64 ± 1.86*de*	95.78 ± 0.93*cd*	97.34 ± 1.18*d*	30.82 ± 9.26*c*	2.25 ± 1.14*a*
15P/8S	92.28 ± 0.58*bcde*	n.d.	96.37 ± 0.48*cd*	n.d.	26.55 ± 10.11*c*	n.d.
8S	n.d.	n.d.	n.d.	n.d.	n.d.	n.d.

3.5 DISCUSSION

Under the conditions used in this study, it appears that starch acted mainly as a filler in the pressure-induced pea protein gel matrix. The addition of starch enhanced the strength of the pressure-induced protein structures, and it enabled the formation of weak gels even at protein concentrations below the minimum required for gelation. This could be due to microscopic phase separation between starch and proteins (Colombo, León, & Ribotta, 2011),

which reduced the volume occupied by protein molecules, leading to a localized increase in protein concentration. In the mixed pea protein-starch systems, the gel strength was however found to be more dependent on protein concentration, as the gel network was primarily made up by pressure-denatured protein molecules.

Remarkably, starch granules in the pea protein-starch systems remained visually intact after pressure treatment. Thermal analyses further revealed that starch was not gelatinized in the pressure-treated samples. This could be due to the limited availability of water for starch gelatinization during the pressure treatment, since both protein and starch compete for water. In pressure treatment, protein denaturation occurs at a lower pressure than starch gelatinization. As water holding capacity of the proteins increases after pressure denaturation (Queirós et al., 2017), this limits the amount of water available for starch gelatinization. It has been reported before that in the absence of water, pea starch did not gelatinize after HPP treatment (Leite et al., 2017). In contrast, heat-treated protein-starch systems of comparable total solids content to the present study led to the formation of starch and protein composite gels, with starch granules visibly disrupted by heat (Joshi et al., 2014; Li et al., 2007). Overall, this data demonstrates that the effect of high pressure on food components can be very different than the effect of thermal treatments, particularly in complex systems.

3.6 CONCLUSIONS

Cold HPP treatment at 600 MPa for 4 min induced gel formation in mixed pea protein-pea starch systems, but starch remained ungelatinized and behaved as a filler in the protein gel matrix. This can have significant implications in the development of food products that contain pea protein, pea flour, or other plant-based ingredients using HPP technology. While

ungelatinized starch contributes to structure formation, the presence of intact starch granules may impact the mouthfeel of the products, which needs to be tested using sensory evaluations. From a nutritional perspective, since ungelatinized starch is poorly digested and acts like a fiber (Wang & Copeland, 2013), pressure-treated protein-starch mixtures may allow the development of high protein products with a low glycemic index.

3.7 ACKNOWLEDGMENTS

This work was funded by the USDA-NIFA grant 2016-67017-24635. We acknowledge the use of the DSC and electron microscope at the Cornell Center for Materials Research (CCMR), supported by NSF-MRSEC (DMR 1120296). We would like to thank Dr. Yifan Cheng from Cornell University for assistance with SEM imaging, AGT Foods for supplying the PPC powder, and World Food Processing for supplying the PS powder.

REFERENCES

Ahmed, J., Singh, A., Ramaswamy, H. S., Pandey, P. K., & Raghavan, G. S. V. (2014). Effect of high-pressure on calorimetric, rheological and dielectric properties of selected starch dispersions. *Carbohydrate Polymers*, *103*, 12–21. https://doi.org/10.1016/J.CARBPOL.2013.12.014

Balasubramaniam, V. M. (Bala), Martínez-Monteagudo, S. I., & Gupta, R. (2015). Principles and Application of High Pressure–Based Technologies in the Food Industry. *Annual Review of Food Science and Technology*, *6*(1), 435–462. https://doi.org/10.1146/annurev-food-022814-015539

Barrios-Peralta, P., Pérez-Won, M., Tabilo-Munizaga, G., & Briones-Labarca, V. (2012). Effect of high pressure on the interactions of myofibrillar proteins from abalone (Haliotis rufencens) containing several food additives. *LWT - Food Science and Technology*, *49*(1), 28–33. https://doi.org/10.1016/j.lwt.2012.04.025

Beliciu, C. M., & Moraru, C. I. (2013). Physico-chemical changes in heat treated micellar casein - Soy protein mixtures. *LWT - Food Science and Technology*, *54*(2), 469–476. https://doi.org/10.1016/j.lwt.2013.06.013

Bogracheva, T. Y., Morris, V. J., Ring, S. G., & Hedley, C. L. (1998). The granular structure of C-type pea starch and its role in gelatinization. *Biopolymers*, *45*(4), 323–332. https://doi.org/10.1002/(SICI)1097-0282(19980405)45:4<323::AID-BIP6>3.0.CO;2-N

Cadesky, L., Walkling-Ribeiro, M., Kriner, K. T., Karwe, M. V., & Moraru, C. I. (2017). Structural changes induced by high-pressure processing in micellar casein and milk protein concentrates. *Journal of Dairy Science*, *100*(9), 7055–7070. https://doi.org/10.3168/jds.2016-12072

Chinma, C. E., Ariahu, C. C., & Abu, J. O. (2013). Chemical composition, functional and pasting properties of cassava starch and soy protein concentrate blends. *Journal of Food Science and Technology*, *50*(6), 1179–1185. https://doi.org/10.1007/s13197-011-0451-8

Chung, H.-J., Liu, Q., Hoover, R., Warkentin, T. D., & Vandenberg, B. (2008). In vitro starch digestibility, expected glycemic index, and thermal and pasting properties of flours from pea, lentil and chickpea cultivars. *Food Chemistry*, *111*(2), 316–321. https://doi.org/10.1016/J.FOODCHEM.2008.03.062

Colombo, A., León, A. E., & Ribotta, P. D. (2011). Rheological and calorimetric properties of corn-, wheat-, and cassava- starches and soybean protein concentrate composites. *Starch/Staerke*, *63*(2), 83–95. https://doi.org/10.1002/star.201000095

Eliasson, A. C. (1994). Interactions between starch and lipids studied by DSC. *Thermochimica Acta*, *246*(2), 343–356. https://doi.org/10.1016/0040-6031(94)80101-0

Henchion, M., Hayes, M., Mullen, A., Fenelon, M., & Tiwari, B. (2017). Future Protein Supply and Demand: Strategies and Factors Influencing a Sustainable Equilibrium. *Foods*, *6*(7), 53. https://doi.org/10.3390/foods6070053

Hunt, A., Getty, K. J. K., & Park, J. W. (2009). Roles of starch in surimi seafood: A review. *Food Reviews International*, *25*(4), 299–312. https://doi.org/10.1080/87559120903155834

Joshi, M., Aldred, P., Panozzo, J. F., Kasapis, S., & Adhikari, B. (2014). Rheological and microstructural characteristics of lentil starch-lentil protein composite pastes and gels. *Food Hydrocolloids*, *35*, 226–237. https://doi.org/10.1016/j.foodhyd.2013.05.016

Leite, T. S., de Jesus, A. L. T., Schmiele, M., Tribst, A. A. L., & Cristianini, M. (2017). High pressure processing (HPP) of pea starch: Effect on the gelatinization properties. *LWT - Food Science and Technology*, *76*, 361–369. https://doi.org/10.1016/j.lwt.2016.07.036

Li, J. Y., Yeh, A. I., & Fan, K. L. (2007). Gelation characteristics and morphology of corn starch/soy protein concentrate composites during heating. *Journal of Food Engineering*, *78*(4), 1240–1247. https://doi.org/10.1016/j.jfoodeng.2005.12.043

Lund, D., & Lorenz, K. J. (1984). Influence of time, temperature, moisture, ingredients, and processing conditions on starch gelatinization. *C R C Critical Reviews in Food Science and Nutrition*, *20*(4), 249–273. https://doi.org/10.1080/10408398409527391

Oh, H. E., Anema, S. G., Pinder, D. N., & Wong, M. (2009). Effects of different components in skim milk on high-pressure-induced gelatinisation of waxy rice starch and normal rice starch. *Food Chemistry*, *113*(1), 1–8. https://doi.org/10.1016/j.foodchem.2008.07.107

Pei-Ling, L., Xiao-Song, H., & Qun, S. (2010). Effect of high hydrostatic pressure on starches: A review. *Starch - Stärke*, *62*(12), 615–628. https://doi.org/10.1002/star.201000001

Queirós, R. P., Saraiva, J. A., & da Silva, J. A. L. (2017). Tailoring structure and technological properties of plant proteins using high hydrostatic pressure. *Critical Reviews in Food Science and Nutrition*, 1–19. https://doi.org/10.1080/10408398.2016.1271770

Ratnayake, W. S., Hoover, R., Shahidi, F., Perera, C., & Jane, J. (2001). Composition, molecular structure, and physicochemical properties of starches from four field pea (Pisum sativum L.) cultivars. *Food Chemistry*, *74*(2), 189–202. https://doi.org/10.1016/S0308-8146(01)00124-8

Shand, P. J., Ya, H., Pietrasik, Z., & Wanasundara, P. K. J. P. D. (2007). Physicochemical and textural properties of heat-induced pea protein isolate gels. *Food Chemistry*, *102*(4), 1119–1130. https://doi.org/10.1016/j.foodchem.2006.06.060

Steffe, J. F. (1996). *Rheological methods in food process engineering*. Freeman press.

Wang, S., & Copeland, L. (2013). Molecular disassembly of starch granules during gelatinization and its effect on starch digestibility: A review. *Food and Function*. https://doi.org/10.1039/c3fo60258c

Yang, Z., Chaib, S., Gu, Q., & Hemar, Y. (2017). Impact of pressure on physicochemical properties of starch dispersions. *Food Hydrocolloids*, *68*, 164–177. https://doi.org/10.1016/j.foodhyd.2016.08.032

CHAPTER FOUR

HIGH PRESSURE PROCESSING OF PEA PROTEIN-STARCH MIXED SYSTEMS: PROTEIN AND STARCH *IN-VITRO* DIGESTIBILITY

4.1 ABSTRACT

This work explores the effects of high pressure processing (HPP) and heat treatment on the protein and starch digestibility of mixed pea protein-starch systems. Reconstituted pea protein concentrate containing 15% (w/w) protein, and a mixed system containing 15% (w/w) protein with 8% (w/w) pea starch were subjected to HPP at 600 MPa for 4 min at 5 °C, or thermal treatments at 95 °C for 15 min. The untreated, pressure-treated, and heat-treated samples then underwent dynamic *in-vitro* digestions using a TIM-1 system. Protein and starch digestibility were investigated using BCA protein and hexokinase-based glucose assays respectively. While the untreated samples had the highest protein and the lowest starch digestibility, pressure treatments led to higher protein and lower starch digestibility than heat treatments. These results show that HPP-treated pea protein-starch mixtures could lead to the creation of novel pea-based products with lower glycemic-index and enhanced protein digestibility.

4.2 INTRODUCTION

With the increase in demand for plant proteins, a major challenge in using pulses as a plant protein source is represented by their lower protein quality compared to animal-based protein sources (Young & Pellett, 1994). Some factors that influence protein quality include the amino acid composition and the digestibility of the protein (Nosworthy & House, 2017).

Pulses contain an array of antinutritional factors such as trypsin inhibitors and lectins, which can reduce protein digestibility (Nosworthy & House, 2017). Traditional processing methods such as soaking and cooking can improve protein digestibility due to the inactivation of the enzyme inhibitors (Boye, Zare, & Pletch, 2010), and the heat denaturation of proteins which allows proteins to become more accessible to digestive proteases (Chitra, Singh, & Venkateswara Rao, 1996).

The use of high pressure processing (HPP) as a nonthermal method to create novel structures is expected to affect the digestibility of proteins. In pure protein systems, HPP was reported to affect protein digestibility through pressure-induced structure changes (Queirós, Saraiva, & da Silva, 2017) and the inactivation of antinutritional factors (Deng, Padilla-Zakour, Zhao, & Tao, 2015; Linsberger-Martin, Weiglhofer, Thi Phuong, & Berghofer, 2013). Pressure-induced structural changes led to improved protein digestibility due to the exposure of more proteolytic cleave sites in the unfolded proteins, but also led to decreased protein digestibility when the unfolded proteins aggregated, which restricted digestive enzymes accessibility to the same cleavage sites (Queirós et al., 2017).

As starch is a major component of pulses, the digestibility of starch is also of interest for high pressure treated pulse-based foods. Native starch is poorly hydrolyzed by amylases due to the low substrate accessibility in the highly crystalline starch structure (Wang & Copeland, 2013). Cooking was found to improve the enzymatic hydrolysis of starch, which increased with the degree of thermal gelatinization due to the breakdown of the crystalline order (Holm, Lundquist, Bjorck, Eliasson, & Asp, 1988). Like in the case of proteins, there are conflicting reports on the effect of HPP on the digestibility of starch in pure starch systems. Pressure-gelatinized starch was found to be more digestible than native starch (Deng

et al., 2014; Hayashi & Hayashida, 1989; Noguchi et al., 2003; Zeng, Li, Gao, Liu, & Yu, 2018; Zhou et al., 2015). There were some studies however that showed that HPP treatments reduced starch digestibility. These occurred in low-moisture systems (Mercier, Charbonn, & Guilbot, 1968) which likely led to incomplete gelatinization of starch (Yang et al., 2017), or in systems where the C-type starch structures converted to more amylase-resistant B-type structures under pressure (Liu et al., 2016; Liu et al., 2017).

In the previous chapters, it was reported that HPP induced gel formation in mixed pea protein-starch systems through the aggregation and network formation of denatured proteins. Pea starch behaved as a filler that mechanically reinforced the protein network, but remained ungelatinized after pressure treatment. In contrast, pea starch in mixed pea protein-starch systems was found to be gelatinized by heat treatment. One implication of these findings is that starch in pressure-treated mixed protein-starch systems may be poorly digested compared to heat-treated samples. There is currently no published literature investigating the effect of HPP on the digestibility of protein-starch mixed systems. Therefore, this work explored the effects of heat and pressure treatment on the protein and starch digestibility in mixed pea protein-starch systems. Filling this knowledge gap might advance the development of novel foods with interesting nutritional benefits.

4.3 MATERIALS AND METHODS

Materials and Chemicals

Pea protein concentrate (PPC) obtained by air classification (Pea Protein 55, AGT Foods, Regina, SK, Canada) was used as a source of pea protein. The composition of PPC powder was: 54.5 % (dry weight) protein, 4.3 % (dry weight) starch, 2.8 % (dry weight) fat,

6.7 % (dry weight) ash, and 7.2 % moisture. Pea starch (PS) was provided by World Food Processing LLC. (Turtle Lake, WI) and contained 0.7 % (dry weight) protein, 94.0 % (dry weight) starch, 0.1 % (dry weight) fat, 0.15 % (dry weight) ash, and 10.7 % moisture. All compositions were determined at Dairy One Laboratories (Ithaca, NY).

Lipase (type II, 100-500 units/mg) and pancreatin (4 x USP specifications, P1750-500G) from porcine pancreas, pepsin A from porcine stomach mucosa (2500-3500 units/mg), and Type II-A α-amylase from Bacillus species (1333 units/mg) were obtained from Sigma-Aldrich (St. Louis, MO). Fresh pig bile was from TNO Zeist (Netherlands). All chemicals used were of analytical grade quality.

Sample Preparation

Two formulations were made to determine if differences in protein-starch interactions or structure formation affect protein and starch digestibility. The first was a 15 % (w/w) protein concentration PPC-only sample (15P) that has been found to form a strong gel under HPP and heat treatments. The other (15P/8S) was a 15 % (w/w) protein concentration PPC sample with PS added to give a final starch concentration of 8% (w/w). The 15P PPC-only system contained 1.19 % (w/w) of starch.

To prepare the solutions, PPC and PS powders were added to Milli-Q water with stirring at 1,200 rpm for 30 min at 25 °C. The solutions were then cooled in an ice bath with continued stirring for 15 min. To achieve good dispersion, the solutions were subsequently high-shear mixed at 18,000 rpm for 7.5 min in an ice bath, using a high shear mixer (UltraTurrax Model T25 fitted with a S25N-18G dispersion tool, IKA Works Inc., Wilmington, NC), ensuring that the solutions did not exceed 25 °C. Finally, the mixed solutions were filled in pre-cut storage bags (FoodSaver Vacuum-Seal Roll, Sunbeam

Products Inc., Boca Raton, FL) and vacuum sealed. The packaged samples were stored overnight at 4 °C before HPP or heat treatments.

HPP Treatment

The samples were high pressure processed using a 55 L HPP unit (Hiperbaric, Spain). Samples were subjected to pressure treatment at 600 MPa for a 4 min hold time, which represent typical processing parameters for microbial inactivation used by the food industry. The initial temperature of the pressurizing medium (filtered water) was 5 °C. The HPP-treated samples were stored at 4 °C to minimize microbial activity until further analyses.

Heat Treatment

Heat-treated samples were obtained by immersing packaged 15P and 15P/8S samples in a water bath at 95 °C for 15 min. The heat-treated samples were immediately cooled in an ice bath for 15 min, then stored at 4 °C until further analyses.

TIM-1 Gastro-Intestinal Model

The untreated, HPP and heat-treated samples were subjected to dynamic *in-vitro* digestion performed in the multi-compartmental TIM-1 system (TNO, The Netherlands) at Rutgers University. The model is described in detail by other authors (Denis et al., 2016; Minekus, 2015). The TIM-1 system was composed of four successive glass compartments (stomach, duodenum, jejunum and ileum) with flexible inner silicone membranes that mimics the human gastrointestinal tract (Figure 4.1). 100 g of the samples were lightly stirred by hand with artificial saliva (95 g electrolyte solution, 100 g distilled water, 5 g gastric start residue, 11 mg α-amylase) and transferred to the stomach compartment, where chyme mixing under controlled temperature was achieved through the pumping of 37 °C water into the space between the glass jacket and inner membrane. The chyme was transported through the

intestinal compartments via peristaltic valve pumps. Gastric and intestinal pH values were monitored and adjusted continually via the addition of hydrochloric acid or sodium bicarbonate. Gastric, bile and pancreatic secretions were injected into the appropriate compartments by computer-controlled pumps. Gastric emptying, intestinal transit times, pH values and secretion fluids were regulated by a computer protocol. Water and digestion products were removed from the jejunum and ileum by dialysis through 10 kDa-cutoff hollow fiber membranes (0.05 µm pore, Spectrum Minikros, Repligen Corp, Boston, MA) and collected as pools (with effluents kept on ice during collection) at 20, 40, 60, 90, 120, 150, 180, 210 and 240 min after the start of digestion. Each pool was weighed and frozen until further analyses. Two independent digests were made for each treatment.

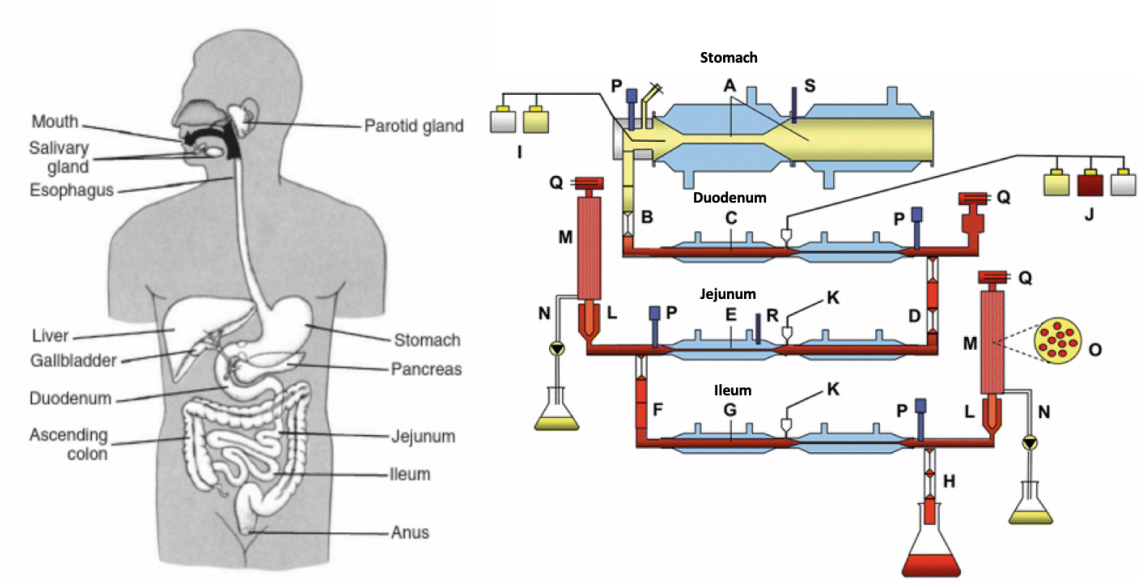

Figure 4.1. Schematic representation of TIM-1 to model the human gastrointestinal tract. A. gastric compartment; B. pyloric sphincter; C. duodenal compartment; D. peristaltic valve; E. jejunal compartment; F. peristaltic valve; G. ileal compartment; H. ileal-cecal valve; I. gastric secretion; J. duodenal secretion; K. bicarbonate secretion; L. pre-filter; M. filtration system; N. filtrate with bio-accessible fraction; O. hollow fiber system (cross section); P. pH

electrodes; Q. level sensors; R. temperature sensors; S. pressure sensor (adapted from Minekus, 2015; Stipanuk and Caudill, 2012).

Protein Digestibility Analyses

The protein concentration of digested samples was determined using a bicinchoninic acid (BCA) protein assay kit (Pierce^{TM} BCA Assay, Thermo Fisher Scientific, Waltham, MA). Digested samples from each collected time point were diluted with distilled water. The samples were then incubated at 37 °C for 30 min, and the absorbance of the cuprous-BCA complex formed due to protein reduction of Cu^{2+} was measured at 562 nm (SpectraMax iD3, Molecular Devices LLC, San Jose, CA). The absorbance values were within the working range recommended by the manufacturer. The final absorbance values were corrected by subtracting the absorbance value of a blank containing distilled water and the BCA working reagent made in the same experimental set. The digested samples protein concentration was determined from a bovine serum albumin (BSA) standard curve also made in the same experimental set. At least two sets of measurements were made for each digested sample, and two independent digests were conducted for each treatment. The differences in absorbance values with an addition of 8 % (w/w) maltose to BSA standards were within the experimental error, indicating that the theoretical maximum concentration of reducing sugars present did not influence the assay.

Starch Digestibility Analyses

The amount of glucose released during digestion was determined using a hexokinase colorimetric assay kit (Glucose (HK) Assay, Sigma-Aldrich, St. Louis, MO). The substrate-specific reaction minimizes the interference of amino acids in detecting the presence of reducing sugars. Briefly, glucose present in the digested samples was initially phosphorylated

to glucose-6-phosphate (G6P) via hexokinase. G6P and NAD^+ were then converted to 6-phosphogluconate and NADH via glucose-6-phosphate dehydrogenase. The amount of NADH produced was measured at 340 nm (GENESYS^{TM} 20, Thermo Fisher Scientific, Waltham, MA), with the concentration of glucose calculated from the absorbance values of NADH as given in the manufacturer's instructions (based on 1:1 stoichiometric ratio of glucose to NADH). At least two sets of measurements were made for each digested sample, and two independent digests were conducted for each treatment.

Starch digestibility was determined according to how rapidly glucose was released during *in-vitro* digestion. Starch from which glucose is released in the first 20 min of digestion was considered rapidly digestible starch. Glucose released from starch between 20 to 120 min came from slowly digestible starch. Any remaining starch after 120 min was classified as resistant starch (Englyst, Kingman, & Cummings, 1992).

4.4 RESULTS

Effect of Pressure and Heat on the Protein Digestibility of the PPC-only and Mixed Systems

Figure 4.2 and Table 4.1 show the average cumulative protein digestion of the untreated, pressure-treated, and heat-treated 15P and 15P/8S samples. There was a greater % protein digested in the jejunum than the ileum, which suggests that the majority of the proteins were digested in the jejunum before the chyme moved to the ileum. For both 15P and 15P/8S samples, overall protein digestibility of untreated > pressure-treated > heat-treated samples (Table 4.1). The cumulative protein digestion followed a sigmoidal curve, and the highest digestion rates occurred between 90-180 min. For the 15P samples, the overall protein

digestion was similar in all treatments during the first 60 min before diverging (Figure 4.2e). By contrast, the overall protein digestion diverged for the different treatments after 150 min for the 15P/8S samples (Figure 4.2f). The 15P/8S samples also had a greater total protein digestibility than the 15P samples for all treatments.

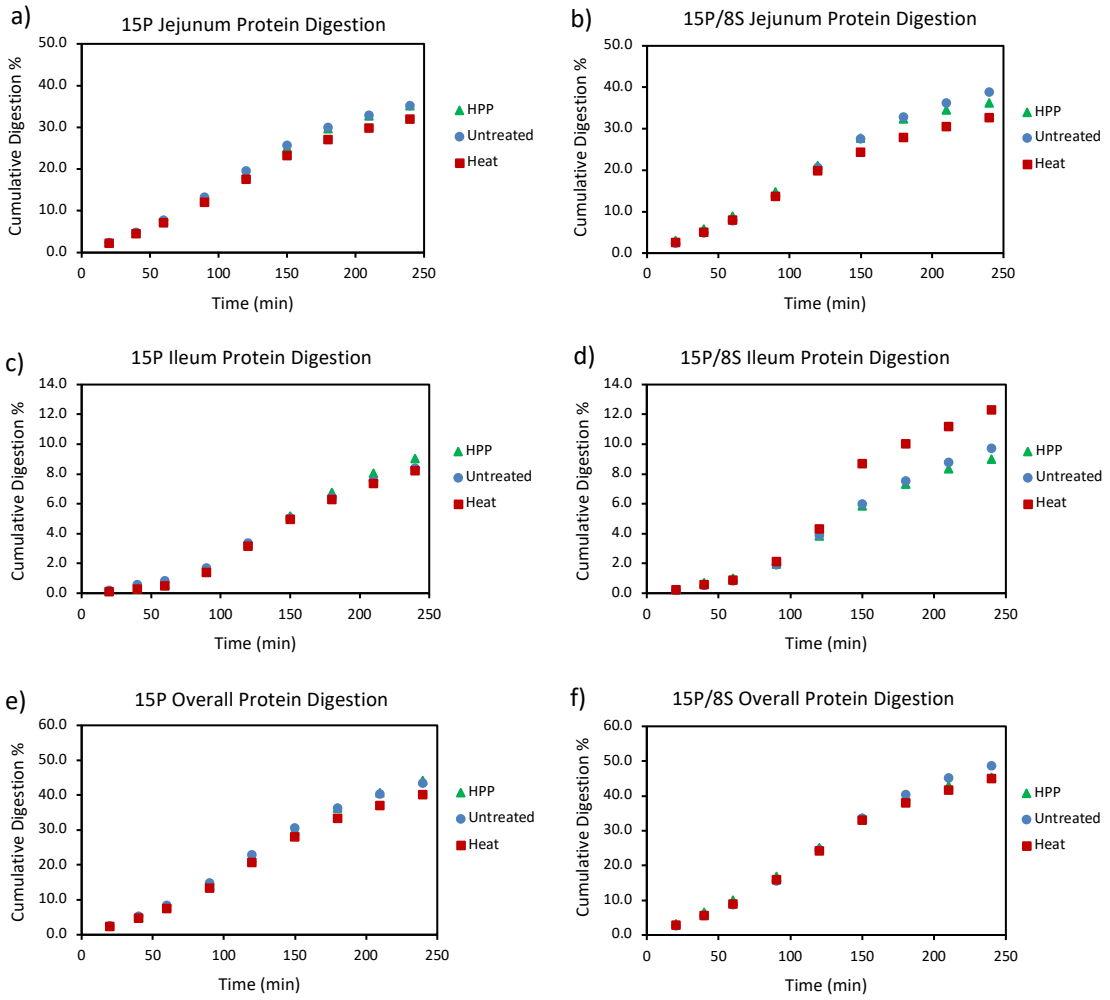

Figure 4.2. Cumulative protein digestibility of untreated, pressure-treated and heat-treated 15 % (w/w) protein PPC-only (15P), and 15 % (w/w) protein with 8 % (w/w) starch mixed (15P/8S) samples taken from the **(a-b)** jejunum, **(c-d)** ileum, **(e-f)** and overall (jejunum + ileum). *The data represent the average of two independent digests conducted for each treatment*.

Table 4.1. Total protein digestibility (in %) after 240 min of *in-vitro* digestion for untreated, pressure-treated, and heat-treated 15 % (w/w) protein PPC-only (15P), and 15 % (w/w) protein with 8 % (w/w) starch mixed (15P/8S) samples. *The data represent the average of two independent digests conducted for each treatment*.

	15P			15P/8S		
Treatment	Jejunum	Ileum	Overall	Jejunum	Ileum	Overall
Untreated	35.12	8.37	43.49	38.90	9.72	48.62
HPP	35.19	9.04	44.23	36.33	8.99	45.32
Heat	31.95	8.23	40.18	32.65	12.29	44.94

Effect of Pressure and Heat on the Starch Digestibility of the PPC-only and Mixed Systems

Figure 4.3 and Table 4.2 show the average cumulative starch digestion, and the proportion of rapidly digestible, slowly digestible and resistant starch, of the untreated, pressure-treated, and heat-treated 15P and 15P/8S samples respectively. Similar to protein digestion, the majority of starch was digested in the jejunum, and the overall digestibility followed a sinusoidal curve with the highest starch digestion rate achieved between 90-180 min (Figure 4.3e-f). For both 15P and 15P/8S samples, overall starch digestibility for all treatments were similar in the first 60 min but diverged after that time. In contrast to protein digestibility however, overall starch digestibility ranked in the order heat-treated > pressure-treated > untreated, for both 15P and 15P/8S samples. This was also reflected in untreated samples having the most amount of resistant starch present (Table 4.2). The 15P/8S samples had a lower overall starch digestibility compared to the 15P samples. This could be due to 15P/8S having much more substrate than amylase present in the *in-vitro* digestion system so relatively less starch was acted on than what was present in the sample.

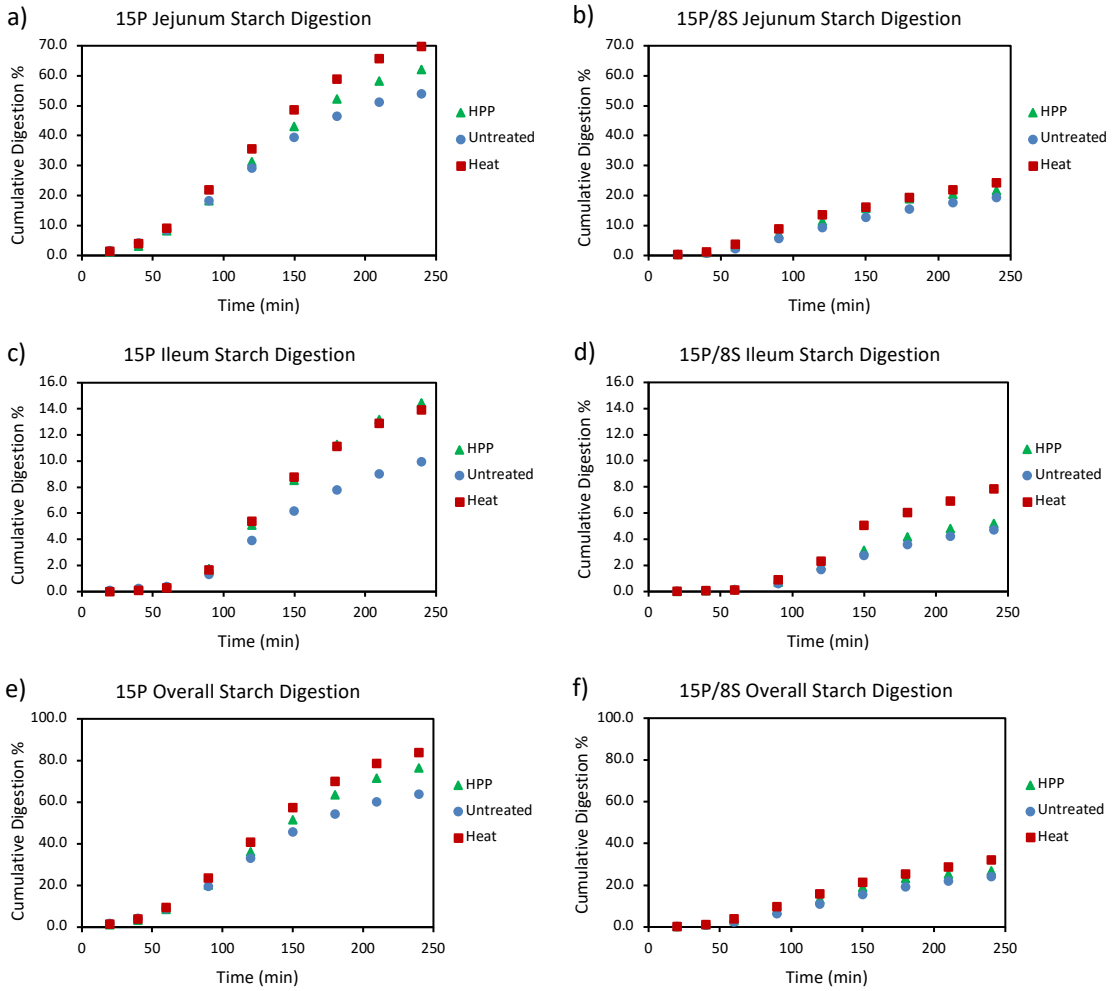

Figure 4.3. Cumulative starch digestibility of untreated, pressure-treated and heat-treated 15 % (w/w) protein PPC-only (15P), and 15 % (w/w) protein with 8 % (w/w) starch mixed (15P/8S) samples taken from the **(a-b)** jejunum, **(c-d)** ileum, **(e-f)** and overall (jejunum + ileum). *The data represent the average of two independent digests conducted for each treatment*.

Table 4.2. Proportion (in %) of rapidly digestible (starch digested between 0-20 min), slowly digestible (starch digested between 20-120 min), and resistant starch (starch digested after 120 min) after *in-vitro* digestion for untreated, pressure-treated, and heat-treated 15 % (w/w) protein PPC-only (15P), and 15 % (w/w) protein with 8 % (w/w) starch mixed (15P/8S) samples. *The data represent the average of two independent digests conducted for each treatment*.

Treatment	15P			15P/8S		
	Rapidly Digestible	Slowly Digestible	Resistant Starch	Rapidly Digestible	Slowly Digestible	Resistant Starch
Untreated	1.637	31.452	66.911	0.232	10.600	89.169
HPP	1.060	35.192	63.748	0.223	13.190	86.588
Heat	1.408	39.492	59.100	0.211	15.602	84.187

4.5 DISCUSSION

The overall protein digestibility decreased after both pressure and heat treatments compared to controls for both 15P and 15P/8S samples. This suggests that the potential improvement to protein digestibility due to increased proteolytic cleavage sites in unfolded proteins was outweighed by the decrease in protein digestibility when the unfolded proteins aggregated, restricting digestive enzymes accessibility to the same cleavage sites (Queirós et al., 2017). The overall protein digestibility due to pressure treatment was greater than for heat treatment, which correlated with the weaker gel strength of pressure-treated samples compared to heat-treated samples reported in Chapter Two, as the pressure-treated samples had less protein aggregation compared to the heat-treated samples. However, the overall protein digestibility values were similar among the treatments, and additional replicates are needed to ascertain if the observed differences are statistically significant.

The overall starch digestibility from pressure treatments was lower than heat treatments for both 15P and 15P/8S samples. This could be because the ungelatinized starch in the pressure-treated samples was less digestible than the gelatinized starch in the heat-

treated samples. Interestingly, the pressure-treated starch had higher digestibility than the untreated samples, which suggests that some structural modifications of starch may have occurred during pressure treatment.

Overall, while the untreated samples had the highest protein and the lowest starch digestibility, heat or pressure treatments are needed to form structures that can be utilized for the development of novel pea-based foods. Between the two processing methods, pressure treatments led to higher protein and lower starch digestibility than heat treatments, although the observed differences were small. It is also important to note that, although the TIM-1 system is one of the most sophisticated *in-vitro* digestion models available today, these findings need to be validated with human *in-vivo* digestibility studies, especially to verify if there are any meaningful nutritional outcomes.

4.6 CONCLUSIONS

This study evaluated the effect of pressure and temperature on the protein and starch digestibility of mixed pea protein-starch systems. Pressure treatments led to higher protein and lower starch digestibility than heat treatments. From a practical angle, HPP-treated pea protein-starch mixtures could be used for the creation of novel pea-based products with lower glycemic-index and enhanced protein digestibility. This may be useful in maximizing the nutritional outcomes of such products, especially in the management of metabolic disorders.

4.7 ACKNOWLEDGMENTS

This work was funded by the USDA-NIFA grant 2016-67017-24635. We would like to thank Ender Arserim from Rutgers University for his assistance with the TIM-1 digestions,

Alexandra Hall from Cornell University for assistance with the BCA and glucose measurements, AGT Foods for supplying the PPC powder, and World Food Processing for supplying the PS powder.

REFERENCES

Boye, J., Zare, F., & Pletch, A. (2010). Pulse proteins: Processing, characterization, functional properties and applications in food and feed. *Food Research International*, *43*(2), 414–431. https://doi.org/10.1016/j.foodres.2009.09.003

Chitra, U., Singh, U., & Venkateswara Rao, P. (1996). Phytic acid, in vitro protein digestibility, dietary fiber, and minerals of pulses as influenced by processing methods. *Plant Foods for Human Nutrition*, *49*(4), 307–316. https://doi.org/10.1007/BF01091980

Deng, Y., Jin, Y., Luo, Y., Zhong, Y., Yue, J., Song, X., & Zhao, Y. (2014). Impact of continuous or cycle high hydrostatic pressure on the ultrastructure and digestibility of rice starch granules. *Journal of Cereal Science*, *60*(2), 302–310. https://doi.org/10.1016/J.JCS.2014.06.005

Deng, Y., Padilla-Zakour, O., Zhao, Y., & Tao, S. (2015). Influences of High Hydrostatic Pressure, Microwave Heating, and Boiling on Chemical Compositions, Antinutritional Factors, Fatty Acids, In Vitro Protein Digestibility, and Microstructure of Buckwheat. *Food and Bioprocess Technology*, *8*(11), 2235–2245. https://doi.org/10.1007/s11947-015-1578-9

Denis, S., Sayd, T., Georges, A., Chambon, C., Chalancon, S., Santé-Lhoutellier, V., & Blanquet-Diot, S. (2016). Digestion of cooked meat proteins is slightly affected by age as assessed using the dynamic gastrointestinal TIM model and mass spectrometry. *Food and Function*, *7*(6), 2682–2691. https://doi.org/10.1039/c6fo00120c

Englyst, H. N., Kingman, S. M., & Cummings, J. H. (1992). Classification and measurement of nutritionally important starch fractions. *European Journal of Clinical Nutrition*, *46 Suppl 2*, S33-50. Retrieved from http://www.ncbi.nlm.nih.gov/pubmed/1330528

Hayashi, R., & Hayashida, A. (1989). Increased Amylase Digestibility of Pressure-Treated Starch. *Agricultural and Biological Chemistry*, *53*(9), 2543–2544. https://doi.org/10.1080/00021369.1989.10869672

Holm, J., Lundquist, I., Bjorck, I., Eliasson, A. C., & Asp, N. G. (1988). Degree of starch gelatinization, digestion rate of starch in vitro, and metabolic response in rats. *American Journal of Clinical Nutrition*, *47*(6), 1010–1016. https://doi.org/10.1093/ajcn/47.6.1010

Linsberger-Martin, G., Weiglhofer, K., Thi Phuong, T. P., & Berghofer, E. (2013). High hydrostatic pressure influences antinutritional factors and in vitro protein digestibility of split peas and whole white beans. *LWT - Food Science and Technology*, *51*(1), 331–336. https://doi.org/10.1016/j.lwt.2012.11.008

Liu, H., Guo, X., Li, Y., Li, H., Fan, H., & Wang, M. (2016). In vitro digestibility and changes in physicochemical and textural properties of tartary buckwheat starch under high hydrostatic pressure. *Journal of Food Engineering*, *189*, 64–71. https://doi.org/10.1016/j.jfoodeng.2016.05.015

Liu, M., Wu, N.-N., Yu, G.-P., Zhai, X.-T., Chen, X., Zhang, M., … Tan, B. (2017). Physicochemical properties, structural properties, and in vitro digestibility of pea starch treated with high hydrostatic pressure. *Starch - Stärke*, 1700082. https://doi.org/10.1002/star.201700082

Mercier, C., Charbonn, R., & Guilbot, A. (1968). Influence of pressure treatment on granular structure and susceptibility to enzymatic amylolysis of various starches. *Starch - Stärke*, *20*(1), 6–11.

Minekus, M. (2015). The TNO gastro-intestinal model (TIM). In *The Impact of Food Bioactives on Health: In Vitro and Ex Vivo Models* (pp. 37–46). Cham: Springer International Publishing. https://doi.org/10.1007/978-3-319-16104-4_5

Noguchi, T., Taniguchi-Yamada, A., Sato, H., Suzuki, T., Matsumoto, S., & Takano, K. (2003). Effect of high-pressure treatment on decomposition of potato and wheat starch by alpha-amylase. *Food Preservation Science*, *29*(6), 335–339. https://doi.org/10.5891/jafps.29.335

Nosworthy, M. G., & House, J. D. (2017, January 1). Factors influencing the quality of dietary proteins: Implications for pulses. *Cereal Chemistry*. John Wiley & Sons, Ltd. https://doi.org/10.1094/CCHEM-04-16-0104-FI

Queirós, R. P., Saraiva, J. A., & da Silva, J. A. L. (2017). Tailoring structure and technological properties of plant proteins using high hydrostatic pressure. *Critical Reviews in Food Science and Nutrition*, 1–19. https://doi.org/10.1080/10408398.2016.1271770

Stipanuk, M. H., & Caudill, M. A. (2012). Biochemical, physiological, and molecular aspects of human nutrition. Retrieved from https://ebookcentral.proquest.com

Wang, S., & Copeland, L. (2013). Molecular disassembly of starch granules during gelatinization and its effect on starch digestibility: A review. *Food and Function*. https://doi.org/10.1039/c3fo60258c

Yang, Z., Chaib, S., Gu, Q., & Hemar, Y. (2017). Impact of pressure on physicochemical properties of starch dispersions. *Food Hydrocolloids*, *68*, 164–177. https://doi.org/10.1016/j.foodhyd.2016.08.032

Young, V. R., & Pellett, P. L. (1994). Plant proteins in relation to human protein and amino acid nutrition. In *American Journal of Clinical Nutrition* (Vol. 59, p. 1203S–1212S). Narnia. https://doi.org/10.1093/ajcn/59.5.1203S

Zeng, F., Li, T., Gao, Q., Liu, B., & Yu, S. (2018). Physicochemical properties and in vitro digestibility of high hydrostatic pressure treated waxy rice starch. *International Journal of Biological Macromolecules*, *120*, 1030–1038. https://doi.org/10.1016/J.IJBIOMAC.2018.08.121

Zhou, Z., Ren, X., Wang, F., Li, J., Si, X., Cao, R., … Blanchard, C. (2015). High pressure processing manipulated buckwheat antioxidant activity, anti-adipogenic properties and starch digestibility. *Journal of Cereal Science*, *66*, 31–36. https://doi.org/10.1016/j.jcs.2015.09.002

CHAPTER FIVE

SUGGESTIONS FOR FUTURE RESEARCH

One of the main motivations for this work as described in Chapter Two is the minimization of the undesirable "cooked" flavor in pressure-treated pea-based products. While this dissertation focused mainly on structure formation, follow-up sensory studies can be done to verify this claim. The textures of the pressure-treated samples could also be compared to the heat-treated samples by the sensory panel, to determine if HPP treatments result in perceivably unique textures.

As HPP affects only non-covalent interactions, an important concern is the structural stability of these physical gels. Hence it may be necessary to conduct shelf life studies to examine how microbial growth, structure breakdown and syneresis occur under cold storage. The results may determine the distribution range of the created products. Structure breakdown and syneresis may however be of lesser concern in products such as HPP-formed yogurt-like products.

Starch was found to remain ungelatinized after HPP in Chapters Two and Three, likely due to the limited availability of water in the mixed systems during HPP. This suggested mechanism could be tested by investigating the water holding capacity of the pea protein concentrate and pea starch to determine the minimum amount of free water required for pea starch to be gelatinized by pressure. Protein-starch ratios could also be investigated to determine its effect on the degree of starch gelatinization. As other biopolymers may be able to bind water under pressure, this strategy to keep starch ungelatinized could be used in other biopolymer-starch mixtures.

In this work, a mainly two-component system was examined. Food products inevitably contain other components such as lipids and minerals. These other components could affect structure formation through phase separation and interactions with protein. Further work into the effects of other components is therefore important in the formulation of new pea-based products.

Finally, protein and starch digestibility were examined in broad strokes in Chapter Four. More in-depth exploration could be done to understand the breakdown of protein, and the formation and efficacy of bioactive peptides. More importantly, the results found in Chapter Four require validation with human subjects.

These studies could potentially lead to the further development of novel pea-based foods with nutritional functions.